

1 Title

2 Large-scale clustering of longitudinal faecal calprotectin and C-reactive protein
3 profiles in inflammatory bowel disease

4 Short title

5 Longitudinal biomarker clustering in inflammatory bowel disease

6 Authors

7 Nathan Constantine-Cooke^{*1,2}, Marie Vibeke Vestergaard^{*3}, Nikolas Plevris^{1,4}, Karla
8 Monterrubio-Gómez^{1,2}, Clara Ramos Belinchón^{1,4}, Solomon Ong⁴, Alexander T.
9 Elford^{4,5}, Beatriz Gros^{4,6}, Aleksejs Sazonovs³, Gareth-Rhys Jones^{4,7}, Tine Jess^{†3,8},
10 Catalina A. Vallejos^{† 2}, and Charlie W. Lees^{† 1,3,4}

11 * Joint first authors,
12 † Joint senior authors

13 Affiliations

- 14 1. Centre for Genomic and Experimental Medicine, Institute of Genetics and
15 Cancer, University of Edinburgh, Edinburgh, UK
- 16 2. MRC Human Genetics Unit, Institute of Genetics and Cancer, University of
17 Edinburgh, Edinburgh, UK
- 18 3. Center for Molecular Prediction of Inflammatory Bowel Disease, PREDICT,
19 Department of Clinical Medicine, Aalborg University, Copenhagen, Denmark
- 20 4. Edinburgh IBD Unit, Western General Hospital, Edinburgh, UK
- 21 5. Faculty of Medicine, The University of Melbourne, Melbourne, Australia
- 22 6. Reina Sofía University Hospital, Gastroenterology and Hepatology. IMIBIC.
23 University of Cordoba. Cordoba, Spain
- 24 7. Centre for Inflammation Research, The Queen's Medical Research Institute,
25 University of Edinburgh, Edinburgh, UK
- 26 8. Department of Gastroenterology & Hepatology, Aalborg University Hospital,
27 Aalborg, Denmark

NOTE: This preprint reports new research that has not been certified by peer review and should not be used to guide clinical practice.

28 Abstract

29 Background

30 Crohn's disease (CD) and ulcerative colitis (UC) are highly heterogeneous, dynamic
31 and unpredictable, with a marked disconnect between symptoms and intestinal
32 inflammation. Attempts to classify inflammatory bowel disease (IBD) subphenotypes
33 to inform clinical decision making have been limited. We aimed to describe the latent
34 disease heterogeneity by modelling routinely collected faecal calprotectin (FC) and
35 CRP data, describing dynamic longitudinal inflammatory patterns in IBD.

36 Methods

37 In this longitudinal study, we analysed patient-level post-diagnosis measurements of
38 FC and CRP in two European cohorts. Latent class mixed models were used to cluster
39 individuals with similar longitudinal profiles. Associations between cluster assignment
40 and baseline characteristics were quantified using multinomial logistic regression.
41 Differences in advanced therapy use across clusters were also explored. Finally, we
42 considered uncertainty in cluster assignments with respect to follow-up length and the
43 overlap between FC and CRP clusters. We included 1036 patients in the FC discovery
44 analysis (Lothian) with a total of 10545 FC observations (median 9 per subject, IQR
45 6–13), and 7880 patients in the replication (Denmark). The CRP discovery analysis
46 consisted of 1838 patients with 49364 measurements (median 20 per subject; IQR
47 10–36), with 10041 patients in the replication cohort.

48 Findings

49 Eight distinct clusters of inflammatory behaviour over time were identified in the FC
50 and CRP analysis for the Scottish cohort. This model was then applied to the Danish
51 replication cohort, with similar patterns observed in both the Scottish and Danish
52 populations. The clusters, FC1–8 and CRP1–8, were ordered from the lowest
53 cumulative inflammatory burden to the highest. The clusters included groups with high
54 diagnostic levels of inflammation which rapidly normalised, groups where high
55 inflammation levels persisted throughout the full seven years of observation, and a
56 series of intermediates including delayed remitters and relapsing remitters.

57 CD and UC patients were unevenly distributed across the clusters. In UC, male sex
58 was associated with the poorest prognostic cluster (FC8). The use and timing of
59 advanced therapy was associated with cluster assignment, with the highest use of
60 early advanced therapy in FC1. Of note, FC8 and CRP8 captured consistently high
61 patterns of inflammation despite a high proportion of patients receiving advanced
62 therapy, particularly for CD individuals. We observed that uncertainty in cluster
63 assignments was higher for individuals with short longitudinal follow-up, particularly
64 between clusters capturing similar earlier inflammation patterns. There was broadly
65 poor agreement between FC and CRP clusters in keeping with the need to monitor
66 both in clinical practice.

67 Interpretation

68 Distinct patterns of inflammatory behaviour over time are evident in patients with IBD.
69 Cluster assignment is associated with disease type and both the use and timing of
70 advanced therapy. These data pave the way for a deeper understanding of disease
71 heterogeneity in IBD and enhanced patient stratification in the clinic.

72 Introduction

73 Inflammatory bowel disease (IBD), an umbrella term for Crohn's disease (CD),
74 ulcerative colitis (UC) and inflammatory bowel disease unclassified (IBDU), has a
75 prevalence of almost 1% in the UK.^{1,2} IBD is characterised by chronic relapsing and
76 remitting inflammation of the gastrointestinal (GI) tract that confers a host of
77 debilitating symptoms, negatively impacting quality of life.^{3,4} Studies have clearly
78 demonstrated that uncontrolled GI tract inflammation increases the risk of disease
79 progression and complications including colorectal cancer,⁵ stricturing/penetrating
80 complications, and surgery.^{6,7} However, IBD is highly heterogeneous with respect to
81 symptoms, inflammatory burden, treatment response, and long-term outcomes.

82
83 Current IBD classification methods are mostly based on historic nomenclature which
84 utilise baseline phenotypic characteristics and do not take into account the dynamic
85 and unpredictable nature of the disease. Attempts at developing prediction tools to
86 identify high risk patients have been made but again use static clinical parameters,
87 dismissing the changing nature of the disease.⁸ Furthermore, they do not take into
88 account the influence of other factors, such as advanced therapy timing, on the
89 disease course. In the wake of the increasing prevalence of IBD and associated
90 healthcare burden,⁹ new methods to characterise the dynamic disease course and
91 help identify at-risk individuals who require aggressive therapy with close monitoring
92 versus those that need less intense input are essential.

93
94 The original IBSEN studies provided the first data on the clinical course of patients
95 with UC and CD during the first 10-years of diagnosis.^{10,11} However, these data were
96 predicated on predefined disease patterns, rather than being data driven, utilising
97 symptoms alone. It is now widely accepted that there is a clear disconnect between
98 inflammation and symptoms in IBD.¹² It is therefore imperative characterisations of
99 disease course include objective parameters of inflammation.

100
101 C-reactive protein (CRP) and faecal calprotectin (FC) are well established tools for
102 monitoring patients with IBD, but are typically interpreted in terms of the most recent
103 measurement or short-term trends. Interrogation of long-term trends of inflammation
104 could greatly assist clinical decision making and improve prediction of future events.

105 Moreover, modelling inflammatory behaviour over time might be a key tool for
106 characterising the largely unexplained heterogeneity seen in IBD, and provide new
107 tools for disease sub-phenotyping beyond the current Montreal classification.¹³

108

109 In this study, we aimed to 1) identify groups of IBD patients with similar longitudinal
110 patterns of inflammation, 2) determine if these groupings were associated with age,
111 sex, IBD type, Montreal classification, or therapy, and 3) explore whether subjects with
112 similar longitudinal FC profiles also share similar CRP profiles. To assess the
113 robustness of our findings, we perform the analysis separately in two population-level
114 cohorts, one covering the NHS Lothian health board in Scotland and one national-level
115 registry in Denmark.

116 Methods

117 Ethics

118 Usage of the Scottish dataset was approved by the local Caldicott Guardian (Project
119 ID: CRD18002, registered NHS Lothian information asset #IAR-954). In Denmark,
120 studies based on registry data alone are not required to obtain permission from the
121 regional ethics committees as confirmed by The Central Denmark Region Committees
122 on Health Research Ethics (legislation: 1–10–72-148-19). Patients or the public were
123 not involved in the design, conduct, reporting or dissemination plans of our research.

124 Study design

125 This was a cohort study carried out separately in two population-level cohorts, based
126 in Scotland and Denmark, respectively. Detailed definitions for each cohort are
127 provided in Supplementary Note 1.

128

129 In Scotland, patients with a confirmed diagnosis of IBD (Lennard-Jones criteria)¹⁴ were
130 followed up for a period of seven years from the date of diagnosis. Baseline phenotype
131 data (sex, age at diagnosis, IBD type, date of diagnosis) were obtained from the
132 Lothian IBD registry (LIBDR), a retrospective cohort of patients receiving IBD care in
133 Lothian, Scotland. The LIBDR is estimated to have identified 94.3% of all IBD patients

134 in the area.¹ Using a population-level cohort reduces potential biases due to
135 recruitment.¹⁵ When available, additional phenotyping was extracted by the clinical
136 team from electronic health records (TrakCare; InterSystems, Cambridge, MA). This
137 includes smoking and Montreal classification for disease location, behaviour and
138 extent, all recorded at the time of diagnosis. Data on prescribing of all advanced
139 therapies, including start/stop dates, were extracted from TrakCare and NHS Lothian
140 pharmacy databases. Primary care prescribing data were not available.

141

142 In Denmark, patients with IBD were identified from national health registries using a
143 methodology previously described by Agrawal et al.¹⁶ Briefly, patients were required
144 to have at least two IBD-related hospital interactions within a period of two years. All
145 Danish residents are assigned a personal identification number which can be used to
146 link interactions across the healthcare system. Montreal classification and smoking
147 status were not available for the Danish cohort. However, this cohort had data on all
148 redeemed primary care prescriptions for corticosteroid and immunosuppressants, in
149 addition to advanced therapy prescribing.

150 Inclusion/exclusion criteria

151 In the LIBDR, subjects were required to have a confirmed diagnosis of IBD at any age
152 and receive secondary care for their condition from the NHS Lothian health board.
153 Only subjects with a recorded date of IBD diagnosis between 2005 and 2019 were
154 included. The lower bound for this criteria was established as FC testing was not
155 routinely performed prior to this date. The upper bound ensured subjects had the
156 possibility of at least five years of follow-up at the time of data extraction. In the Danish
157 cohort, subjects were required to have a date of diagnosis between January 2015 and
158 September 2022. The lower bound was set based on when the Danish nationwide
159 Register of Laboratory Results for Research became nationwide. The upper bound
160 was set based on data availability.

161

162 In both cohorts, the following criteria were separately applied to longitudinal FC and
163 CRP measurements. Subjects were required to have a diagnostic measurement (\pm
164 three months of diagnosis, Figures [S1](#), [S2](#)) and have a further two observations
165 available within the follow up periods of five and seven years for the Danish and LIBDR

166 cohorts respectively. If any biomarker measurements were observed within three
167 months prior to the recorded diagnosis date, measurements were realigned with
168 respect to diagnosis ([Figure S3](#)). Only non-censored observations were considered in
169 this calculation for FC. For CRP, this filtering was applied after preprocessing (see
170 “Longitudinal measurements and preprocessing” section), and subjects with constant
171 biomarker measurements over time were excluded.

172 Statistical analysis

173 Cohort description

174 Continuous variables were summarised as their median and interquartile range (IQR).
175 Categorical variables were summarised as counts and percentages.

176 Longitudinal measurements and preprocessing

177 For the LIBDR, FC and CRP measurements were obtained from an extract by the local
178 biochemistry team describing tests recorded up to August 13, 2024. For each
179 individual, all measurements within seven years from diagnosis were considered.
180 Failed tests, for example due to contamination, were discarded. All FC tests were
181 performed from stool samples using the same ELISA technology.¹⁷ Due to limits of
182 detection, observations $<20 \mu\text{g/g}$ were recoded to $20 \mu\text{g/g}$ whilst observations >1250
183 $\mu\text{g/g}$ were mapped to $1250 \mu\text{g/g}$. Such observations were treated as censored when
184 applying the inclusion exclusion criteria described above. CRP was measured from
185 blood samples; observations for which only an upper bound was available, e.g. <1
186 mg/L , were mapped to the corresponding upper bound.

187
188 Test results for the Danish data were obtained from subjects’ local biochemistry teams.
189 As national biochemistry data were only nationwide from 2015, only measurements
190 within five years from the date of diagnosis were considered. Test results between
191 January 2015 and September 2022 were considered. For FC, observations $>1800\mu\text{g/g}$
192 were censored, whilst CRP observations $<4\text{mg/L}$ were censored. As with the LIBDR,
193 censored observations were recoded to their respective threshold.

194

195 To smooth out short-term fluctuations CRP measurements were further processed by
196 considering median values within fixed time intervals (Supplementary Note 2).

197 Longitudinal biomarker clustering

198 The Scottish and Danish data were analysed separately. FC and CRP trajectories
199 (after log-transformation) were modelled separately using latent class mixed models
200 (LCMMs),¹⁸ enabling clustering of subjects that share similar longitudinal trajectories.
201 LCMM consists of two submodels: one which captures longitudinal behaviour, and one
202 which captures cluster assignment. Fixed effects for the longitudinal submodel were
203 specified as natural cubic splines. The intercept was used as a patient-level random
204 effect. The cluster assignment submodel used IBD type as a covariate. Model
205 definitions and hyper-parameter choices are shown in Supplementary Note 3.

206
207 As the number of clusters is not known a priori, the optimal model was found using a
208 grid search approach. We considered models with 2–10 clusters for both FC and CRP.
209 ¹⁹ Akaike information criterion (AIC),¹⁹ Bayesian information criterion (BIC), and visual
210 inspection of cluster trajectories were used to compare models with different
211 specifications and determine the most appropriate number of assumed clusters. The
212 optimal number of clusters was chosen based on the LIBDR dataset as it has a more
213 precise phenotyping (date of diagnosis, IBD type and additional information). The
214 chosen number of clusters was then applied when analysing the Danish cohort.

215
216 LCMM calculates, for each individual, the probability of being assigned to each cluster.
217 In subsequent analyses, each individual was assigned to the cluster with the highest
218 probability. The distribution of cluster assignment probabilities was used to assess
219 uncertainty in these allocations with respect to follow-up length. This was defined as
220 the time difference between diagnosis and the last available biomarker measurement
221 (FC or CRP, depending on the analysis). For each cluster, the average probability of
222 individual-specific probabilities of cluster assignment were reported.

223
224 To avoid displaying potentially identifiable individual-level data, exemplar trajectories
225 within each cluster were visualised as aggregated trends, with measurements
226 summarised as the median across six randomly selected individuals. For the LIBDR

227 analysis, clusters were ordered based on the area under the overall biomarker trend
228 inferred for each cluster (a proxy for cumulative inflammatory burden). The clusters
229 found in the Danish cohort were ordered manually to resemble similar trajectories.

230 Associations with respect to cluster assignments

231 To facilitate the interpretation of each cluster, we considered potential associations
232 between cluster assignments and patient phenotypes. Violin plots and percentage bar
233 plots were used as a visual summary when considering continuous (age) and discrete
234 (sex, IBD type and, for LIBDR, additional phenotyping) covariates, respectively.

235

236 Multinomial logistic regression was used to quantify associations between cluster
237 assignments and patient phenotypes (covariates). Multivariate models were
238 considered, and the associated 95% confidence intervals are reported. Individuals with
239 missing covariate values were excluded when fitting each model. As a sensitivity
240 analysis, the analysis was repeated after excluding individuals with a low probability
241 for cluster assignment (<0.5).

242 Prescribing trends

243 To compare patterns of advanced therapy (AT) across clusters, the cumulative
244 distribution of first-line advanced therapy use was calculated for both the Scottish and
245 Danish cohorts. As primary care prescribing data were available for Danish subjects,
246 patterns for systemic corticosteroid and immunomodulator use were also investigated.
247 Results are reported stratified by IBD type (CD and UC only).

248 Comparison between FC and CRP cluster assignments

249 For subjects meeting the criteria for both FC and CRP analyses, the relationship
250 between FC and CRP cluster assignment was visualised using alluvial plots and side-
251 by-side comparisons of mean cluster trajectories for the optimal models. Stratified
252 results for CD and UC subjects are also reported.

253 Software

254 All analysis was performed in the R statistical software²⁰; software/package versions
255 are shown in Supplementary Note 4. Analytical reports for the LIBDR have been

256 generated using the Quarto scientific publishing system and are hosted online
 257 (<https://vallejosgroup.github.io/IBD-Inflammatory-Patterns/>) with code used to perform
 258 the LIBDR and Danish analyses publicly available under an open source license
 259 (<https://github.com/VallejosGroup/IBD-Inflammatory-Patterns>).

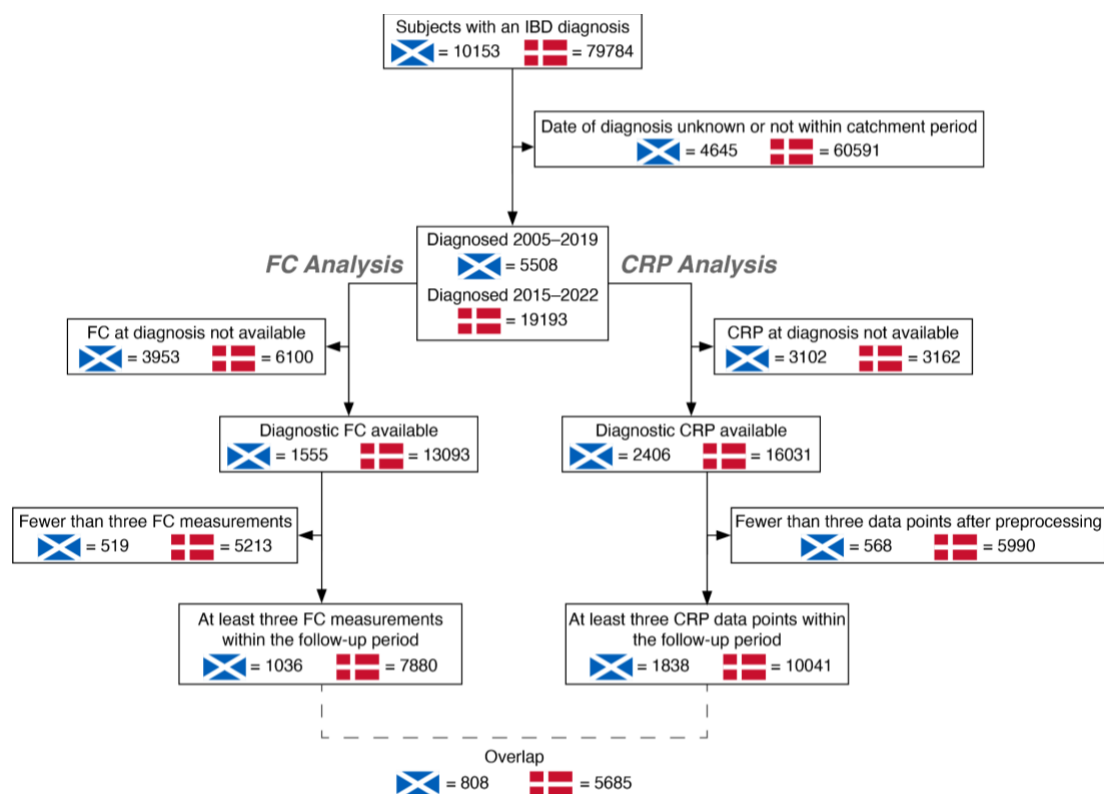
260 Role of the funding source

261 Funders were not involved in the study design, collection, analysis, or interpretation
 262 of the data, writing, or decision to submit the paper for publication.

263 Results

264 Cohort derivation and description

265 In the Scottish cohort, 10545 FC and 49364 (9898 after preprocessing) CRP
 266 observations were available. In the Danish cohort, 67986 FC and 207141 (40648 after
 267 preprocessing) CRP observations were available. [Figure 1](#) outlines the derivation of
 268 the cohorts; [Table 1](#) describes key demographic factors. The distribution of log-
 269 transformed FC and CRP values is shown in [Figure S4](#).



270

271 *Figure 1. Derivation of the study cohorts based on separate faecal calprotectin (FC) and C-reactive*
 272 *protein (CRP) inclusion/exclusion criteria. A 7-year follow-up period was used for LIBDR, a 5-year*
 273 *follow-up period was used for the Danish cohort.*
 274

| | The Lothian IBD Registry | | | Danish national registry | | |
|---|---------------------------|----------------------------|----------------------|---------------------------|-----------------------------|-----------------------|
| | FC analysis (n = 1036) | CRP analysis (n = 1838) | Overlap (n = 808) | FC analysis (n = 7880) | CRP analysis (n = 10041) | Overlap (n = 5685) |
| Age at diagnosis | 33 (25–75) | 37 (24–55) | 32 (20–50) | 33 (22–53) | 38 (24–57) | 32 (22-52) |
| Male sex | 503 (48.6%) | 956 (52.0%) | 397 (49.1%) | 3648 (46.3%) | 4693 (46.7%) | 2594 (45.6%) |
| IBD type | | | | | | |
| Crohn's disease (CD) | 544 (52.5%) | 805 (43.8%) | 451 (55.8%) | 3931 (49.9%) | 4415 (44.0%) | 2954 (52.0%) |
| Ulcerative colitis (UC) | 380 (36.7%) | 847 (46.1%) | 276 (34.2%) | 3949 (50.1%) | 5626 (56.0%) | 2731 (48.0%) |
| IBDU | 112 (10.8%) | 186 (10.1%) | 81 (10.0%) | .. | .. | |
| Baseline FC (µg/g) | 740 (320–1070) | .. | 760 (330–1081) | 574 (148-1613) | .. | 652 (171-1737) |
| FC observations | 9 (6–13) | .. | 9 (6–14) | 7 (4–11) | .. | 8 (5-12) |
| Baseline CRP (µg/mL) | .. | 8 (3–24) | 8 (3–20) | .. | 12 (3-45) | 20 (3-38) |
| Total unprocessed CRP observations | .. | 20 (10–36) | 26 (14–36) | .. | 19 (9–32) | 22 (12-34) |
| Total CRP observations after pre-processing | .. | 6 (4–7) | 6 (5–7) | .. | 4 (3–5) | 4 (3-5) |
| Advanced therapies (AT) | | | | | | |
| AT within follow-up for CD | 270 (49.6%) | 374 (46.5%) | | 2108 (53.6%) | 2246 (50.9%) | |
| AT within one year for CD | 129 (23.7%) | 167 (20.7%) | | 1517 (38.6%) | 1549 (35.1%) | |
| AT within follow-up for UC | 108 (28.4%) | 85 (10.0%) | | 1293 (32.7%) | 1702 (30.3%) | |
| AT within one year for UC | 42 (11.1%) | 35 (4.1%) | | 789 (20.0%) | 978 (17.4%) | |
| Crohn's disease | | | | | | |
| Montreal location | | | | | | |
| L1 | 168 (30.9%) | 249 (30.9%) | 136 (30.2%) | | | |

| | | | |
|------------------------------|---------------|-------------|-------------|
| L2 | 200 (36.8%) | 287 (35.7%) | 157 (34.8%) |
| L3 | 169 (31.1%) | 246 (30.6%) | 153 (33.9%) |
| Missing | 7 (1.3%) | 23 (2.9%) | 5 (1.1%) |
| Upper GI inflammation | | | |
| Present | 77 (14.2%) | 87 (10.8%) | 68 (15.1%) |
| Not Present | 467 (85.8.4%) | 718 (89.2%) | 383 (84.9%) |
| Montreal behaviour | | | |
| B1 | 443 (81.4%) | 607 (75.4%) | 364 (80.7%) |
| B2 | 63 (11.5%) | 110 (13.7%) | 54 (12.0%) |
| B3 | 28 (5.1%) | 61 (7.6%) | 25 (5.5%) |
| Missing | 10 (1.8%) | 27 (3.4%) | 8 (1.8%) |
| Perianal disease | | | |
| Present | 79 (14.5%) | 113 (14.0%) | 68 (15.1%) |
| Not Present | 459 (84.4%) | 673 (83.6%) | 379 (84.0%) |
| Missing | 6 (1.1%) | 19 (2.4%) | 4 (0.9%) |
| Smoking status | | | |
| Current or previously | 166 (30.5%) | 274 (34.0%) | 138 (30.6%) |
| Never | 352 (64.7%) | 484 (60.1%) | 293 (65.0%) |
| Missing | 26 (4.8%) | 47 (5.8%) | 20 (4.4%) |
| Ulcerative colitis | | | |
| Montreal extent | | | |
| E1 | 50 (13.2%) | 155 (18.3%) | 27 (9.8%) |
| E2 | 155 (40.8%) | 330 (39.0%) | 111 (40.2%) |
| E3 | 170 (44.7%) | 341 (40.3%) | 133 (48.1%) |

| | | | |
|-----------------------|-------------|-------------|-------------|
| Missing | 5 (1.3%) | 21 (2.5%) | 5 (1.8%) |
| Smoking status | | | |
| Current or previously | 121 (31.8%) | 336 (39.7%) | 89 (32.2%) |
| Never | 237 (62.4%) | 444 (52.4%) | 167 (60.5%) |
| Missing | 22 (5.8%) | 67 (7.9%) | 20 (7.2%) |

275 *Table 1. Demographic and clinical data at diagnosis for subjects meeting the faecal calprotectin (FC)*
 276 *or C-reactive protein (CRP) study inclusion criteria. Continuous data are presented as median and*
 277 *interquartile range. Categorical data are presented as counts and percentages. Missingness is only*
 278 *directly reported if values were missing. The column labelled as “Overlap” denotes subjects which met*
 279 *the inclusion criteria for both FC and CRP modelling. Missing observations for upper gastrointestinal*
 280 *inflammation were assumed to be “not present” (Supplementary Note 1). Missingness was not*
 281 *inferred to be a value for any other variable. There are no IBDU diagnoses reported for the Danish*
 282 *cohort as these were mapped to either CD or UC (Supplementary Note 1).*

283 Modelling of FC trajectories

284 For the LIBDR cohort, AIC suggested the 10-cluster model ([Figure S5](#)), whilst BIC
 285 suggested the 9-cluster model ([Figure S6](#)) was most appropriate ([Table S1](#), [Figure S7](#)
 286 [\(A\)](#)). However, the 8-cluster model was chosen as a parsimonious choice, as it
 287 captures the main observed longitudinal patterns without generating very small
 288 clusters (<50 individuals) which could be difficult to interpret.

289
 290 [Figure 2](#) (A) shows representative cluster profiles for the 8-cluster model in the Lothian
 291 population, ordered from lowest (FC1) to highest (FC8) cumulative inflammatory
 292 burden. FC2 (n=67; ~6%) represents low FC values throughout the whole observation
 293 period. Instead, FC1 (n=140; ~14%), FC3 (n=157; ~15%), and FC7 (n=244; ~24%)
 294 were characterised by initially high FC values (>250 µg/g) which decreased over time
 295 at different rates. Whilst FC1 exhibited a sharp decrease within the first year, the
 296 decrease was more gradual for FC3 and FC7, where FC was normalised (<250 µg/g)
 297 approximately around two and five years post diagnosis, respectively. Furthermore,

298 FC4 (n=103; ~10%), FC5 (n=67; ~6%) and FC6 (n=64; ~6%) captured relapsing and
299 remitting patterns of gastrointestinal inflammation. Finally, FC8 (n=194; ~19%)
300 represented individuals with consistently high FC values.

301
302 The 8-cluster model was then applied to the Danish data. Despite being a completely
303 independent analysis, using data from another healthcare system, and with a shorter
304 follow-up period, the shape of the cluster-specific trajectories largely matched those
305 found for the LIBDR cohort ([Figure 2](#) (B)). In particular, the same rapid remitters (FC1),
306 delayed remitters (FC3 and FC7), and non-remitters (FC8) clusters were observed.
307 The most marked difference is within the relapsing-remitting clusters (FC4-6), which
308 may be partly explained by the smaller size of these clusters in the LIBDR cohort. The
309 proportion of individuals allocated to each cluster differed between cohorts. For
310 example, whilst FC2 represented ~6.5% in the Scottish cohort, nearly one third of
311 patients (~30.1%) were assigned to FC2 in the Danish cohort.

312 Associations with respect to FC cluster assignments

313 Associations with respect to age, sex and IBD type were considered in both cohorts
314 with the relapsing-remitting clusters (FC4–6) grouped for ease of comparison. Effect
315 sizes were largely consistent between both cohorts ([Figures S8–S10](#)). The effect of
316 age differed across clusters ([Figure S8](#)), but this may be partially due to differences in
317 treatment between younger and older individuals. Males were more likely to be
318 assigned to the clusters with the highest inflammatory burden, FC7 and FC8 ([Figure](#)
319 [S9](#), [S10](#) and [S11](#)). IBD type was associated with cluster assignments ([Figure S12](#)).
320 For example, FC1 (rapid remitters) was enriched by patients with CD in both cohorts
321 (62.9% in LIBDR and 63.0% in the Danish data vs 50.9% and 45.6% respectively
322 elsewhere). However, whilst the relapsing-remitting clusters (FC4–6) mostly consists
323 of individuals with UC in the Danish cohort (87.7%), this was not the case for LIBDR.

324
325 For the LIBDR cohort, a similar analysis was performed after stratifying by IBD type
326 (UC and CD only) and considering additional phenotyping ([Figures S13–S19](#)). In most
327 cases, effect sizes were not statistically significant (in some cases this was due to low
328 counts and small cluster sizes). However, amongst patients with CD, those without
329 upper GI inflammation were more likely to be assigned to the clusters with the lowest

330 inflammatory burden, FC1 or FC2 (2.4% and 3.03% L4 vs 18.1% elsewhere; Figure
331 [S13](#)). Finally, UC patients with ulcerative proctitis were found to be less likely to be
332 assigned to FC3 (2.44% E1 versus 14.2% elsewhere; Figure [S19](#)).

333 FC cluster assignment and IBD therapy usage

334 In Scottish and Danish patients with CD, 23.7% and 38.6% received an advanced
335 therapy (AT) within one year of diagnosis, respectively ([Table 1](#)). This increased to
336 49.6% and 53.6% by the end of the observation period (seven and five years
337 respectively). For patients with UC, 11.1% and 20.0% received an AT within one year
338 of diagnosis, respectively for Scottish and Danish patients. This increased to 28.4%
339 and 32.7% by the end of the observation period. Overall AT rates and the distribution
340 of time to first AT were not homogeneous across clusters ([Figure 3](#)). For example,
341 whilst AT prescription rates in FC1 largely matched the overall FC cohort, prescriptions
342 were generally earlier in this cluster, especially in patients with CD. In both FC7 (the
343 very delayed remitting cluster) and in FC8 (the cluster with consistently high
344 inflammation levels), the cumulative AT rates for CD were high. By the end of follow-
345 up in Scotland and Denmark, 55.1% and 80.9% were on AT in FC7 and 56.8% and
346 56.7% in FC8. However, early prescriptions of AT were noticeably lower than in other
347 clusters including FC1.

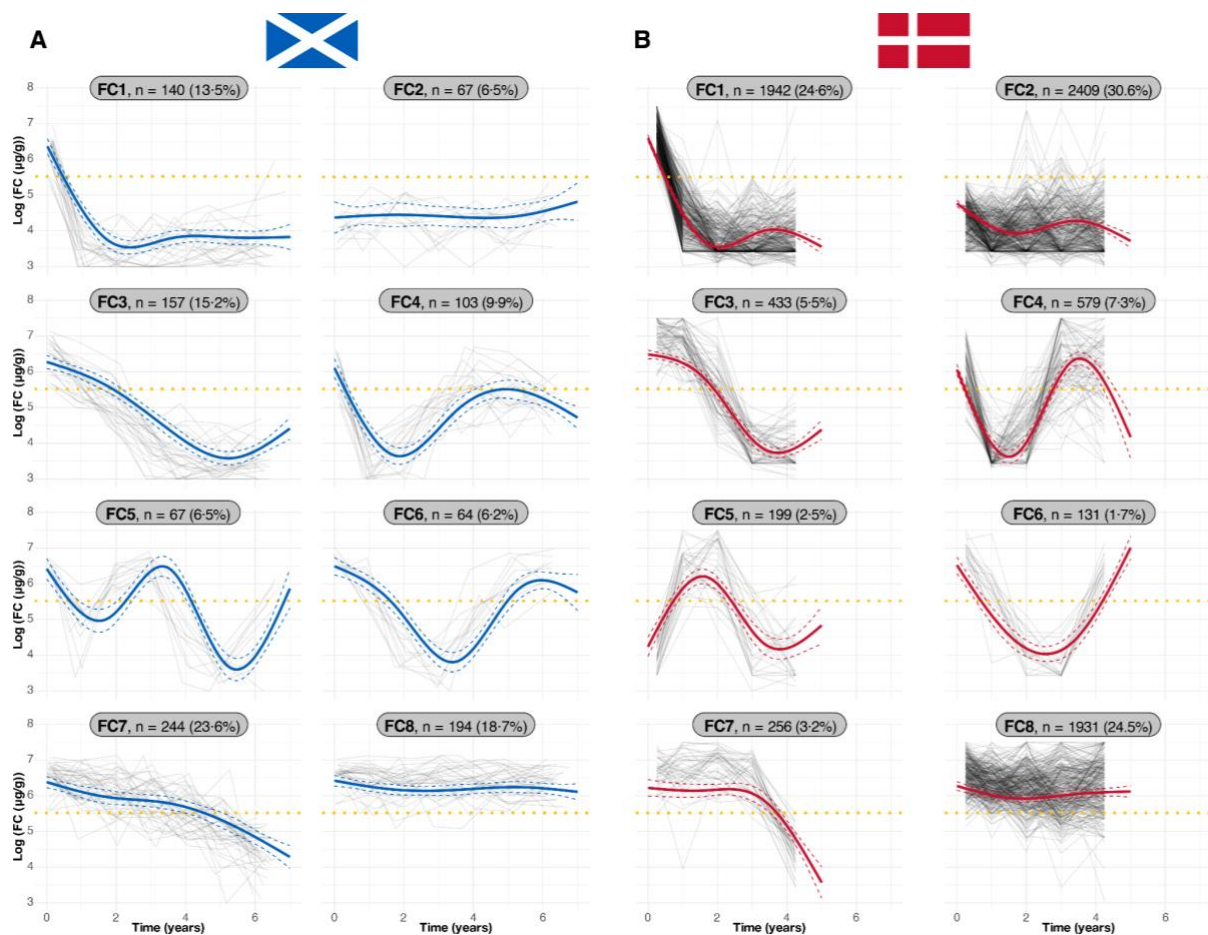
348

349 The detailed therapy data available from the Danish registries allows for a more
350 granular exploration of multiple lines of advanced therapy, immunosuppressant use
351 and courses of corticosteroids separately for CD ([Figure S34](#)) and UC ([Figure S35](#)).
352 In CD, FC1 is characterised by the early introduction of steroids, AT and
353 immunosuppressants, with therapy remaining remarkably stable throughout (no
354 additional lines of AT and no further courses of steroids). FC2 has the highest number
355 of patients not on AT after 1 (72.3%) and 5 years (62.5%). In FC3 (delayed remitters),
356 FC4 and FC6 (the two main relapsing remitting clusters for patients with CD), second,
357 third and fourth line AT prescriptions are noted along with multiple courses of
358 corticosteroids. These observations would be consistent with the challenges of treating
359 patients with IBD, where in some patients it takes time to find the right drug for the
360 right patient to induce deep remission, with multiple steroid courses used along the
361 way. A similar pattern is seen in FC7, where 25.5% had 3 or more different advanced

362 therapies, 23.7% had 5 or more steroid courses and 87.2% received an
363 immunomodulator within the five years. These are the largest numbers across all the
364 clusters, suggesting that multiple attempts are being made with different therapies to
365 control active disease with eventual success. In FC8, 29.3% and 13.1% of patients
366 had tried ≥ 2 and ≥ 3 different types of AT respectively, suggesting the persistently
367 elevated inflammation levels during follow-up are at least in part due to non-response
368 to multiple lines of therapy.

369 In patients with UC, FC2 has the highest percentage of patients without treatment,
370 FC1 is relatively stable over time, and FC8 has the highest percentage of multiple
371 types of treatment.

372 Surgical resections for patients with CD are shown in [Figure S36](#). It is noteworthy that
373 some of the patients assigned to a delayed remitting group (FC3 and FC7) were having
374 surgical resections later in follow-up. Colectomy rates in UC were overall very low
375 ([Figure S37](#)), but not evenly distributed with higher rates in those clusters with higher
376 cumulative inflammatory burdens (10.5% in FC8 compared to 2.8% and 1.4% in FC1
377 and FC2).



378

379

380 *Figure 2. Cluster trajectories obtained from LCMM assuming eight clusters fitted to FC data (log-*
 381 *transformed) in (A) the Lothian IBD Registry and (B) Danish national registry data. The blue and red*
 382 *lines indicate predicted mean cluster profiles with 95% confidence intervals for the Lothian IBD*
 383 *Registry and Danish data respectively. The yellow dotted lines indicate log(250µg/g). For visualisation*
 384 *purposes, pseudo subject-specific trajectories have been generated by amalgamating observations*
 385 *from randomly selected groups of six subjects. Clusters are ordered from lowest (FC1) to highest*
 386 *(FC8) cumulative inflammatory burden in the Lothian data with Danish cluster labels chosen based on*
 387 *visual similarity to the former clusters. Cluster sizes are shown as panel titles.*

388 Modelling of CRP trajectories

389 AIC and BIC both suggested the 8-cluster model was the most appropriate ([Table S2](#))
 390 for the LIBDR cohort. Visual inspection supported this finding as the 9-cluster model
 391 did not identify new trajectories when compared to the 8-cluster model, producing two
 392 trajectories with consistently low CRP ([Figure S20](#)). In contrast, the 7-cluster model
 393 ([Figure S21](#)) lacks one of the clinically interesting trajectories, characterised by an

394 initially elevated CRP which then decreases to slightly above biochemical remission
395 after one year, when compared to the 8-cluster model.

396

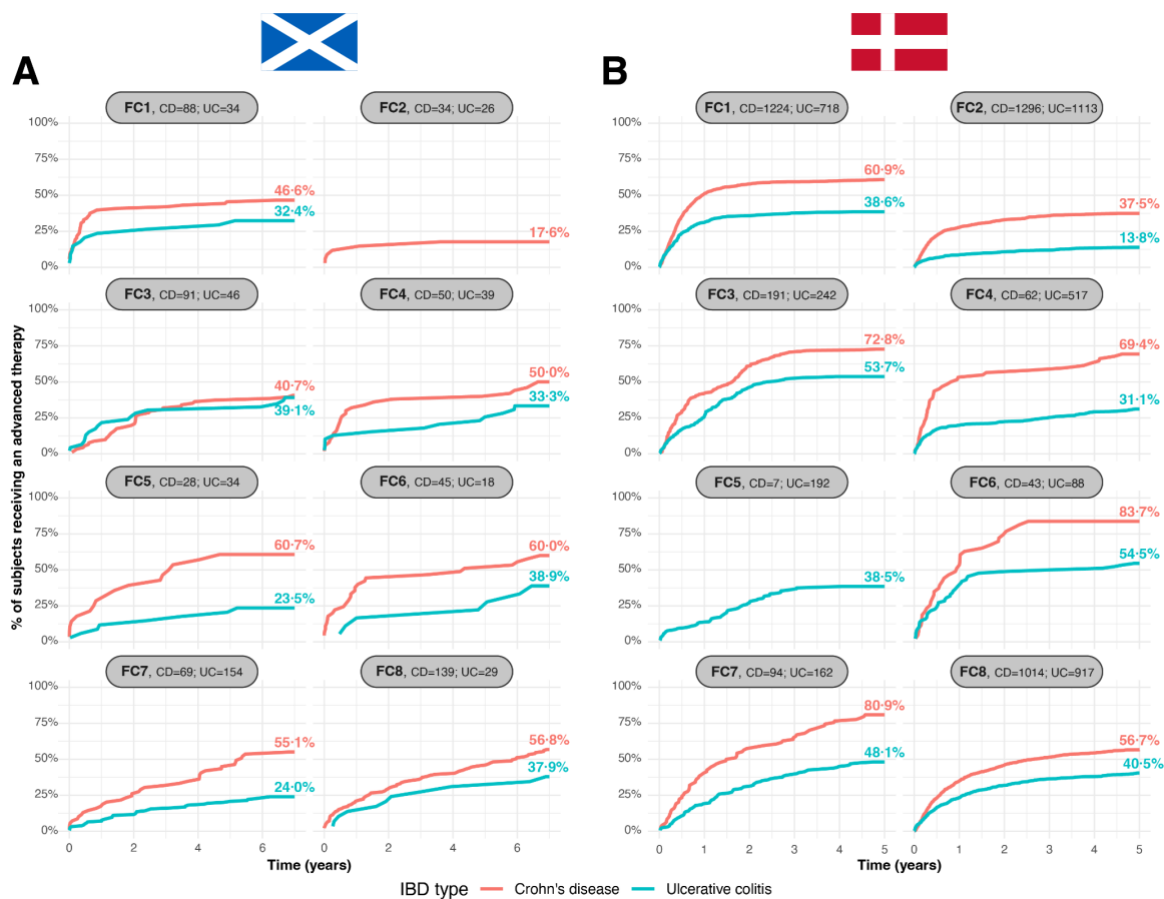
397 [Figure 4](#) (A) presents exemplar cluster profiles for the 8-cluster model. Over a third of
398 subjects (n=702; ~38%) were assigned to CRP1, defined by consistently low CRP (<
399 5µg/mL). CRP2 (n=225; ~12%) was characterised by high CRP at diagnosis which
400 rapidly decreased shortly thereafter remaining low. CRP3 (n=51; ~3%) and CRP4
401 (n=60; ~3%) are both small clusters with the former described by low CRP until the
402 last year of follow-up and the latter presenting low inflammation within the first year
403 before increasing until the third year where the inflammation then decreases again.
404 CRP5 (n=110; 6%) is characterised by elevated CRP at diagnosis which then
405 decreases gradually over time. CRP6 (n=434; 24%) consists of trajectories which are
406 elevated at diagnosis which then falls slightly for the first two years after diagnosis,
407 remaining elevated across the remaining duration of follow-up. CRP8 (n=172; 9%) is
408 consistently elevated and does not change over time. As in the FC analysis, the shape
409 of CRP clusters inferred for the LIBDR cohort was largely recapitulated when the 8-
410 cluster model was applied to the Danish cohort ([Figure 4](#) (B)).

411 Associations with CRP cluster assignments

412 Figures [S22–S24](#) visualise the distribution of age, sex and IBD type within each CRP
413 cluster. Results were largely consistent across the cohorts. Older patients were more
414 likely to be assigned to a CRP cluster with higher cumulative inflammatory burden
415 (Figure [S22](#)). IBD type was not evenly distributed among clusters ([Figure S24](#)), with
416 CRP1, CRP3, CRP4 and CRP7 enriched for UC patients (59.3%, 56.8%, 61.7% and
417 72.6% vs 32.3% elsewhere in LIBDR, with similar proportions for the Danish data. The
418 association plots for CD and UC disease sub-phenotypes and CRP cluster assignment
419 are shown in Figures [S25–S30](#).

420

421 AT prescribing patterns in CRP clusters are shown in [Figure S31](#).



422

423

424

425

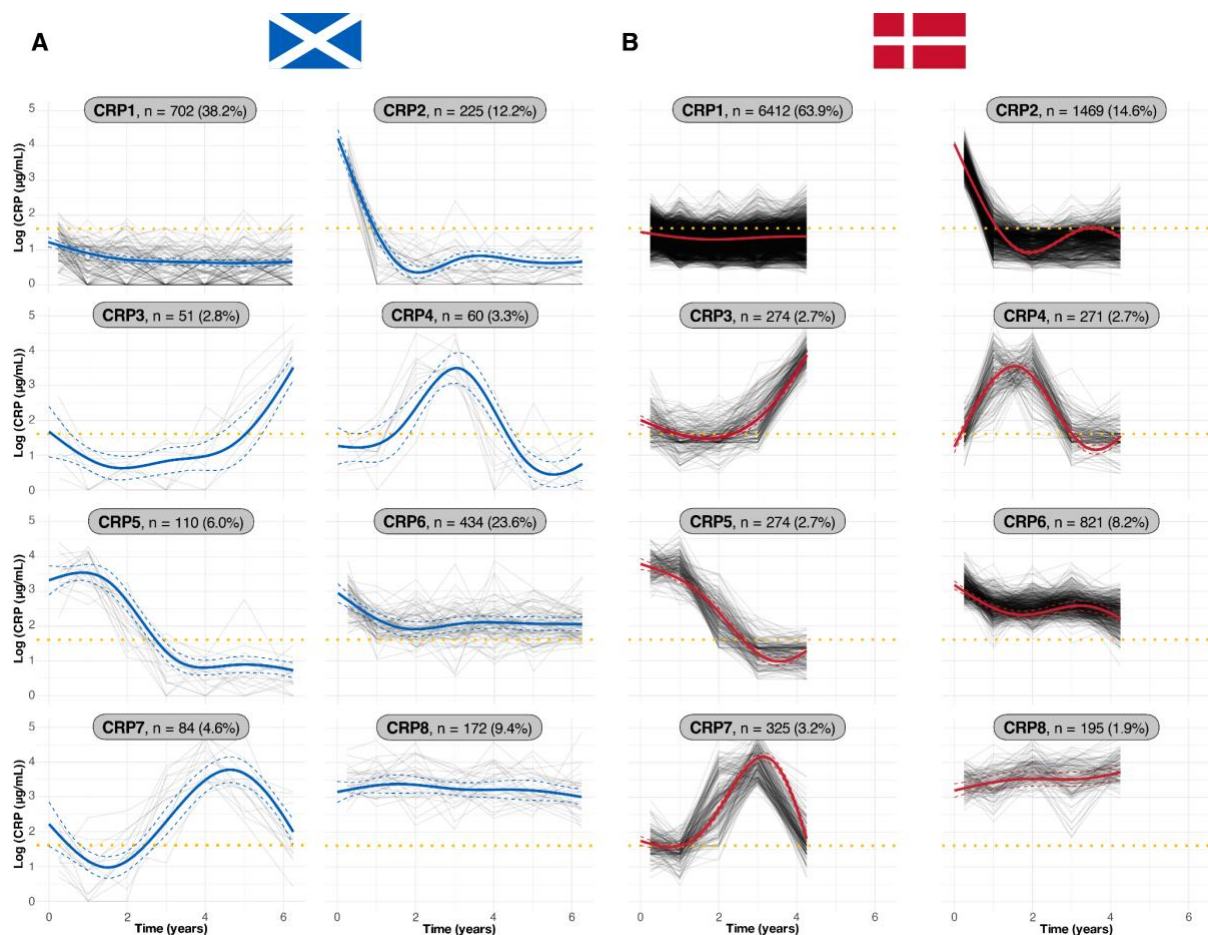
426

427

428

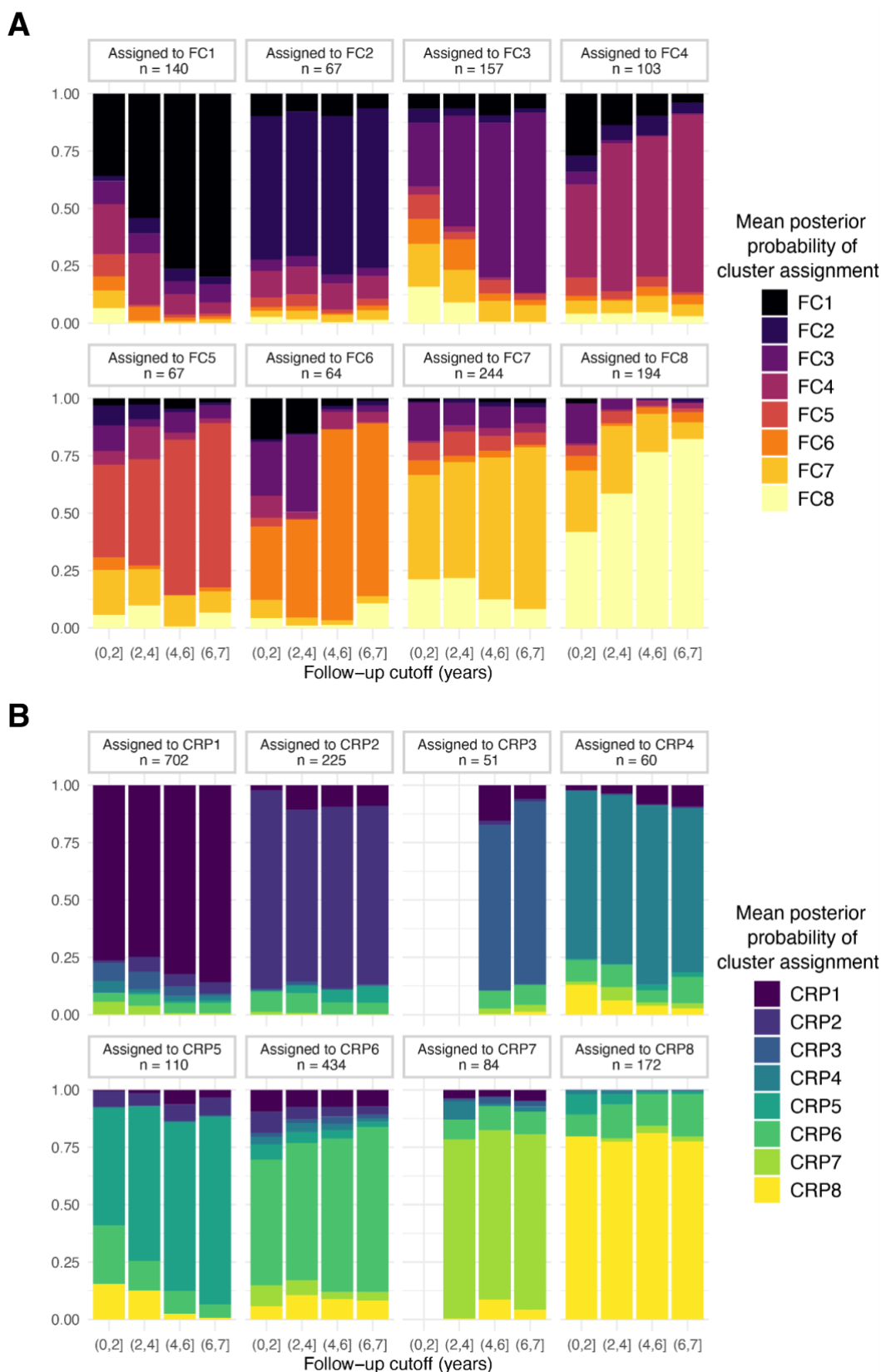
429

Figure 3. FC cluster-specific cumulative distribution for first-line advanced therapy prescribing for Crohn's disease (red) and ulcerative colitis (teal) subjects in (A) the Lothian IBD Registry and (B) national Danish registry data. Clusters are ordered from lowest (FC1) to highest (FC8) cumulative inflammatory burden. The number of CD and UC subjects present in each cluster is displayed as panel titles. Total advance therapy prescribing (as a percentage of the corresponding group) within seven/five years from diagnosis is shown next to each distribution curve. Curves which would describe fewer than ten subjects are not shown.



430
431
432
433
434
435
436
437

Figure 4. Cluster trajectories obtained from LCMM assuming eight clusters fitted to processed CRP data (log-transformed) for subjects in (A) the Lothian IBD Registry and (B) national Danish registry data. Blue and red lines indicate predicted mean cluster profiles with 95% confidence intervals. The yellow dotted lines indicate log(5 µg/mL). For visualisation purposes, pseudo subject-specific trajectories have been generated by amalgamating observations from randomly selected groups of six subjects. Clusters are ordered from lowest (CRP1) to highest (CRP8) cumulative inflammatory burden. Cluster sizes are shown as panel titles.



438
439
440
441
442

Figure 5. Exploration of cluster assignment uncertainty for A) faecal calprotectin (FC) and B) CRP clusters in the Lothian IBD Registry cohort. LCMM assigns individuals to the cluster with the highest estimated probability. For individuals assigned to a given cluster, bars show the average probability of cluster assignment to each possible cluster. Results are stratified according to follow-up length,

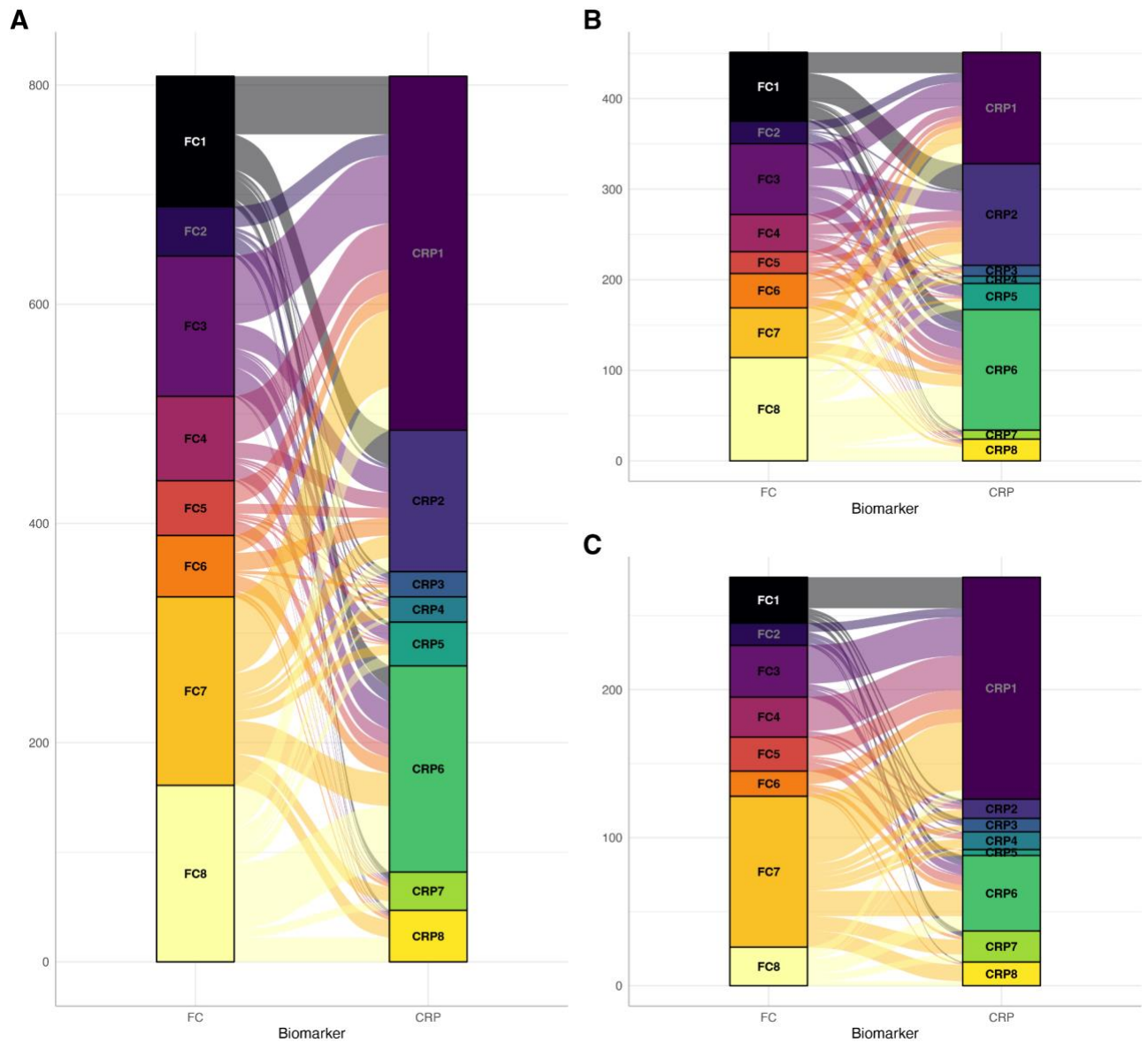
443 *defined as the time difference between diagnosis and the last available biomarker measurement (FC*
444 *or CRP for A) and B), respectively). Clusters are ordered from lowest (FC1 and CRP1) to highest*
445 *(FC8 and CRP8) cumulative inflammatory burden, with adjacent clusters coloured sequentially in the*
446 *plots for FC (black to yellow) and CRP (blue to yellow).*

447 Uncertainty in cluster assignments

448 The relationship between the uncertainty in cluster assignments and follow-up length
449 was explored for the LIBDR cohort. In the FC analysis, with the exception of FC2,
450 cluster assignments were on average more uncertain for those with a short follow-up
451 ([Figure 5](#) (A)). This is particularly the case for FC clusters that share similar earlier
452 trends. For example, individuals assigned to FC1 (rapid remitters) had a low average
453 probability of being assigned to FC8 (non-remitters) and vice-versa, even for those
454 with a short follow-up. This is not the case for FC3 and FC6, both of which capture
455 similar FC trajectories within the first two years. Indeed, those assigned to FC6 with
456 less than two years of follow-up also have, on average, a high probability of being
457 assigned to FC3. On average, cluster assignments were less uncertain in the CRP
458 analysis, even for individuals with a short follow-up ([Figure 5](#) (B)). This is expected as
459 CRP clusters are associated with more distinct early trajectories.

460 Comparison of FC and CRP clustering

461 In the LIBDR cohort, all FC clusters were well represented amongst the 808 subjects
462 included in both analyses (*overlap sub-cohort*), but the proportion in CRP8 was low
463 (~27% of CRP8 was in the overlap sub-cohort vs ~46% elsewhere; [Figure S32](#)). As
464 shown in [Figure 6](#) (A), there was low agreement between FC and CRP clustering in
465 the overlap sub-cohort (the same occurred in the Danish data, [Figure S33](#)). Whilst
466 most subjects in FC1 (71.6%) were also in CRP1 or CRP2, this relationship was not
467 mirrored as 81.2% of subjects in the latter two CRP clusters were assigned to
468 substantially different FC clusters. However, CRP8 did overlap with elevated FC as
469 the majority of subjects in this cluster (80.8%) were assigned to either FC7 or FC8.



470
471
472
473
474
475
476

Figure 6. Comparison between faecal calprotectin (FC) and processed CRP for models with chosen specification (three NCS) assuming eight clusters for subjects in the Lothian IBD Registry cohort. Results are reported based on the overlap cohort, consisting of 808 subjects included in both the FC and CRP analysis. (A) all subjects; (B) Crohn's disease; and (C) ulcerative colitis. Each segment denotes the size of the cluster whilst the alluvial segments connecting the nodes visualises the number of subjects shared between clusters.

477 Discussion

478 We have characterised IBD behaviour using long-term longitudinal trends of objective
479 inflammatory markers routinely collected for clinical care. Our analysis has uncovered
480 eight clusters with distinct inflammatory profiles based on FC and CRP, respectively.
481 This was replicated in two independent cohorts, one based in Scotland (Lothian) and

482 one in Denmark (nationwide). Our data highlights the heterogeneity of the disease
483 course, and presents a novel approach for understanding real-world inflammatory
484 activity patterns in IBD patients. For the first time, we are capturing the dynamic nature
485 of the disease in a more biologically nuanced way than traditional behaviour endpoints
486 such as treatment escalation, surgery and “Montreal progression”. This represents a
487 marked shift from the traditional symptom-based behaviour profiles exemplified by the
488 IBSEN cohorts over a decade ago.^{10,11}

489

490 This study builds on our earlier proof-of-concept work, where we first demonstrated
491 the feasibility of using long-term individualised profiles of FC to cluster IBD patients
492 with CD.¹⁷ In our previous analysis of Lothian patients, we identified four distinct FC
493 clusters: one cluster with persistently high FC (non-remitters) and three clusters with
494 different downward longitudinal trends. Here, we expand upon this by considering a
495 substantially larger Lothian IBD cohort (FC cohort, n=1036; CRP cohort, n=1838), with
496 longer follow-up, not excluding patients based on indicators of disease severity, and
497 also including patients with UC or IBDU. In addition, we modelled CRP. This has
498 generated results with greater representativeness across IBD phenotypes, uncovering
499 more granular structure with eight distinct FC clusters rather than four. Whilst the
500 modelling suggested further partitioning of the FC data was possible ([Figure S5](#),
501 [Figure S7 \(A\)](#)), we selected the eight-cluster model as a parsimonious choice that
502 captured the key inflammatory patterns ([Figure 2](#)). Notably, the CRP data also
503 partitioned into eight distinct clusters. Together, the clusters broadly fall into four
504 patterns of inflammatory behaviour mirroring those recognised by gastroenterologists
505 managing IBD patients (i) rapid remitters (FC1 and CRP2), (ii) delayed remitters (FC3,
506 FC7 and CRP5), (iii) relapsing-remitters (FC4–6 and CRP4 and CRP7), and (iv) non-
507 remitters (FC8 and CRP6 and CRP8). These classifications provide new insights into
508 the inflammatory course of IBD patients.

509

510 Critically, replication in two independent IBD cohorts demonstrates the robustness of
511 our findings, indicating that the longitudinal patterns described above characterise
512 inherent properties of the disease course. Both cohorts represent real-world IBD
513 populations with complementary properties. The Danish cohort is larger (n = 7880 and
514 n = 10041 for FC and CRP, respectively), has nation-wide coverage, and more
515 detailed treatment information (including primary care prescribing), but phenotyping is

516 more limited (e.g. no Montreal classification). Instead, LIBDR represents a single
517 Scottish health board and is more moderate in size (n = 1036 and n = 1838 for FC and
518 CRP, respectively), but has a longer longitudinal follow-up. Moreover, extensive data
519 curation provides more accurate diagnostic data and additional phenotyping, helping
520 to understand how the clusters relate to well-established IBD classifications.

521
522 We observed broadly poor agreement between FC and CRP clusters, although there
523 was overlap amongst those at the varying ends of the inflammatory spectrum with FC1
524 and FC2 correlating with CRP1 and CRP2 (rapid remitters with low cumulative
525 inflammatory burden), and FC7 and FC8 correlating with CRP6-8 (non-remitters with
526 high cumulative inflammatory burdens). Broadly though, the lack of overlap between
527 the two is not surprising. CRP is a marker of systemic inflammation, whilst FC is more
528 specific for detecting inflammation at a mucosal level. Hence, why both biomarkers
529 are complimentary when monitoring patients with IBD. Studies have also shown that
530 a proportion of IBD patients will have lower CRP values at diagnosis,²² as is seen in
531 CRP1 which is significantly enriched for UC cases.

532
533 We observed several important observations regarding cluster assignment. All IBD
534 subtypes featured in each cluster, but cluster assignment was unevenly distributed
535 across IBD types (Figures [S12](#) and [S24](#)). In CD, although patients with L4 disease
536 were less represented in FC1 and FC2, there was no association with ileal versus
537 colonic disease location. Males were slightly overrepresented in the FC8 cluster, which
538 is characterised by persistently elevated values. Interestingly, in the recent SEXEII
539 study, they observed male patients with UC were more likely to have extensive colonic
540 involvement and abdominal surgery, which may account for this finding.²³ CRP cluster
541 membership was also associated with smoking and older age, with both more likely to
542 have higher inflammatory burdens.

543
544 Multiple lines of evidence, including the recent PROFILE study,²⁴ have clearly
545 demonstrated improved disease control and outcomes in Crohn's patients receiving
546 early AT. As such, we anticipated that the biggest driver of inflammatory patterns over
547 time would be AT and that this effect would be more pronounced in CD versus UC
548 especially given the era of our cohort. Indeed, rates of AT use were not homogenous
549 across clusters or IBD subtypes. Overall, in the FC LIBDR cohort, AT were used in

550 49.6% of CD patients of which 47.7% started AT in the first year. In FC1, similar rates
551 of AT were used for CD patients, however they were used earlier, suggesting their
552 positive benefit in rapidly inducing and maintaining remission. Rates of AT
553 prescriptions for patients with CD in FC8 (persistently high levels of inflammatory
554 behaviour) were similar, but started later in the disease course, which may have
555 negatively affected the ability to bring about remission of disease. This cluster may
556 also represent a more refractory group of patients, with a higher risk phenotype. Whilst
557 this may provide additional support for the use of early AT, a causal interpretation of
558 these effects is not possible in this study, which is based on observational data.
559 Additional work with alternative cohorts where treatment assignment is randomised is
560 planned.

561
562 Our study also highlights the importance of using a probabilistic approach to account
563 for uncertainty in cluster assignments. Indeed, we observed higher uncertainty for
564 subjects with a shorter longitudinal follow-up, particularly for FC clusters ([Figure 5](#)). In
565 such cases, we cannot confidently assign individuals to a specific cluster. Instead,
566 cluster assignment probabilities are sometimes evenly split across multiple clusters,
567 mostly between those with similar earlier behaviour and inflammatory burdens. This
568 effect is less prominent in CRP cluster assignments, partly due to the more distinct
569 early trajectories across CRP clusters. As such, we anticipate that a multivariate
570 approach which simultaneously considers other biomarkers of disease activity, such
571 as haemoglobin, albumin, and platelet count, may further increase the robustness of
572 cluster assignments. Such analysis may also consider pre-diagnostic biomarker
573 measurements, following the recent observations in Danish registry data,²⁵ as well as
574 metabolomics, genetics or microbiome data to inform cluster assignments.

575
576 Critically, this study is limited by the use of observational data. Beyond AT use, the
577 frequency and amount of biomarker measurements is likely to be higher for those with
578 a more severe disease, and very mild cases may be excluded from our cohort.
579 Moreover, FC and CRP clusters cannot be directly used in a prognostic way. Indeed,
580 future work is needed to assess associations between clusters and IBD related
581 complications (such as steroid use, hospitalisations and surgery) but also non-
582 conventional complications related to a high cumulative inflammatory burden, such as
583 major cardiovascular adverse events, neuropsychiatric illness, and malignancy. Such

584 analyses will ultimately support the development of a low cost clinical support tool to
585 help deliver precision medicine to patients with IBD.

586

587 Classifying patients by their inflammatory behaviour may better inform therapy
588 decisions, including timing of AT, as well as monitoring and follow-up requirements.
589 This is a paradigm shift in thinking about disease behaviour compared with the
590 previous symptom based profiles first reported by the IBSEN cohorts. Moreover, this
591 approach - rooted in data that is widely available in clinical settings²⁶ and probabilistic
592 modelling- paves the way for predictive analytics integrated into a clinical support tool
593 for population wide risk stratification and individual patient level prognostication and
594 treatment.

595 Data sharing statement

596 As the data collected for this study has been derived from unconsented patient data,
597 it is not possible to share subject-level data with external entities. Detailed summary
598 level data is available online at [https://vallejosgroup.github.io/IBD-Inflammatory-](https://vallejosgroup.github.io/IBD-Inflammatory-Patterns)
599 [Patterns](https://vallejosgroup.github.io/IBD-Inflammatory-Patterns). The code used to conduct the analysis is also publicly available
600 (<https://github.com/VallejosGroup/IBD-Inflammatory-Patterns>).

601 Analyses performed on the DK cohort is based on data from the Danish National
602 Health registries (<https://sundhedsdatastyrelsen.dk>). It is protected by the Danish Act
603 on Processing of Personal Data and access requires application to the Danish Data
604 Protection Agency and the Danish Health Data Authority. In addition, data handling
605 must be carried out by a Danish institution.

606 Author contributions

607 CAV, CWL, and NCC were involved in conceptualising the study. CRB, SO, ATE, GRJ,
608 and NP curated the LIBDR data. NCC and CAV implemented computer code, tested
609 existing code components, and conducted the formal analysis and visualisation for the
610 LIBDR. TJ obtained funding for and built the Danish PREDICT data infrastructure on
611 which the Danish analyses were performed. MVV curated the Danish data and
612 conducted the validation analyses and visualization on the Danish data. The original
613 draft was written by NCC, NP, ATE, CMR, MVV, CWL and CAV with all authors

614 involved in reviewing and editing the manuscript. KMG, CWL, CAV, AS and TJ
615 provided supervisory support.

616 Competing interests

617 NP has served as a speaker for Janssen, Takeda and Pfizer. BG has acted as
618 consultant to Galapagos and Abbvie and as speaker for Abbvie, Jansen, Takeda,
619 Pfizer and Galapagos. GRJ has served as a speaker for Takeda, Janssen, Abbvie,
620 Fresenius and Ferring. TJ has served as a speaker and/or consultant for Ferring and
621 Pfizer. CWL has acted as a speaker and/or consultant to AbbVie, Janssen, Takeda,
622 Pfizer, Galapagos, GSK, Gilead, Vifor Pharma, Ferring, Dr Falk, BMS, Boehringer
623 Ingelheim, Eli Lilly, Merck, Novartis, Sandoz, Celltrion, Cellgene, Amgen, Samsung
624 Bioepis, Fresenius Kabi, Tillotts, Kuma Health, Trelus Health and Iterative Health.
625 None of the other authors report any conflicts of interest.

626 Funding

627 CWL is funded by a UKRI (UK Research and Innovation) Future Leaders Fellowship
628 'Predicting outcomes in IBD' (MR/S034919/1). G-RJ is funded by a Wellcome Trust
629 Clinical Research Career Development Fellowship. NC-C was partially supported by
630 the Medical Research Council and The University of Edinburgh via a Precision
631 Medicine PhD studentship (MR/N013166/1). MVV, AS, and TJ are funded by a Center
632 of Excellence Grant (DNRF148) to TJ from the Danish National Research Foundation.

633 Acknowledgements

634 This work uses data provided by patients and collected by the NHS as part of their
635 care and support. The Lothian component of this work has made use of the
636 resources provided by the Edinburgh Compute and Data Facility (ECDF). The
637 analysis of the Danish cohort was performed using the National Genome Center
638 platform.

639 References

640

641 1. Jones GR, Lyons M, Plevris N, et al. IBD prevalence in Lothian, Scotland, derived
642 by capture–recapture methodology. *Gut*. 2019;68(11):1953-1960.

- 643 doi:10.1136/gutjnl-2019-318936
- 644 2. Hamilton B, Green H, Heerasing N, et al. Incidence and prevalence of
645 inflammatory bowel disease in Devon, UK. *Frontline Gastroenterol.*
646 2021;12(6):461-470. doi:10.1136/flgastro-2019-101369
- 647 3. Cushing K, Higgins PDR. Management of Crohn disease: A review. *JAMA.*
648 2021;325(1):69. doi:10.1001/jama.2020.18936
- 649 4. Gros B, Kaplan GG. Ulcerative colitis in adults: A review. *JAMA.*
650 2023;330(10):951. doi:10.1001/jama.2023.15389
- 651 5. Zhou RW, Harpaz N, Itzkowitz SH, Parsons RE. Molecular mechanisms in colitis-
652 associated colorectal cancer. *Oncogenesis.* 2023;12(1):48. doi:10.1038/s41389-
653 023-00492-0
- 654 6. Kennedy NA, Jones GR, Plevris N, Patenden R, Arnott ID, Lees CW. Association
655 between level of fecal calprotectin and progression of Crohn's disease. *Clin*
656 *Gastroenterol Hepatol.* 2019;17(11):2269-2276.e4. doi:10.1016/j.cgh.2019.02.017
- 657 7. Plevris N, Fulforth J, Lyons M, et al. Normalization of fecal calprotectin within 12
658 months of diagnosis is associated with reduced risk of disease progression in
659 patients with Crohn's disease. *Clin Gastroenterol Hepatol.* 2021;19(9):1835-
660 1844.e6. doi:10.1016/j.cgh.2020.08.022
- 661 8. Verstockt B, Noor NM, Marigorta UM, et al. Results of the Seventh Scientific
662 Workshop of ECCO: Precision medicine in IBD—Disease outcome and response
663 to therapy. *J Crohns Colitis.* 2021;15(9):1431-1442. doi:10.1093/ecco-jcc/jjab050
- 664 9. Alatab S, Sepanlou SG, Ikuta K, et al. The global, regional, and national burden of
665 inflammatory bowel disease in 195 countries and territories, 1990–2017: A
666 systematic analysis for the Global Burden of Disease Study 2017. *Lancet*
667 *Gastroenterol Hepatol.* 2020;5(1):17-30. doi:10.1016/S2468-1253(19)30333-4
- 668 10. Solberg IC, Vatn MH, Høie O, et al. Clinical course in Crohn's disease:
669 Results of a Norwegian population-based ten-year follow-up study. *Clin*
670 *Gastroenterol Hepatol.* 2007;5(12):1430-1438. doi:10.1016/j.cgh.2007.09.002
- 671 11. Solberg IC, Lygren I, Jahnsen J, et al. Clinical course during the first 10 years
672 of ulcerative colitis: Results from a population-based inception cohort (IBSEN
673 Study). *Scand J Gastroenterol.* 2009;44(4):431-440.
674 doi:10.1080/00365520802600961
- 675 12. Peyrin-Biroulet L, Reinisch W, Colombel JF, et al. Clinical disease activity, C-
676 reactive protein normalisation and mucosal healing in Crohn's disease in the
677 SONIC trial. *Gut.* 2014;63(1):88-95. doi:10.1136/gutjnl-2013-304984
- 678 13. Silverberg MS, Satsangi J, Ahmad T, et al. Toward an integrated clinical,
679 molecular and serological classification of inflammatory bowel disease: Report of a
680 working party of the 2005 Montreal World Congress of Gastroenterology. *Can J*
681 *Gastroenterol Hepatol.* 2005;19:5A-36A. doi:10.1155/2005/269076
- 682 14. Lennard-Jones JE. Classification of inflammatory bowel disease. *Scand J*
683 *Gastroenterol.* 1989;24(sup170):2-6. doi:10.3109/00365528909091339
- 684 15. Sorlie P, Wei GS. Population-based cohort studies: Still relevant? *J Am Coll*
685 *Cardiol.* 2011;58(19):2010-2013. doi:10.1016/j.jacc.2011.08.020
- 686 16. Agrawal M, Christensen HS, Bøgsted M, Colombel JF, Jess T, Allin KH. The
687 rising burden of inflammatory bowel disease in Denmark over two decades: A
688 nationwide cohort study. *Gastroenterology.* 2022;163(6):1547-1554.e5.
689 doi:10.1053/j.gastro.2022.07.062
- 690 17. Constantine-Cooke N, Monterrubio-Gómez K, Plevris N, et al. Longitudinal
691 fecal calprotectin profiles characterize disease course heterogeneity in Crohn's
692 disease. *Clin Gastroenterol Hepatol.* 2023;21(11):2918-2927.e6.

- 693 doi:10.1016/j.cgh.2023.03.026
694 18. Proust-Lima C, Philipps V, Liquet B. Estimation of extended mixed models
695 using latent classes and latent processes: The R package lcmm. *J Stat Softw.*
696 2017;78(2):1-56. doi:10.18637/jss.v078.i02
697 19. Stoica P, Selen Y. Model-order selection: A review of information criterion
698 rules. *IEEE Signal Process Mag.* 2004;21(4):36-47.
699 doi:10.1109/MSP.2004.1311138
700 20. R Core Team. *R: A Language and Environment for Statistical Computing.* R
701 Foundation for Statistical Computing; 2022. <https://www.R-project.org/>
702 21. Clough J, Colwill M, Poullis A, Pollok R, Patel K, Honap S. Biomarkers in
703 inflammatory bowel disease: A practical guide. *Ther Adv Gastroenterol.*
704 2024;17:17562848241251600. doi:10.1177/17562848241251600
705 22. Henriksen M, Jahnsen J, Lygren I, et al. C-reactive protein: A predictive factor
706 and marker of inflammation in inflammatory bowel disease. Results from a
707 prospective population-based study. *Gut.* 2008;57(11):1518-1523.
708 doi:10.1136/gut.2007.146357
709 23. Gargallo-Puyuelo CJ, Ricart E, Iglesias E, et al. Sex-related differences in the
710 phenotype and course of inflammatory bowel disease: SEXEII study of ENEIDA.
711 *Clin Gastroenterol Hepatol.* 2024;22(11):2280-2290.
712 doi:10.1016/j.cgh.2024.05.013
713 24. Noor NM, Lee JC, Bond S, et al. A biomarker-stratified comparison of top-
714 down versus accelerated step-up treatment strategies for patients with newly
715 diagnosed Crohn's disease (PROFILE): A multicentre, open-label randomised
716 controlled trial. *Lancet Gastroenterol Hepatol.* 2024;9(5):415-427.
717 doi:10.1016/S2468-1253(24)00034-7
718 25. Vestergaard MV, Allin KH, Poulsen GJ, Lee JC, Jess T. Characterizing the
719 pre-clinical phase of inflammatory bowel disease. *Cell Rep Med.*
720 2023;4(11):101263. doi:10.1016/j.xcrm.2023.101263
721 26. Markowitz F. All models are wrong and yours are useless: Making clinical
722 prediction models impactful for patients. *Npj Precis Oncol.* 2024;8(1):54.
723 doi:10.1038/s41698-024-00553-6

724 Supplemental display items

725 Table of contents

726 Supplemental figures

- 727 • [Figure S1](#). Distribution of observation times for diagnostic FC
- 728 • [Figure S2](#). Distribution of observation times for diagnostic CRP
- 729 • [Figure S3](#). Illustration of how biomarker (faecal calprotectin or CRP)
730 observation times were adjusted based on time of diagnostic biomarker
731 observation

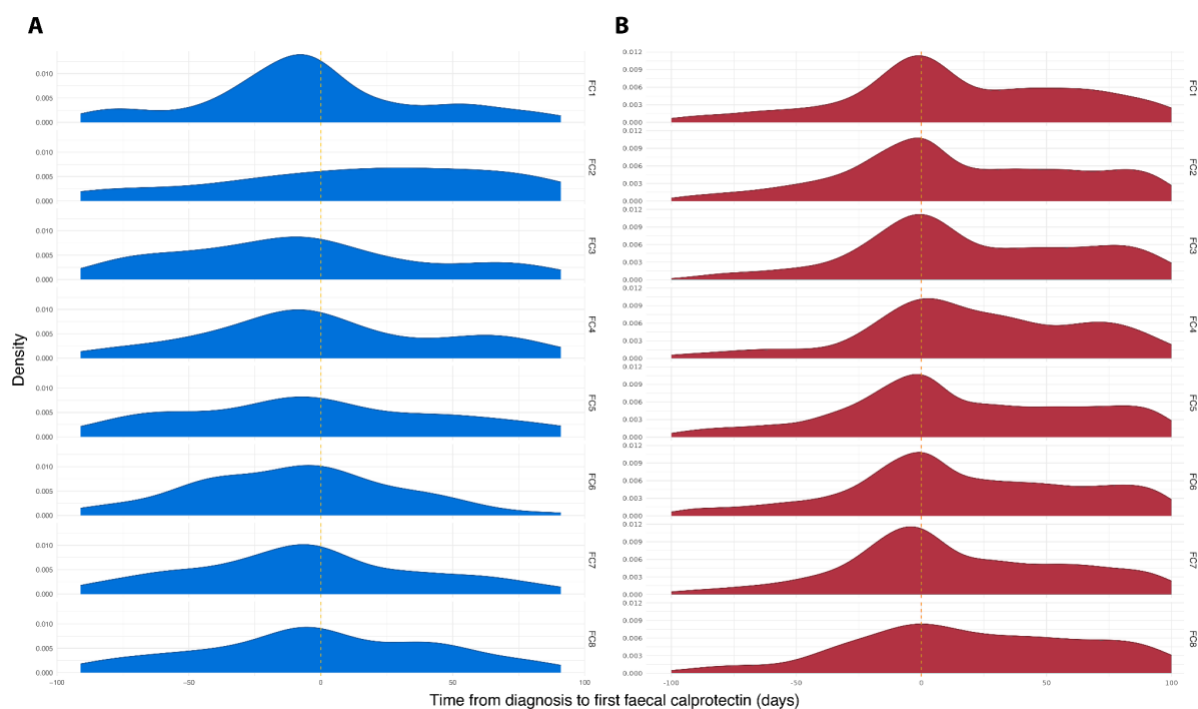
- 732 ● [Figure S4](#). Distribution of diagnostic biomarker measurements across the
- 733 LIBDR study cohort
- 734 ● [Figure S5](#). Cluster trajectories obtained from LCMM assuming ten clusters
- 735 fitted to FC LIBDR data
- 736 ● [Figure S6](#). Cluster trajectories obtained from LCMM assuming nine clusters
- 737 fitted to FC LIBDR data
- 738 ● [Figure S7](#). Alluvial plot visualising cluster assignment for the LIBDR cohort as
- 739 the number of assumed clusters increases
- 740 ● **Associations with FC cluster membership**
- 741 ○ [Figure S8](#). Age
- 742 ○ [Figure S9](#) Sex
- 743 ○ [Figure S10](#). IBD type
- 744 ○ [Figure S11](#). Smoking for CD subjects
- 745 ○ [Figure S12](#). Montreal location for CD subjects
- 746 ○ [Figure S13](#). L4 for CD subjects
- 747 ○ [Figure S14](#). Montreal behaviour for CD subjects
- 748 ○ [Figure S15](#). Perianal disease for CD subjects
- 749 ○ [Figure S16](#). Smoking for UC subjects
- 750 ○ [Figure S17](#). Montreal extent for UC subjects
- 751 ○ [Figure S18](#). Sex for UC subjects
- 752 ○ [Figure S19](#). Sex for CD subjects
- 753 ● [Figure S20](#). Cluster trajectories obtained from model assuming nine clusters
- 754 fitted to CRP LIBDR data
- 755 ● [Figure S21](#). Cluster trajectories obtained from model assuming seven clusters
- 756 fitted to CRP LIBDR data
- 757 ● **Associations with CRP cluster membership**
- 758 ○ [Figure S22](#). Age
- 759 ○ [Figure S23](#). Sex
- 760 ○ [Figure S24](#). IBD type
- 761 ○ [Figure S25](#). Smoking for CD subjects
- 762 ○ [Figure S26](#). Montreal location for CD subjects
- 763 ○ [Figure S27](#). L4 for CD subjects
- 764 ○ [Figure S28](#). Montreal behaviour for CD subjects
- 765 ○ [Figure S29](#). Smoking for UC subjects

- 766 ○ [Figure S30](#). Montreal extent for UC subjects
- 767 ● [Figure S31](#). Time to first-line advanced therapy by CRP cluster assignment
- 768 ● [Figure S32](#). Proportion of individuals included in the overlap cohort by FC and
- 769 CRP cluster assignment
- 770 ● [Figure S33](#). Comparison between FC and CRP cluster assignment in the
- 771 Danish cohort.

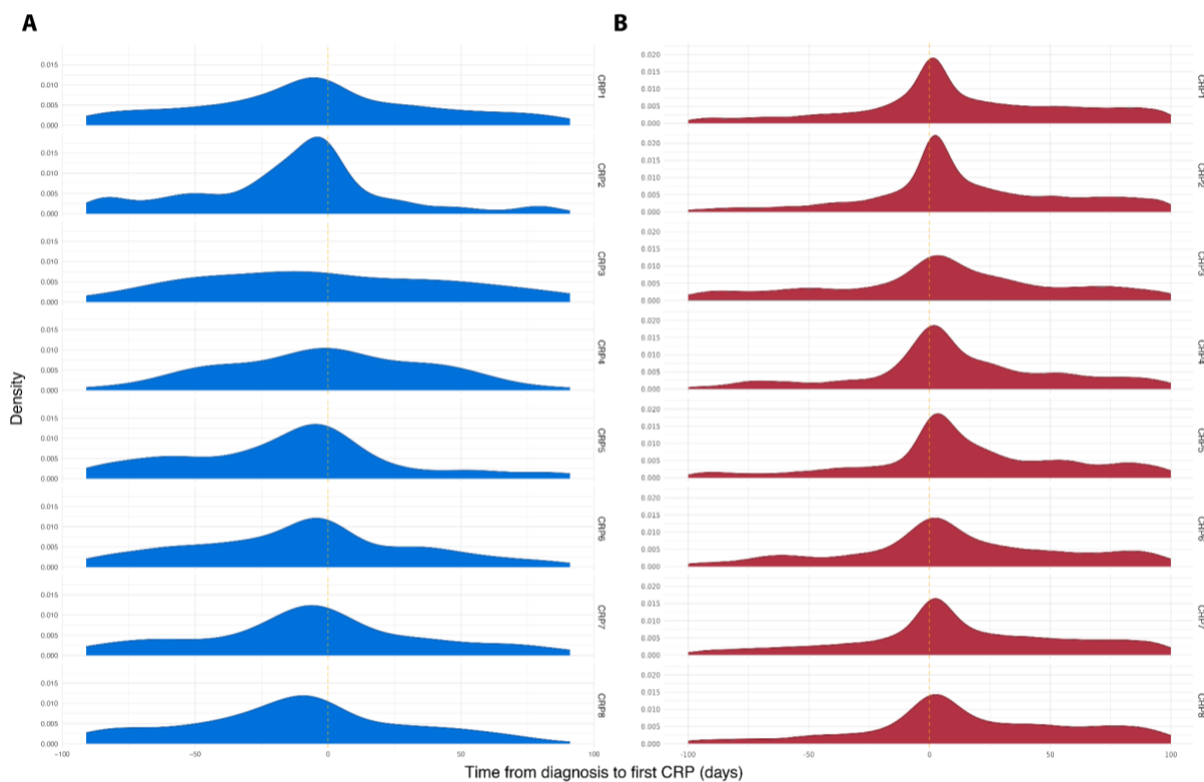
772 Supplemental tables

- 773 ● [Table S1](#). Model statistics for models fitted to FC data
- 774 ● [Table S2](#). Model statistics for models fitted to CRP data

775 Supplemental figures



776
777 *Figure S1. Distribution of observation times for diagnostic faecal calprotectin (FC) relative to reported*
778 *date of diagnosis for (A) the Lothian IBD registry cohort and (B) the Danish national registry cohort.*
779 *Stratified by FC cluster assignment. Diagnostic FC was defined as the first FC test within ± 90 days of*
780 *diagnosis.*

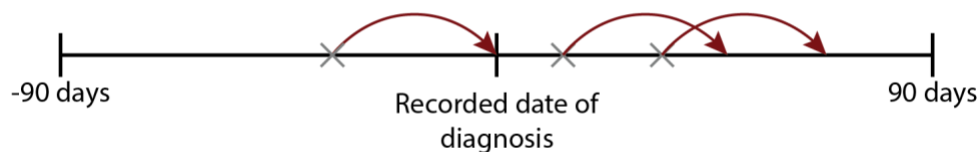


781
782
783
784
785

Figure S2. Distribution of observation times for diagnostic C-reactive protein (CRP) relative to reported date of diagnosis for (A) the Lothian IBD registry cohort and (B) the Danish national registry cohort. Stratified by CRP cluster assignment. Diagnostic CRP was defined as the first CRP test within ± 90 days of diagnosis.

Scenario 1:

First biomarker measurement within 90 days of reported date of diagnosis is *before* diagnosis



Biomarker observations are re-timed by the same amount so the first observation now corresponds to diagnosis

Scenario 2:

First biomarker measurement within 90 days of reported date of diagnosis is *after* diagnosis



Biomarker observations are not re-timed

786

787 *Figure S3. Illustration of how biomarker (faecal calprotectin or CRP) observation times were adjusted*
788 *depending on if the diagnostic observation was before or after the date of diagnosis recorded in*
789 *electronic health records.*

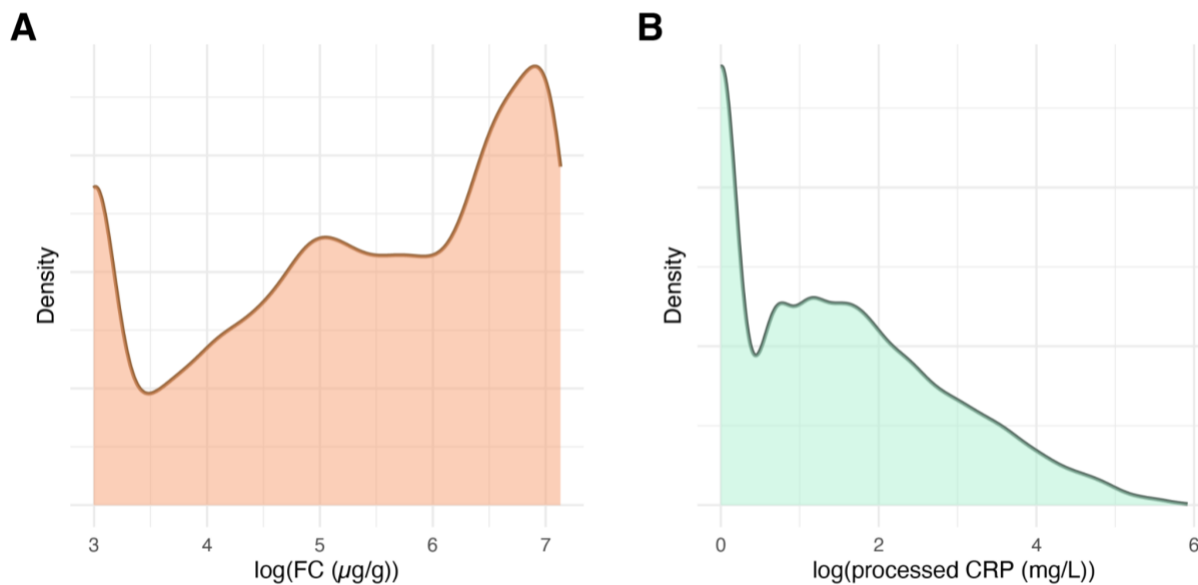
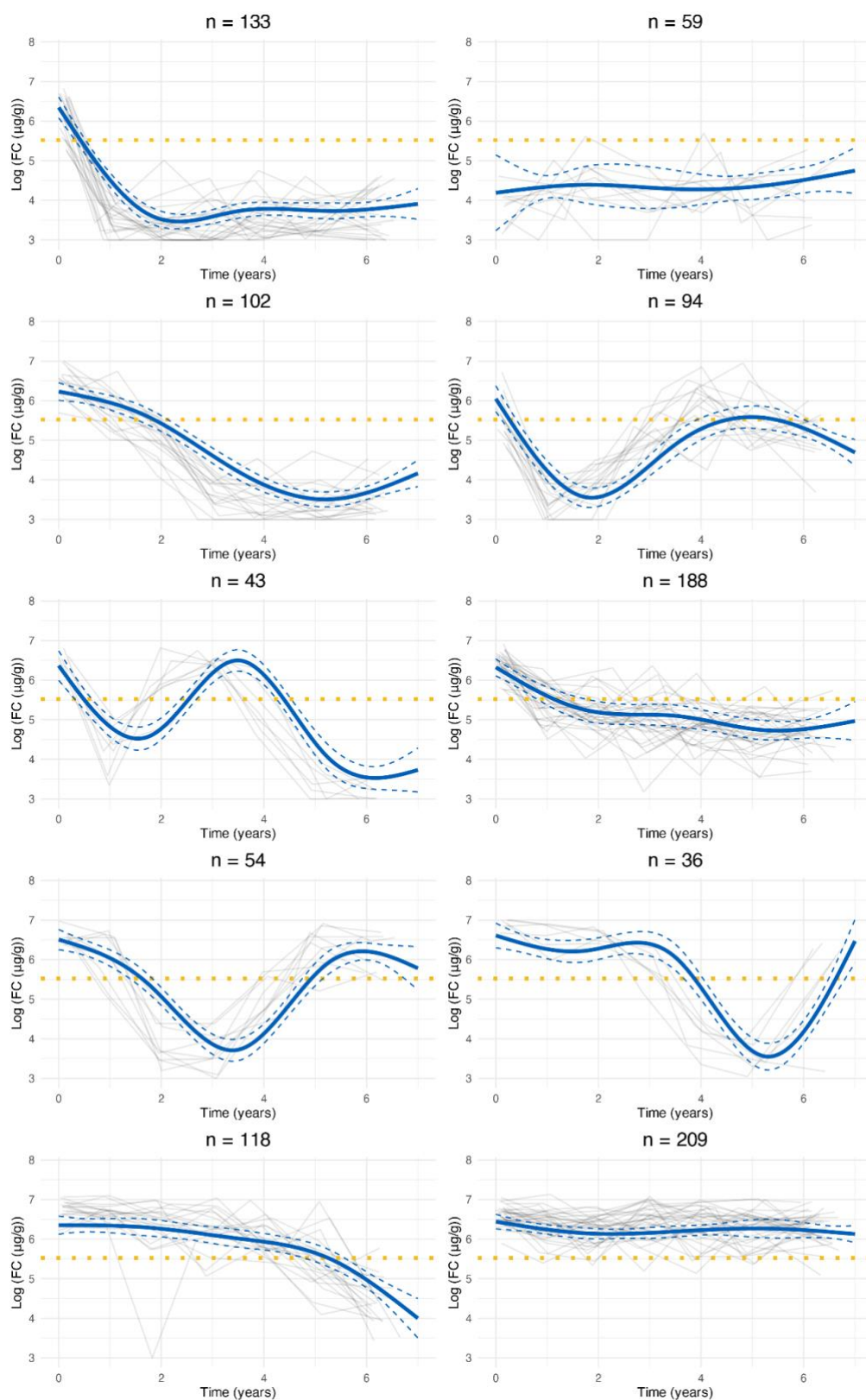
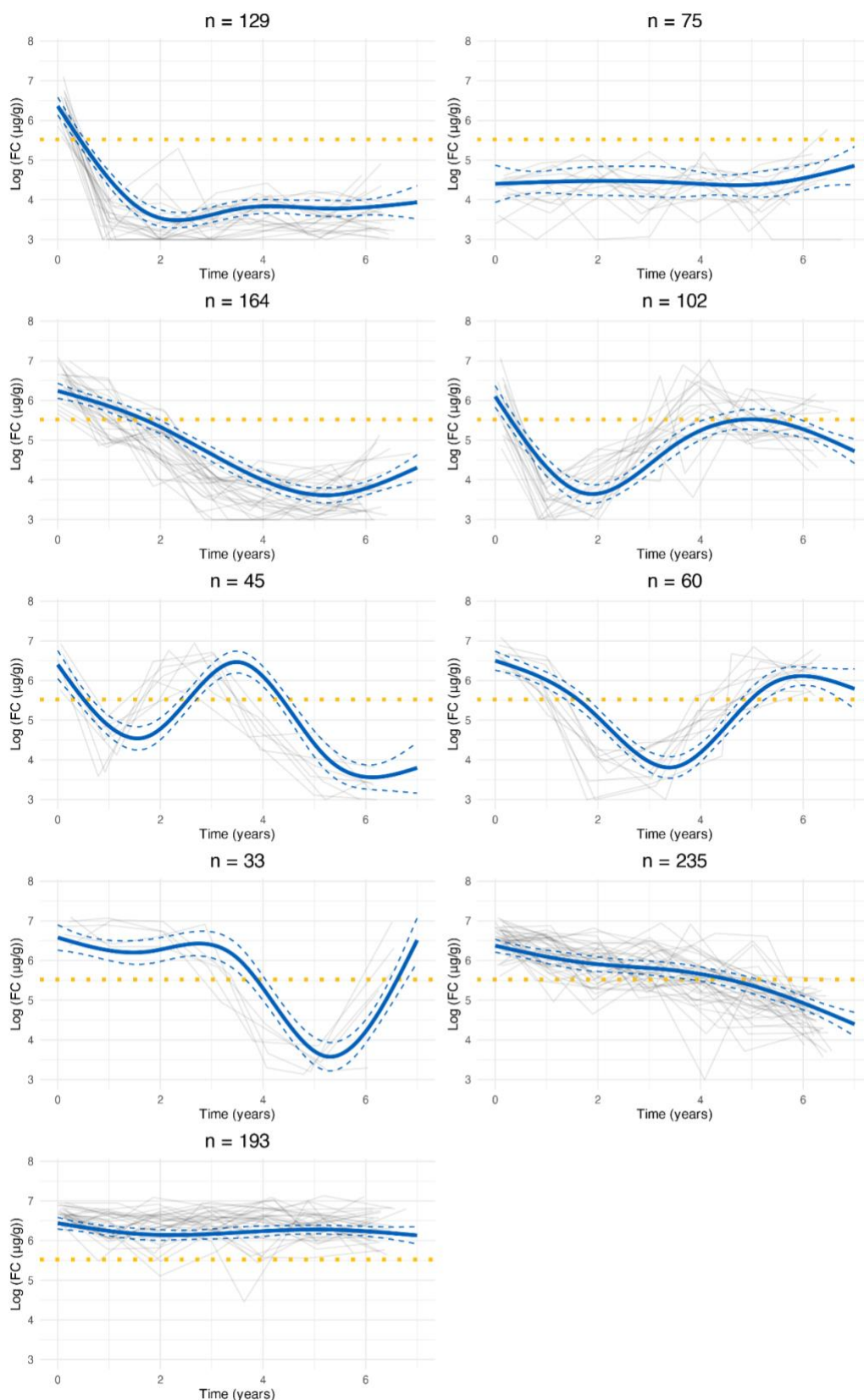


Figure S4. Distribution of diagnostic biomarker measurements across the LIBDR study cohort. (A) faecal calprotectin after applying a logarithmic transformation; (B) pre-processed (grouped into time intervals with the median used for multiple measurements) CRP after logarithmic transformation.



794
795
796
797
798
799

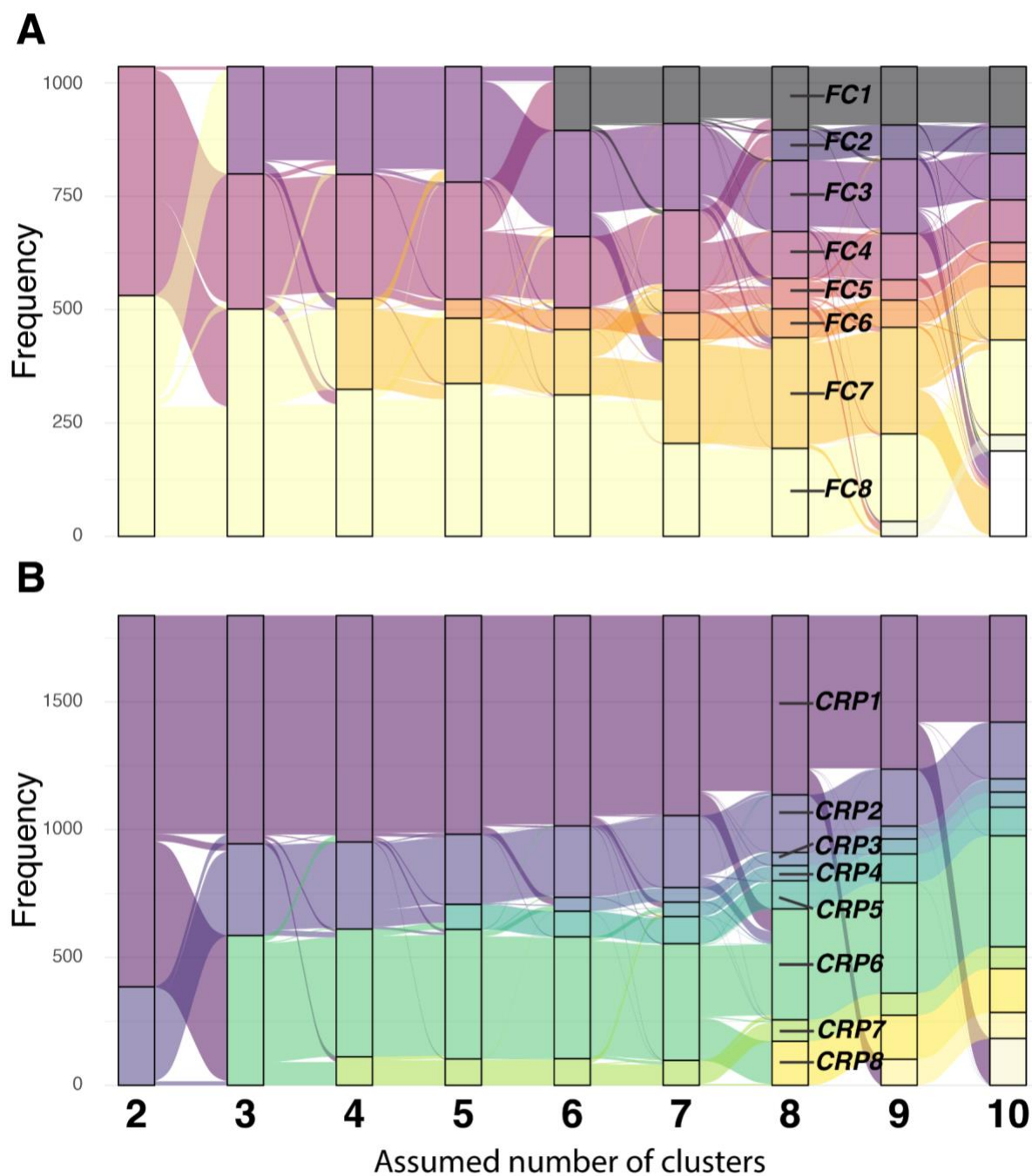
Figure S5. Cluster trajectories obtained from LCMM assuming ten clusters fitted to faecal calprotectin data in the Lothian IBD Registry. Red lines indicate predicted mean cluster profiles with 95% confidence intervals. Dotted horizontal lines indicate $\log(250\mu\text{g/g})$. For visualisation purposes, pseudo subject-specific trajectories have been generated by amalgamating observations from groups of six subjects.



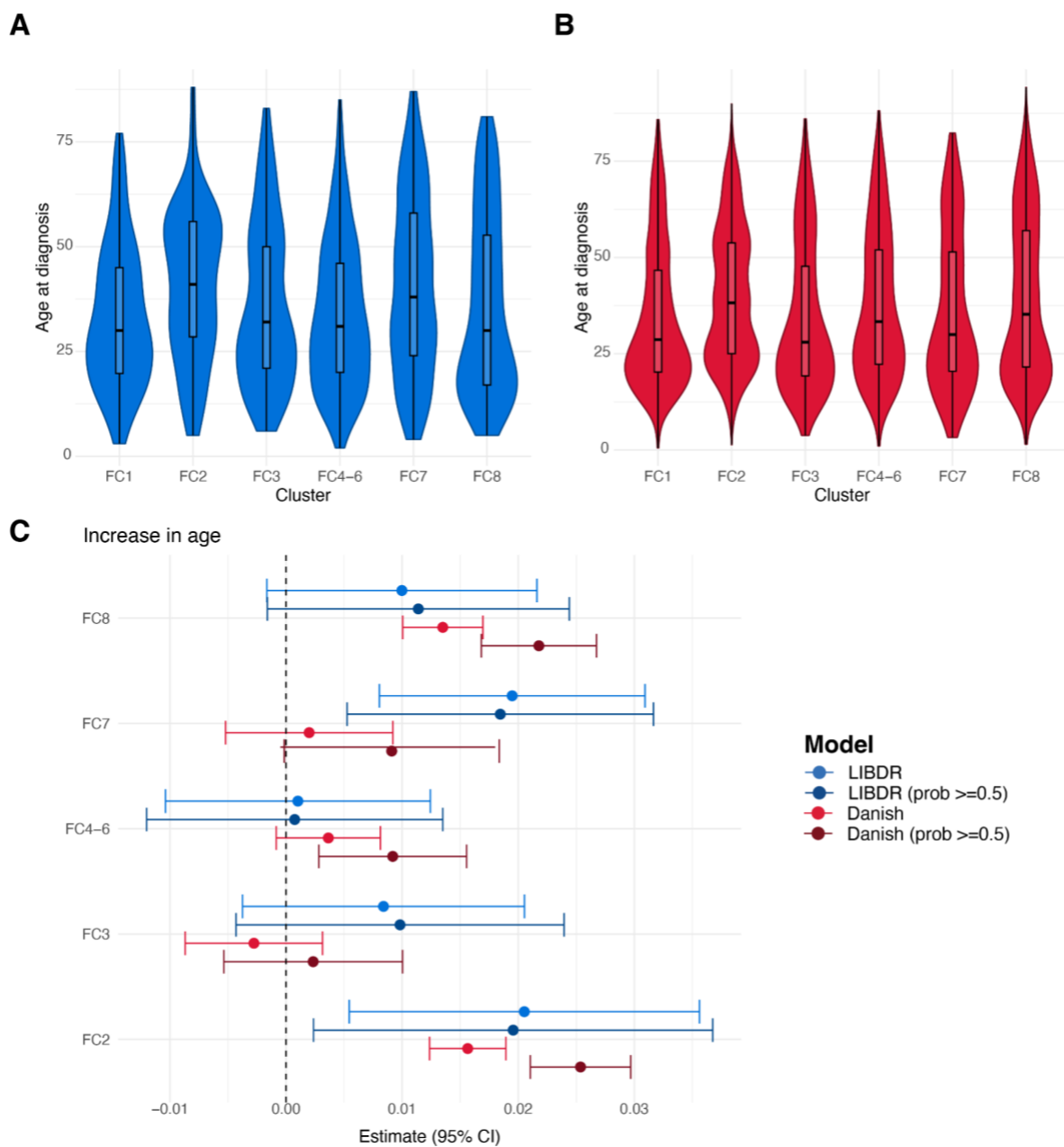
800
801
802
803

Figure S6. Cluster trajectories obtained from LCMM assuming nine clusters fitted to faecal calprotectin data in the Lothian IBD Registry. Red lines indicate predicted mean cluster profiles with 95% confidence intervals. Dotted horizontal lines indicate $\log(250\mu\text{g/g})$. For visualisation purposes,

804 *pseudo subject-specific trajectories have been generated by amalgamating observations from groups*
805 *of six subjects.*

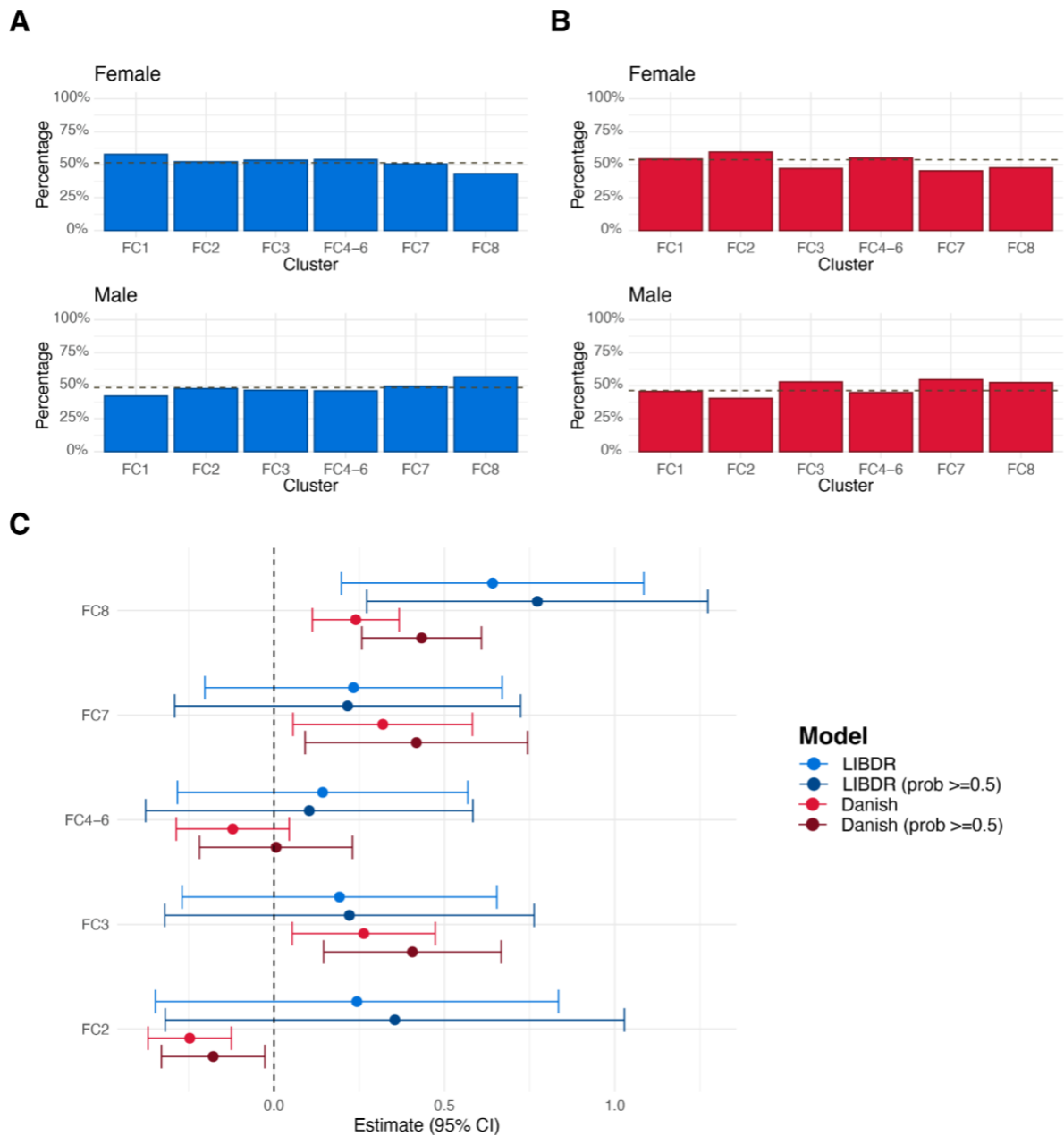


806
807 *Figure S7. Alluvial plot demonstrating how cluster assignment changes for the Lothian IBD registry*
808 *cohort as the number of assumed clusters increases for the chosen models for (A) faecal calprotectin*
809 *and (B) C-reactive protein. The clusters found by the 8-cluster models are labelled.*



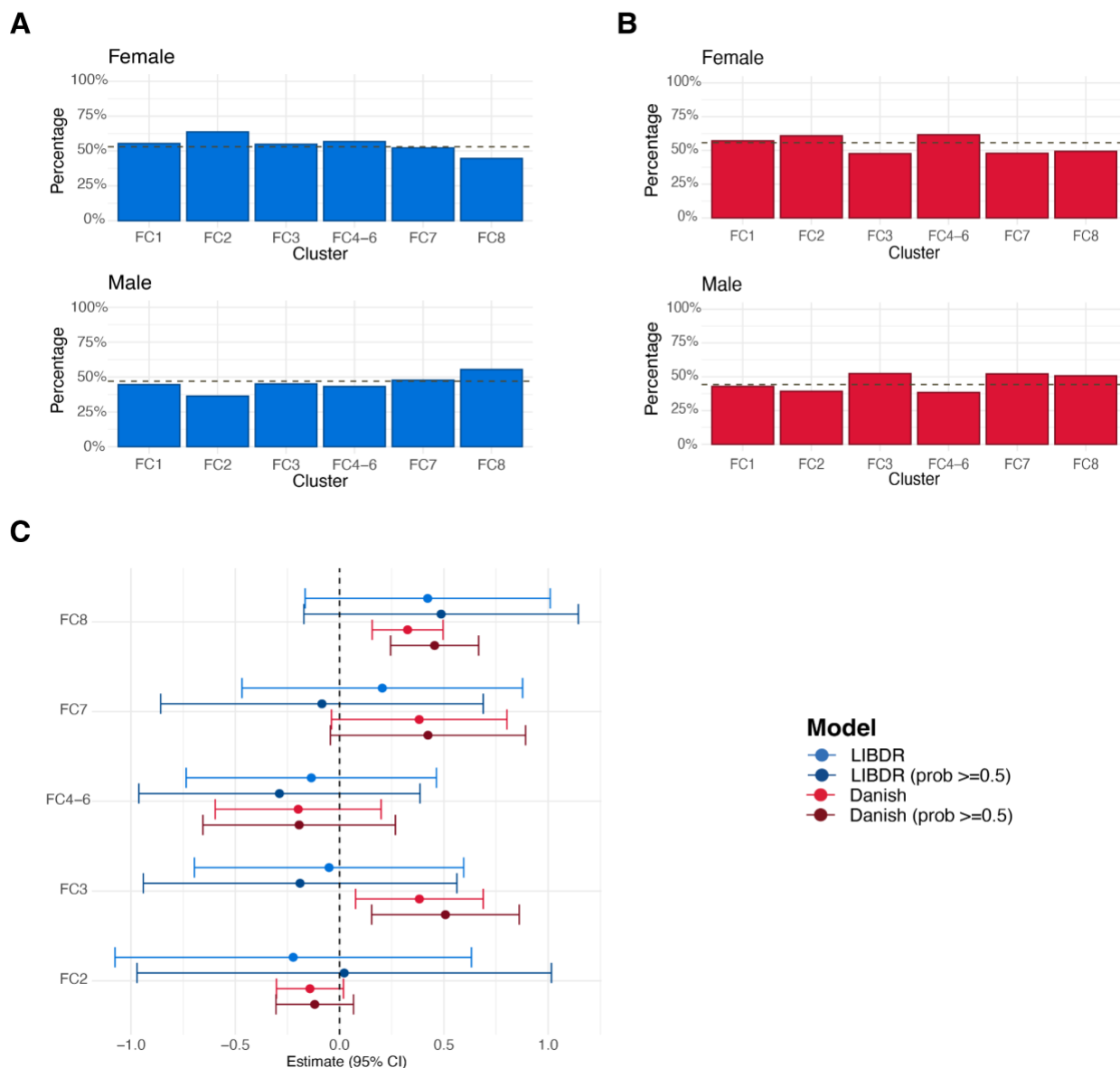
810
811
812
813
814
815
816
817
818

Figure S8. For each FC cluster, violin plots show the distribution of age at diagnosis across subjects, highlighting median and interquartile ranges for (A) the Lothian IBD Registry and (B) Danish national registry data. (C) Forest plot showing the estimated effect sizes and associated 95% confidence intervals for age in a multinomial logistic regression model that uses FC cluster assignment as outcome. Subjects with a posterior probability of belonging to their assigned cluster greater than 0.5 were considered in addition to all subjects in the cohort. Effect sizes are with respect to the reference cluster (in this case FC1). The multivariate model includes age, sex and IBD type as covariates. The dashed vertical lines are used as a reference to indicate no effect.



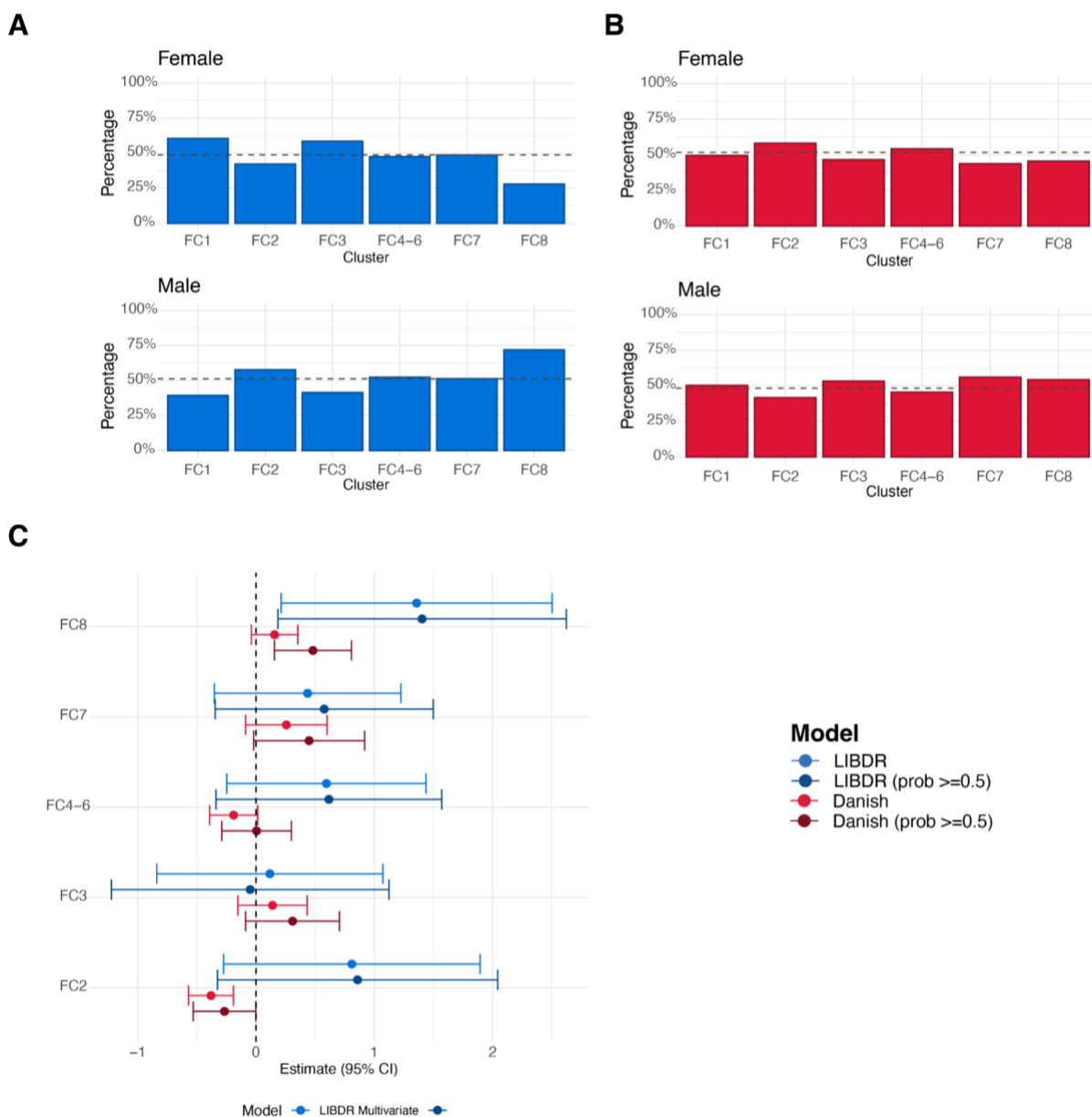
819
820
821
822
823
824
825
826
827
828

Figure S9. For each FC cluster, barplots show the proportion of individuals with female and male sex. The dashed horizontal line represents overall proportions for (A) the Lothian IBD Registry and (B) Danish national registry data. (C) Forest plot showing the estimated effect sizes and associated 95% confidence intervals for male sex versus females (baseline category) in a multinomial logistic regression model that uses FC cluster assignment as outcome. Subjects with a posterior probability of belonging to their assigned cluster greater than 0.5 were considered in addition to all subjects in the cohort. In (C), effect sizes are with respect to the reference cluster (in this case FC1). The multivariate model includes age, sex and IBD type as covariates. The dashed vertical line is used as a reference to indicate no effect.



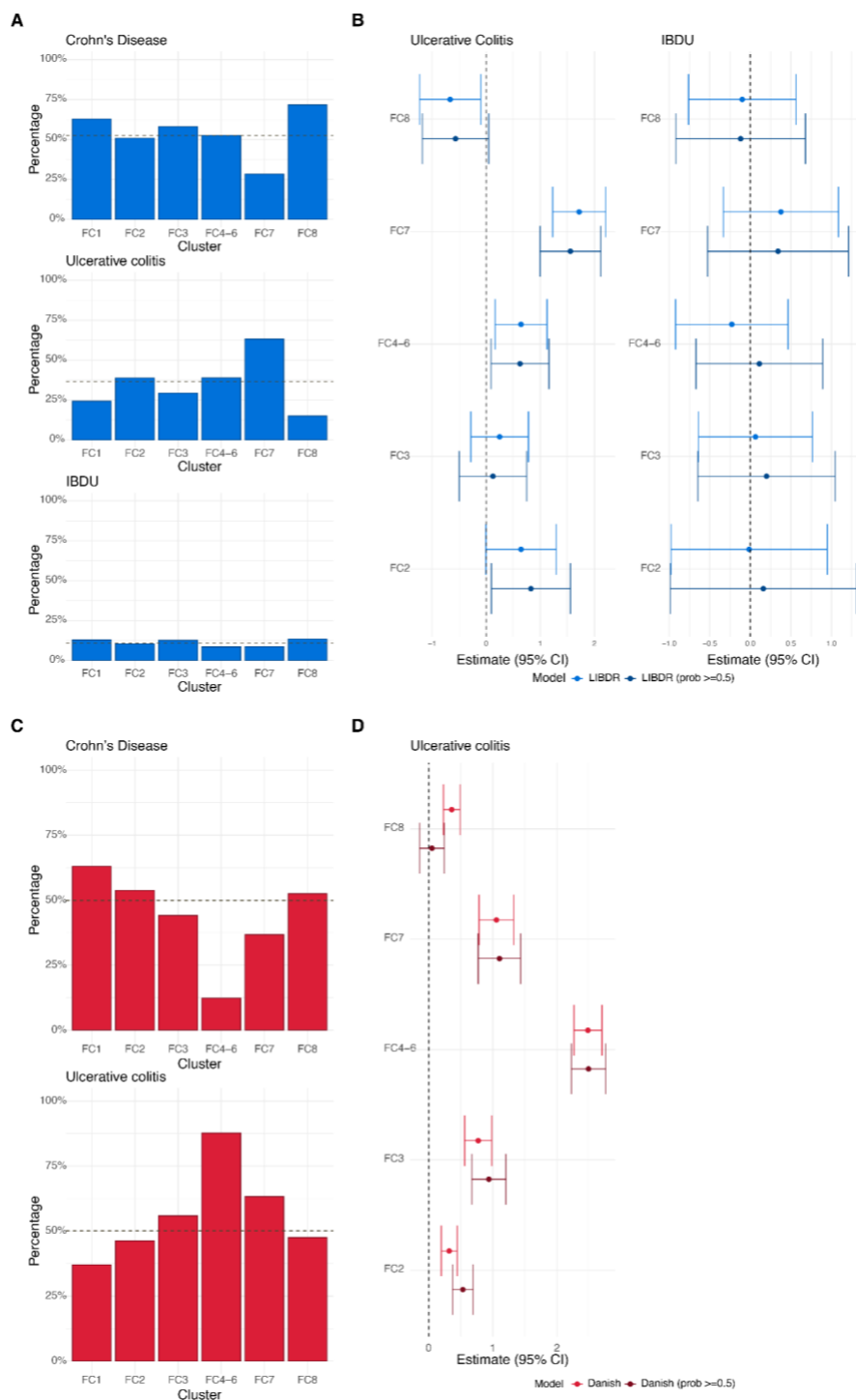
829
830
831
832
833
834
835
836
837
838
839

Figure S10. Crohn's disease subjects only. For each FC cluster, barplots show the proportion of individuals with female and male sex. The dashed horizontal line represents overall proportions for (A) the Lothian IBD Registry and (B) Danish national registry data. (C) Forest plot showing the estimated effect sizes and associated 95% confidence intervals for male sex versus females (baseline category) in a multinomial logistic regression model that uses FC cluster assignment as outcome. Subjects with a posterior probability of belonging to their assigned cluster greater than 0.5 were considered in addition to all subjects in the cohort. In (C), effect sizes are with respect to the reference cluster (in this case FC1). The multivariate model includes age, sex and IBD type as covariates. The dashed vertical lines are used as a reference to indicate no effect.



840
841
842
843
844
845
846
847
848
849

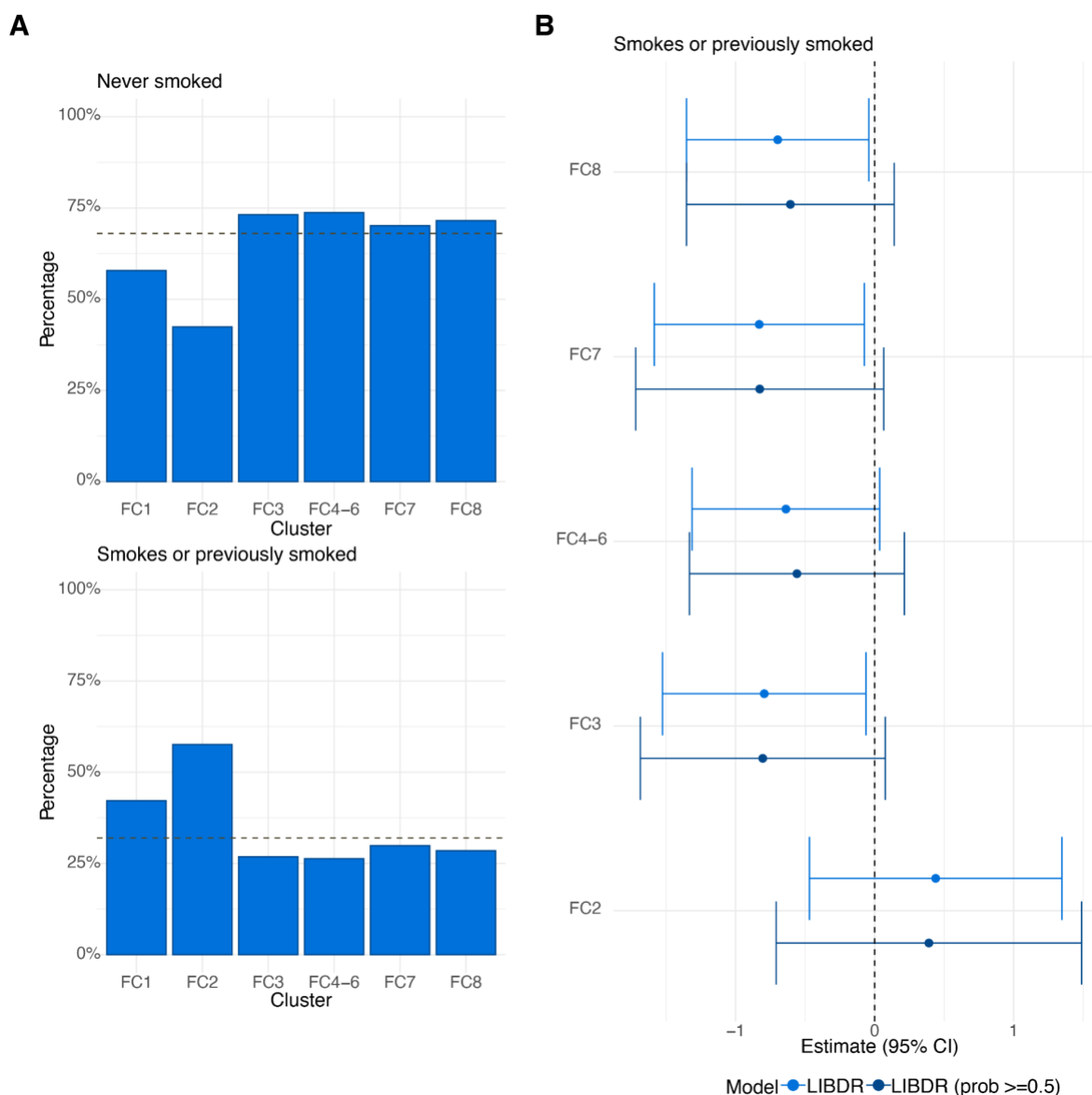
Figure S11. Ulcerative colitis subjects only. For each FC cluster, barplots show the proportion of individuals with female and male sex. The dashed horizontal line represents overall proportions for (A) the Lothian IBD Registry and (B) Danish national registry data. (C) Forest plot showing the estimated effect sizes and associated 95% confidence intervals for male sex versus females (baseline category) in a multinomial logistic regression model that uses FC cluster assignment as outcome. Subjects with a posterior probability of belonging to their assigned cluster greater than 0.5 were considered in addition to all subjects in the cohort. In (C), effect sizes are with respect to the reference cluster (in this case FC1). The multivariate model includes age, sex and IBD type as covariates. The dashed vertical lines are used as a reference to indicate no effect.



850
851
852
853
854
855
856
857
858

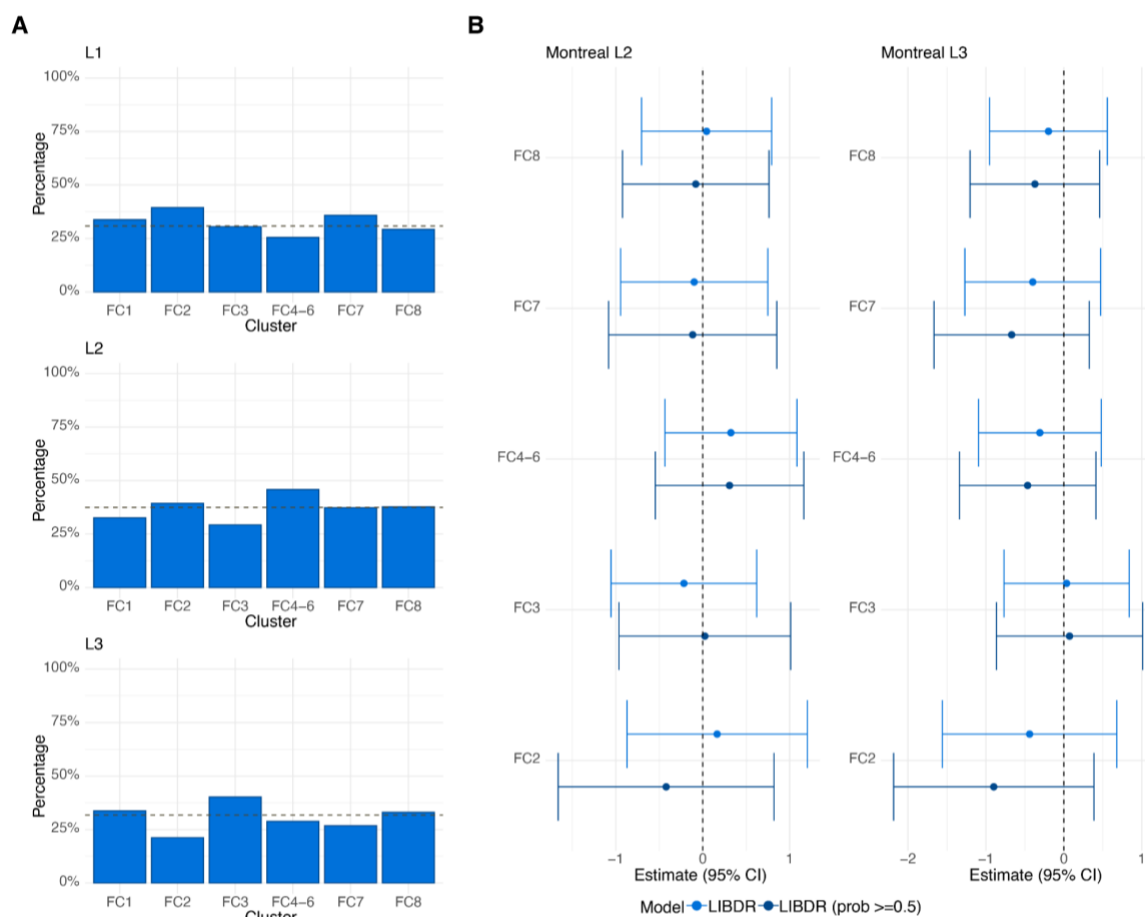
Figure S12. (A) For each FC cluster, panels show the proportion of individuals with Crohn's disease, ulcerative colitis and IBDU respectively in the Lothian IBD Registry. (B) Forest plot showing the estimated effect sizes and associated 95% confidence intervals for IBD type in the Lothian IBD Registry: ulcerative colitis and IBDU versus Crohn's disease (baseline category) in a multinomial logistic regression model that uses FC cluster assignment as outcome. (C) For each FC cluster, panels show the proportion of individuals with Crohn's disease and ulcerative colitis respectively in the Danish cohort. (D) Forest plot showing the estimated effect sizes and associated 95% confidence intervals for IBD type in the Danish cohort: ulcerative colitis versus Crohn's disease (baseline

859 category) in a multinomial logistic regression model that uses FC cluster assignment as outcome. In
 860 the Danish cohort, subjects were not assigned a subtype of “IBDU”. Instead, they were assigned
 861 either Crohn’s disease or ulcerative colitis. Subjects with a posterior probability of belonging to their
 862 assigned cluster greater than 0.5 were considered in addition to all subjects in the cohort. In (A) and
 863 (C), the dashed horizontal line represents overall proportions across the FC cohorts. In (B) and (D),
 864 effect sizes are with respect to the reference cluster (in this case FC1). In both cases, the multivariate
 865 model includes age, sex and IBD type as covariates. The dashed vertical lines are used as a
 866 reference to indicate no effect.

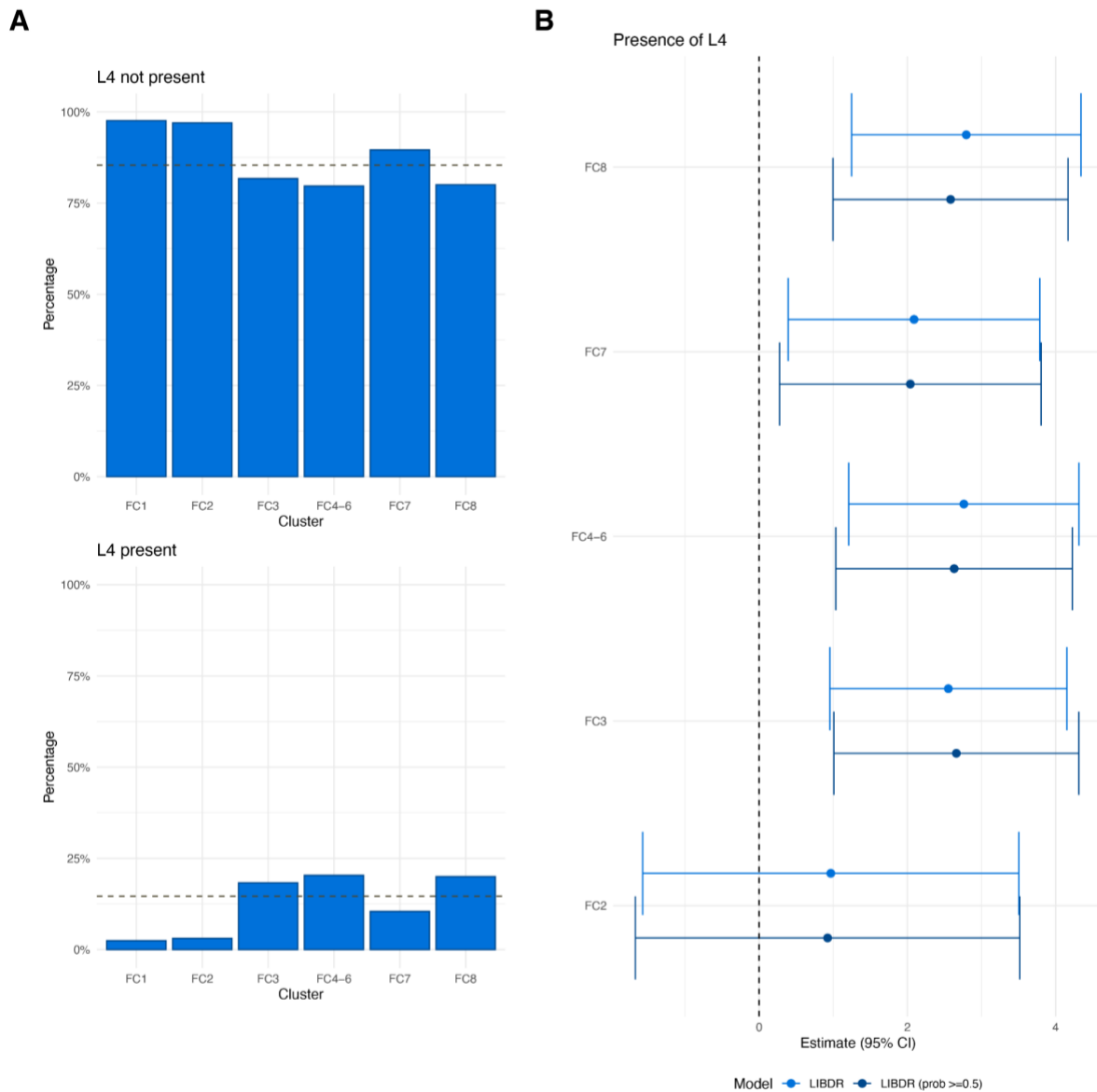


867
 868
 869 Figure S13. Crohn’s disease patients in the Lothian IBD Registry only. (A) For each FC cluster, panels
 870 show the proportion of individuals with smoking behaviour recorded as “no” (no and never) and “yes”
 871 (current or previously smoked) at diagnosis respectively. The dashed horizontal line represents
 872 overall proportions across the entire FC cohort. (B) Forest plot showing the estimated effect sizes and
 873 associated 95% confidence intervals for smoking: yes versus no (baseline category) in a multinomial

874 *logistic regression model that uses FC cluster assignment as outcome. Subjects with a posterior*
 875 *probability of belonging to their assigned cluster greater than 0.5 were considered in addition to all*
 876 *subjects in the cohort, Effect sizes are with respect to the reference cluster (in this case FC1). The*
 877 *multivariate model includes age, sex, smoking, Montreal location (L1, L2, L3), upper gastrointestinal*
 878 *inflammation (L4), perianal disease (yes, no) and Montreal behaviour (B1, B2/B3) as covariates. The*
 879 *dashed vertical lines are used as a reference to indicate no effect.*



880
 881 *Figure S14. Crohn's disease patients in the Lothian IBD Registry only. (A) For each FC cluster, panels*
 882 *show the proportion of individuals with Montreal Location recorded as L1, L2 and L3 respectively. The*
 883 *dashed horizontal line represents overall proportions across the entire FC cohort. (B) Forest plot*
 884 *showing the estimated effect sizes and associated 95% confidence intervals for Montreal Location: L2*
 885 *and L3 versus L1 (baseline category) in a multinomial logistic regression model that uses FC cluster*
 886 *assignment as outcome. Subjects with a posterior probability of belonging to their assigned cluster*
 887 *greater than 0.5 were considered in addition to all subjects in the cohort. Effect sizes are with respect*
 888 *to the reference cluster (in this case FC4). The multivariate model includes age, sex, smoking,*
 889 *Montreal location (L1, L2, L3), upper gastrointestinal inflammation (L4), perianal disease (yes, no) and*
 890 *Montreal behaviour (B1, B2/B3) as covariates. The dashed vertical lines are used as a reference to*
 891 *indicate no effect.*



892

893 *Figure S15. Crohn's disease patients in the Lothian IBD Registry only. (A) For each FC cluster, panels*

894 *show the proportion of individuals with Montreal L4 (upper gastrointestinal inflammation), recorded as*

895 *present or non present. The dashed horizontal line represents overall proportions across the entire FC*

896 *cohort. (B) Forest plot showing the estimated effect sizes and associated 95% confidence intervals for*

897 *L4: present versus not present (baseline category) in a multinomial logistic regression model that uses*

898 *FC cluster assignment as outcome. Subjects with a posterior probability of belonging to their assigned*

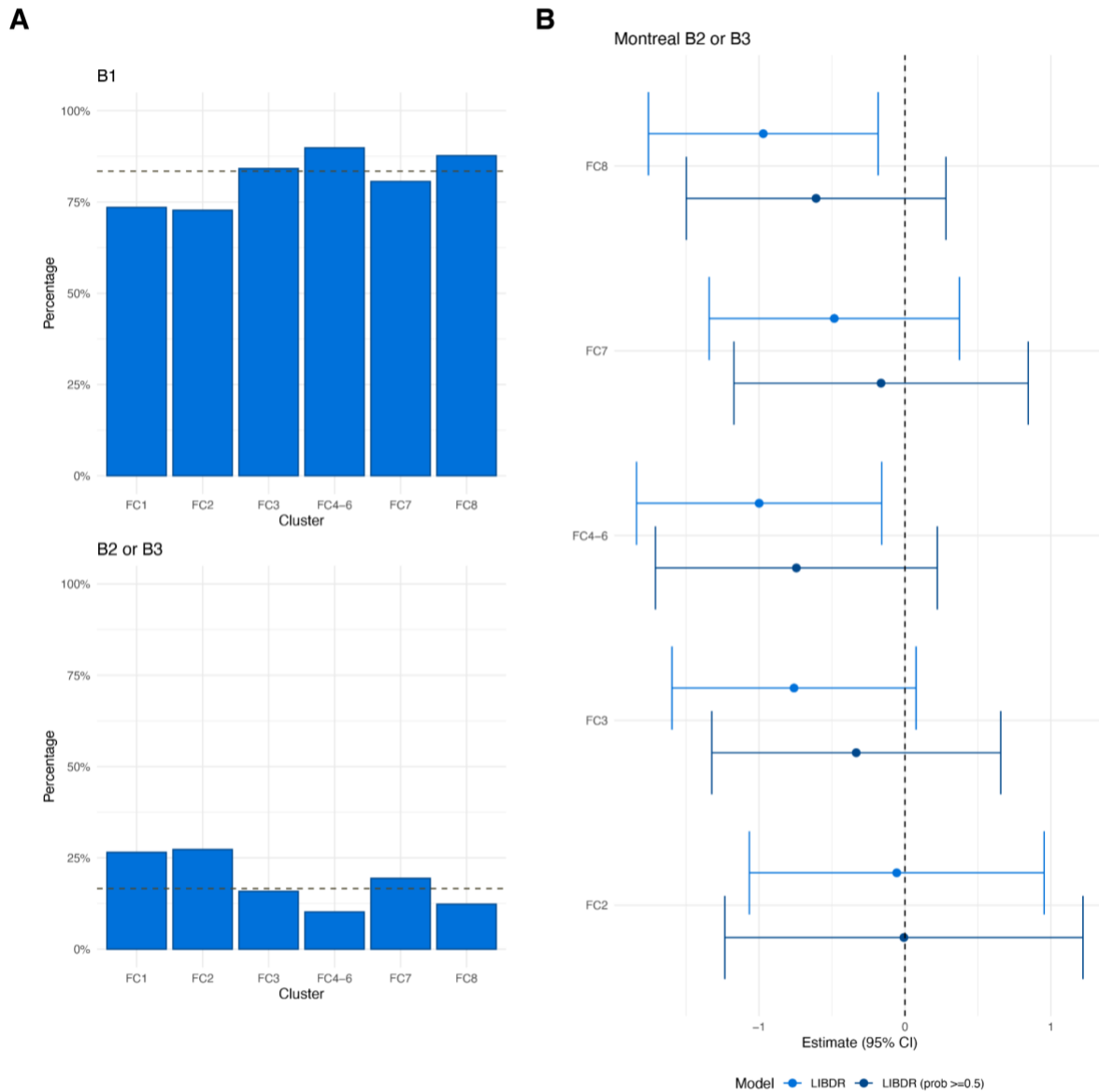
899 *cluster greater than 0.5 were considered in addition to all subjects in the cohort. Effect sizes are with*

900 *respect to the reference cluster (in this case FC1). The multivariate model includes age, sex, smoking,*

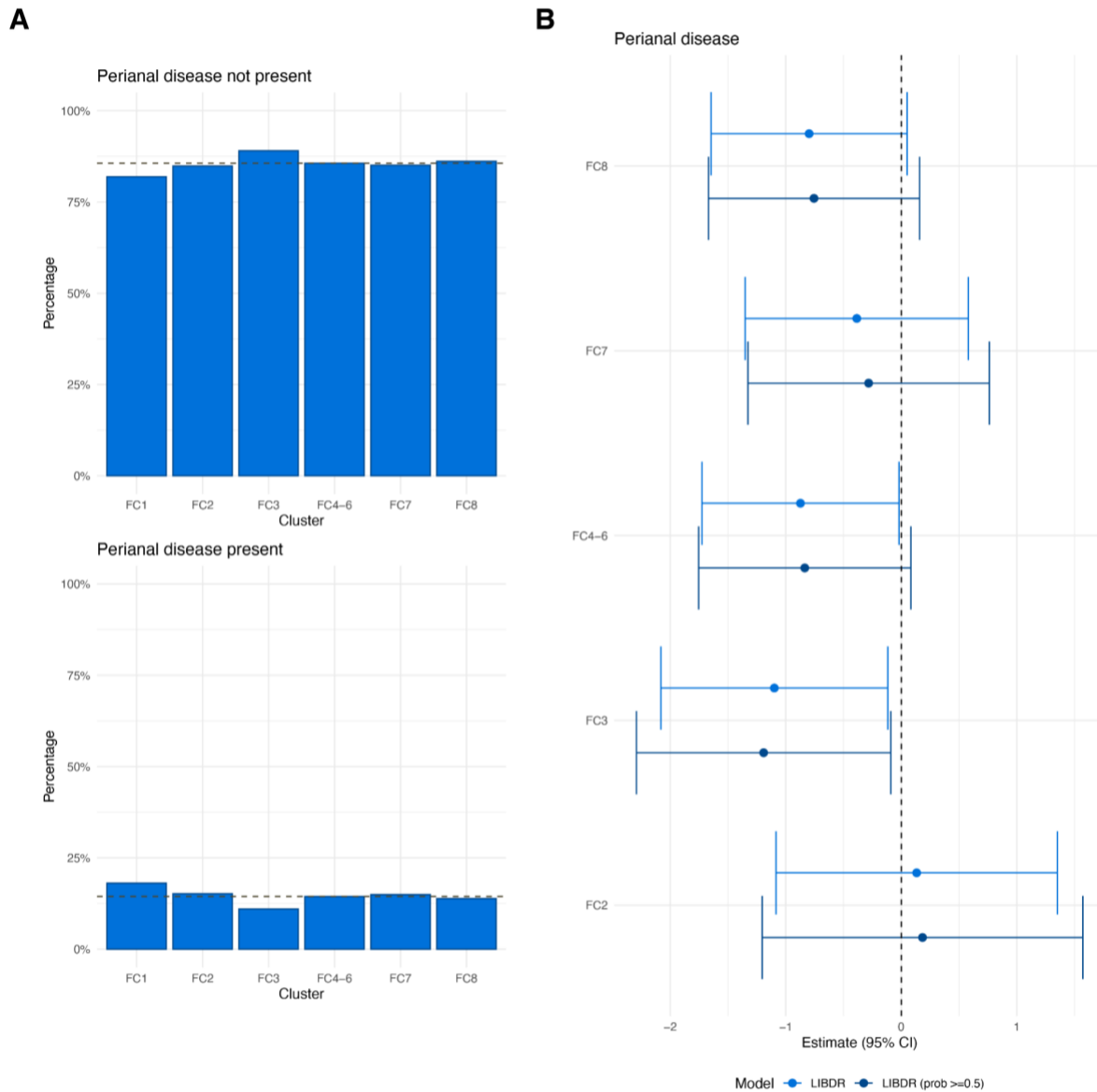
901 *Montreal location (L1, L2, L3), upper gastrointestinal inflammation (L4), perianal disease (yes, no) and*

902 *Montreal behaviour (B1, B2/B3) as covariates. The dashed vertical lines are used as a reference to*

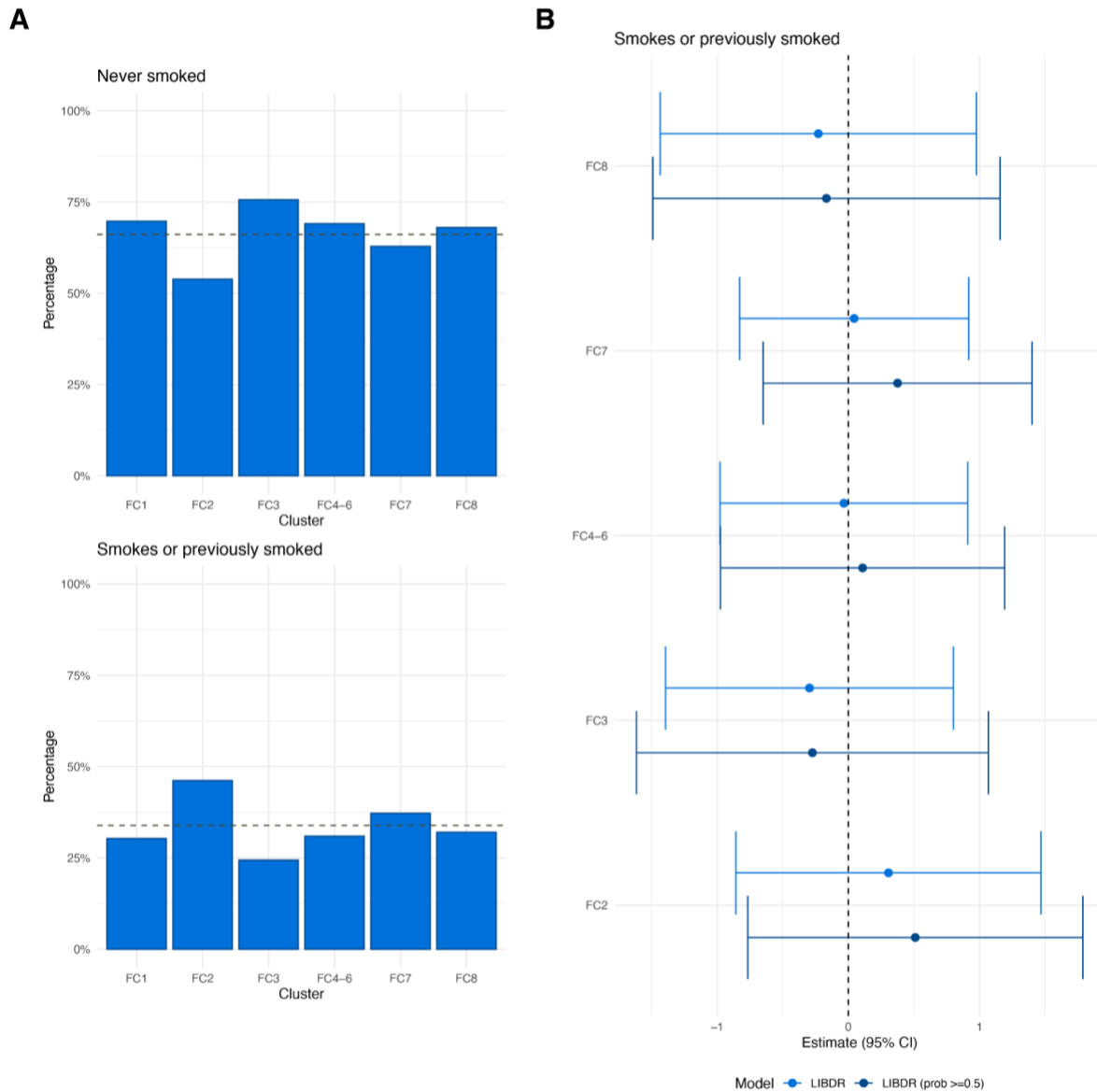
903 *indicate no effect.*



904
 905 *Figure S16. Crohn's disease patients in the Lothian IBD Registry only. (A) For each FC cluster, panels*
 906 *show the proportion of individuals with Montreal behaviour recorded as B1 or B2/B3 respectively. The*
 907 *dashed horizontal line represents overall proportions across the entire FC cohort. (B) Forest plot*
 908 *showing the estimated effect sizes and associated 95% confidence intervals for Montreal behaviour:*
 909 *B2/B3 versus B1 (baseline category) in a multinomial logistic regression model that uses FC cluster*
 910 *assignment as outcome. Subjects with a posterior probability of belonging to their assigned cluster*
 911 *greater than 0.5 were considered in addition to all subjects in the cohort. Effect sizes are with respect*
 912 *to the reference cluster (in this case FC4). The multivariate model includes age, sex, smoking,*
 913 *Montreal location (L1, L2, L3), upper gastrointestinal inflammation (L4), perianal disease (yes, no) and*
 914 *Montreal behaviour (B1, B2/B3) as covariates. The dashed vertical lines are used as a reference to*
 915 *indicate no effect.*

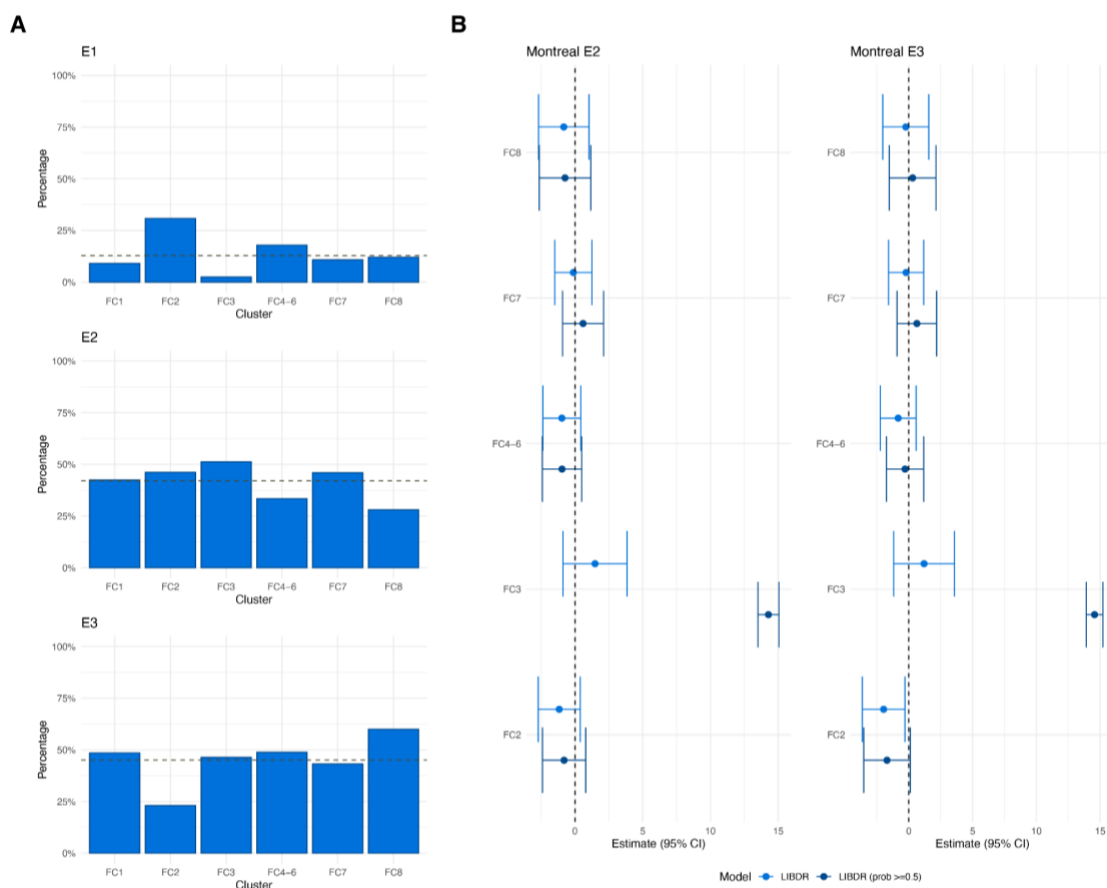


916
 917 *Figure S17. Crohn's disease patients in the Lothian IBD Registry only. (A) For each FC cluster, panels*
 918 *show the proportion of individuals with perianal disease recorded as present or not present. The*
 919 *dashed horizontal line represents overall proportions across the entire FC cohort. (B) Forest plot*
 920 *showing the estimated effect sizes and associated 95% confidence intervals for perianal disease:*
 921 *present versus not present (baseline category) in a multinomial logistic regression model that uses FC*
 922 *cluster assignment as outcome. Subjects with a posterior probability of belonging to their assigned*
 923 *cluster greater than 0.5 were considered in addition to all subjects in the cohort. Effect sizes are with*
 924 *respect to the reference cluster (in this case FC1). The multivariate model includes age, sex, smoking,*
 925 *Montreal location (L1, L2, L3), upper gastrointestinal inflammation (L4), perianal disease (yes, no) and*
 926 *Montreal behaviour (B1, B2/B3) as covariates. The dashed vertical lines are used as a reference to*
 927 *indicate no effect.*



928
929
930
931
932
933
934
935
936
937
938
939

Figure S18. Ulcerative colitis patients in the Lothian IBD Registry only. (A) For each FC cluster, panels show the proportion of individuals with smoking behaviour recorded as “no” (no and never) and “yes” (current or previously smoked) at diagnosis respectively. The dashed horizontal line represents overall proportions across the entire FC cohort. (B) Forest plot showing the estimated effect sizes and associated 95% confidence intervals for smoking: yes versus no (baseline category) in a multinomial logistic regression model that uses FC cluster assignment as outcome. Subjects with a posterior probability of belonging to their assigned cluster greater than 0.5 were considered in addition to all subjects in the cohort. Effect sizes are with respect to the reference cluster (in this case FC1). The multivariate model includes age, sex, smoking and Montreal extent (E1, E2, E3). The dashed vertical lines are used as a reference to indicate no effect.



940

941

942

943

944

945

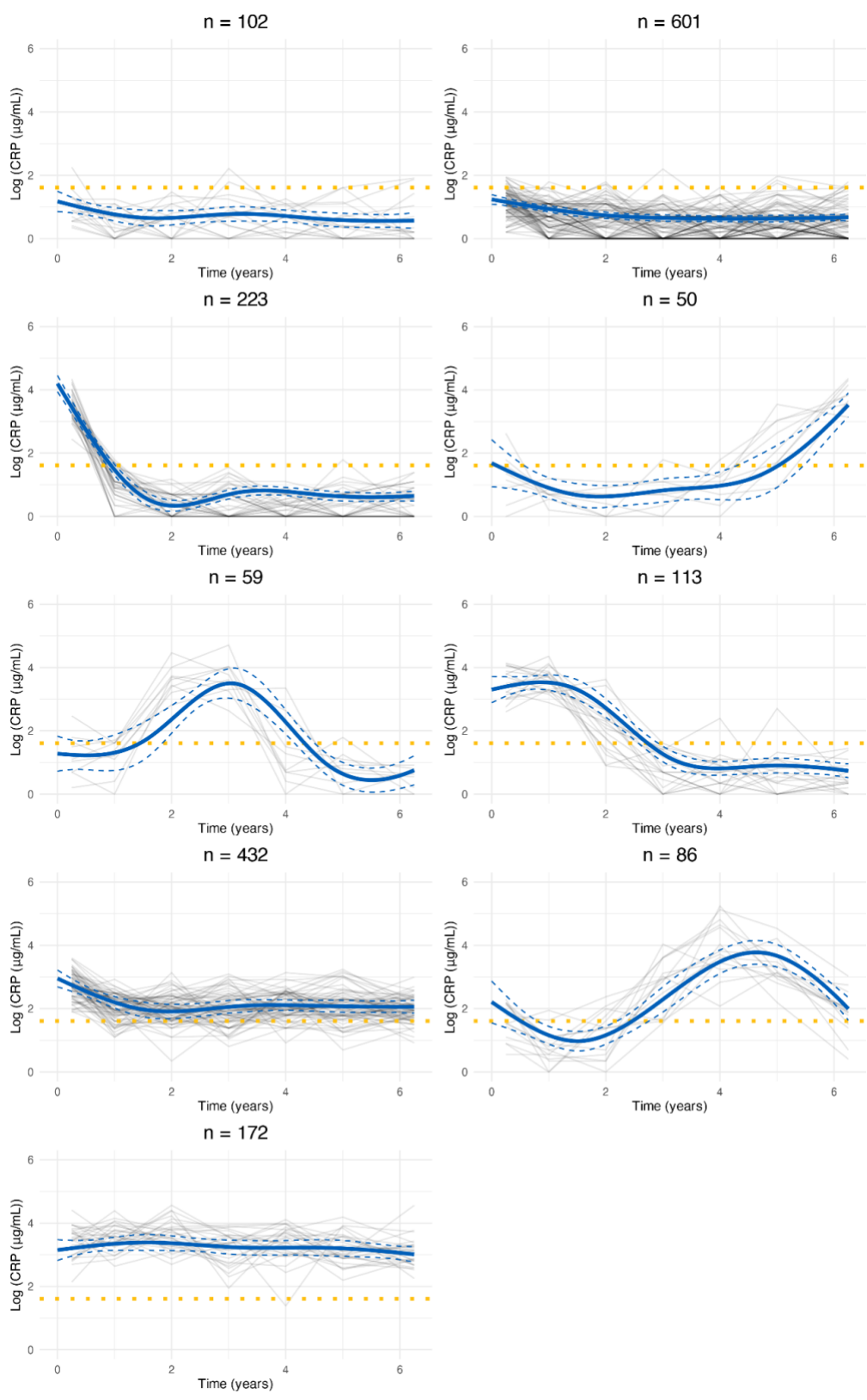
946

947

948

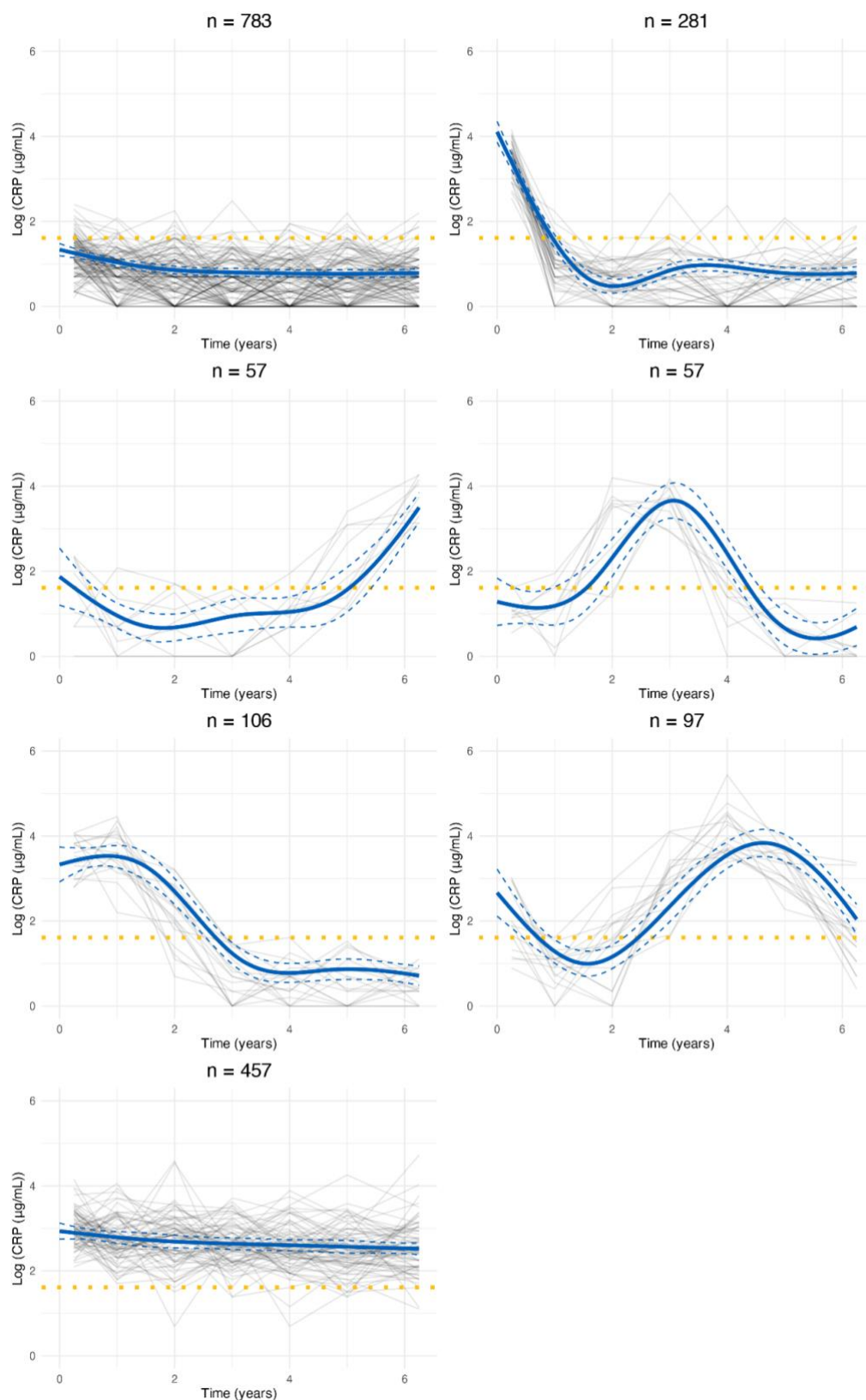
949

Figure S19. Ulcerative colitis patients in the Lothian IBD Registry only. (A) For each cluster, panels show the proportion of individuals with Montreal extent recorded as E1, E2 and E3 respectively. The dashed horizontal line represents overall proportions across the entire FC cohort. (B) Forest plot showing the estimated effect sizes and associated 95% confidence intervals for Montreal extent: E2 and E3 versus E1 (baseline category) in a multinomial logistic regression model that uses FC cluster assignment as outcome. Subjects with a posterior probability of belonging to their assigned cluster greater than 0.5 were considered in addition to all subjects in the cohort. Effect sizes are with respect to the reference cluster (in this case FC1). The multivariate model includes age, sex, smoking and Montreal extent (E1, E2, E3). The dashed vertical lines are used as a reference to indicate no effect.



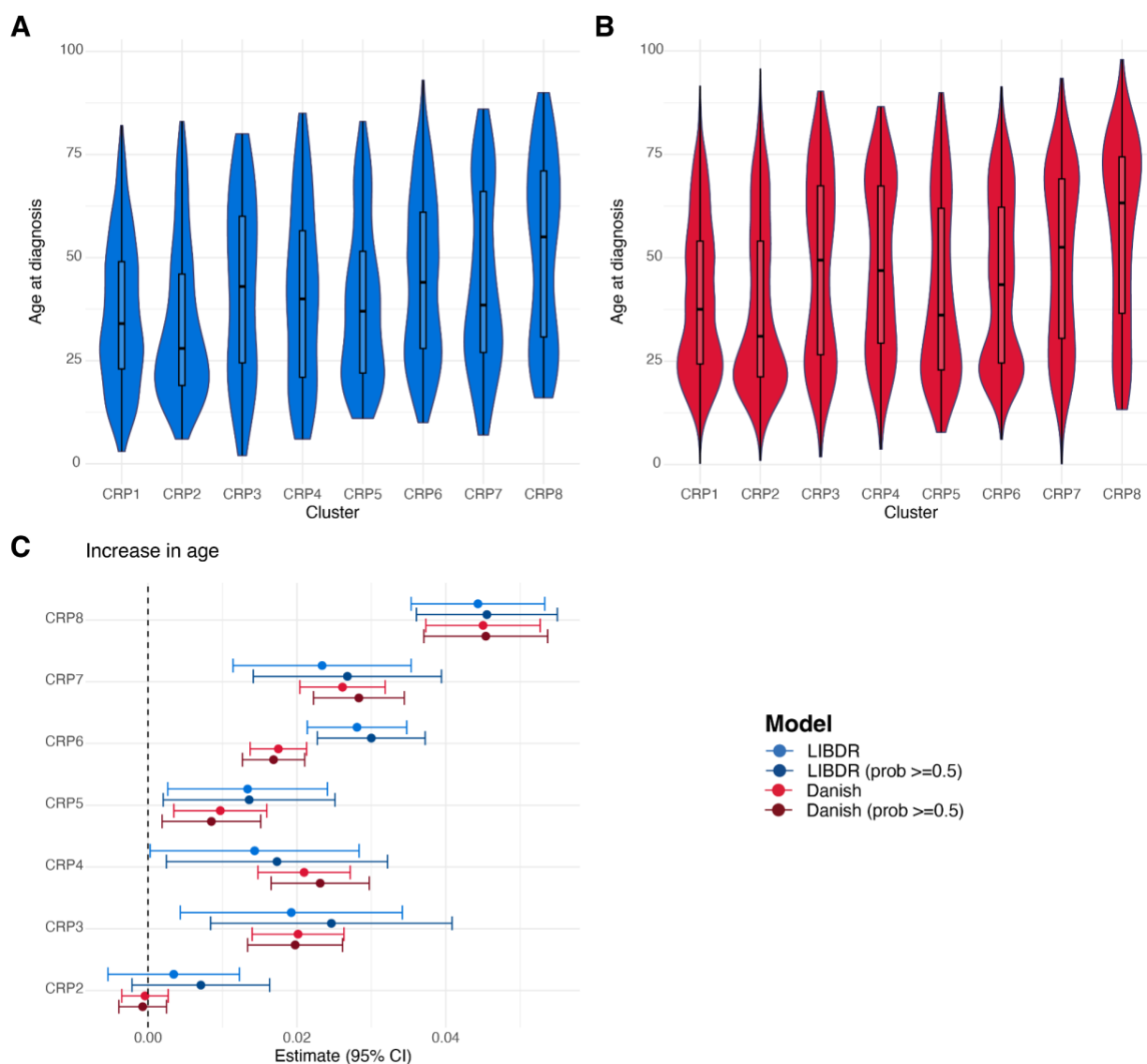
950
951
952
953
954
955

Figure S20. Cluster trajectories obtained from LCMM assuming nine clusters fitted to C-reactive protein data in the Lothian IBD Registry. Red lines indicate predicted mean cluster profiles with 95% confidence intervals. Dotted horizontal lines indicate $\log(5\mu\text{g/mL})$. For visualisation purposes, pseudo subject-specific trajectories have been generated by amalgamating observations from groups of six subjects.



956
957
958
959
960
961

Figure S21. Cluster trajectories obtained from LCMM assuming seven clusters fitted to C-reactive protein data in the Lothian IBD Registry. Red lines indicate predicted mean cluster profiles with 95% confidence intervals. Dotted horizontal lines indicate $\log(5\mu\text{g/mL})$. For visualisation purposes, pseudo subject-specific trajectories have been generated by amalgamating observations from groups of six subjects.

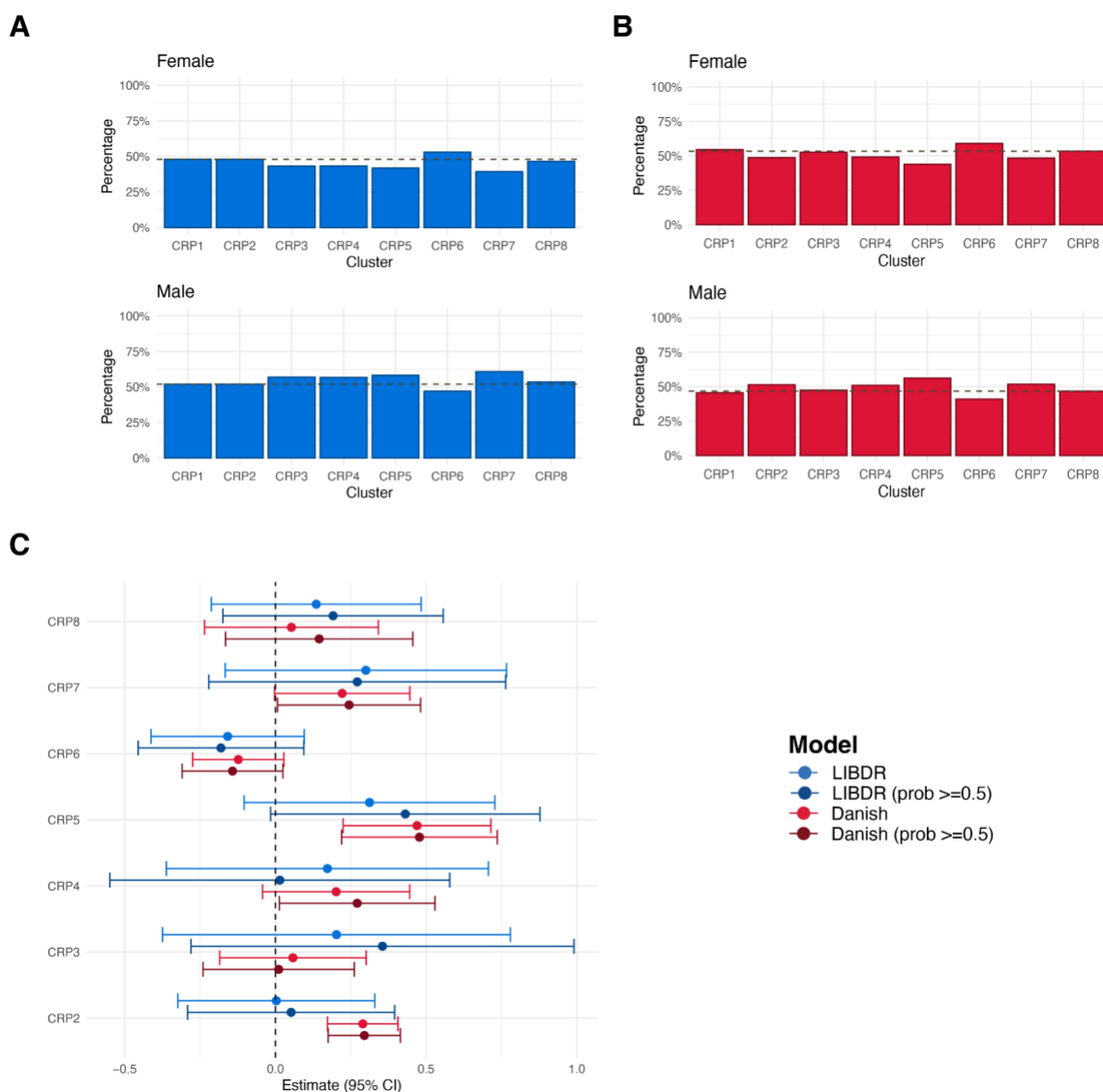


962
963
964
965
966
967
968
969

Figure S22. For each CRP cluster, violin plots show the distribution of age at diagnosis across subjects, highlighting median and interquartile ranges for (A) the Lothian IBD Registry and (B) Danish national registry data. (C) Forest plot showing the estimated effect sizes and associated 95% confidence intervals for age in a multinomial logistic regression model that uses CRP cluster assignment as outcome. Subjects with a posterior probability of belonging to their assigned cluster greater than 0.5 were considered in addition to all subjects in the cohort. Effect sizes are with respect to the reference cluster (in this case CRP1). The multivariate model includes age, sex and IBD type

970

as covariates. The dashed vertical lines are used as a reference to indicate no effect.



971

972

973

974

975

976

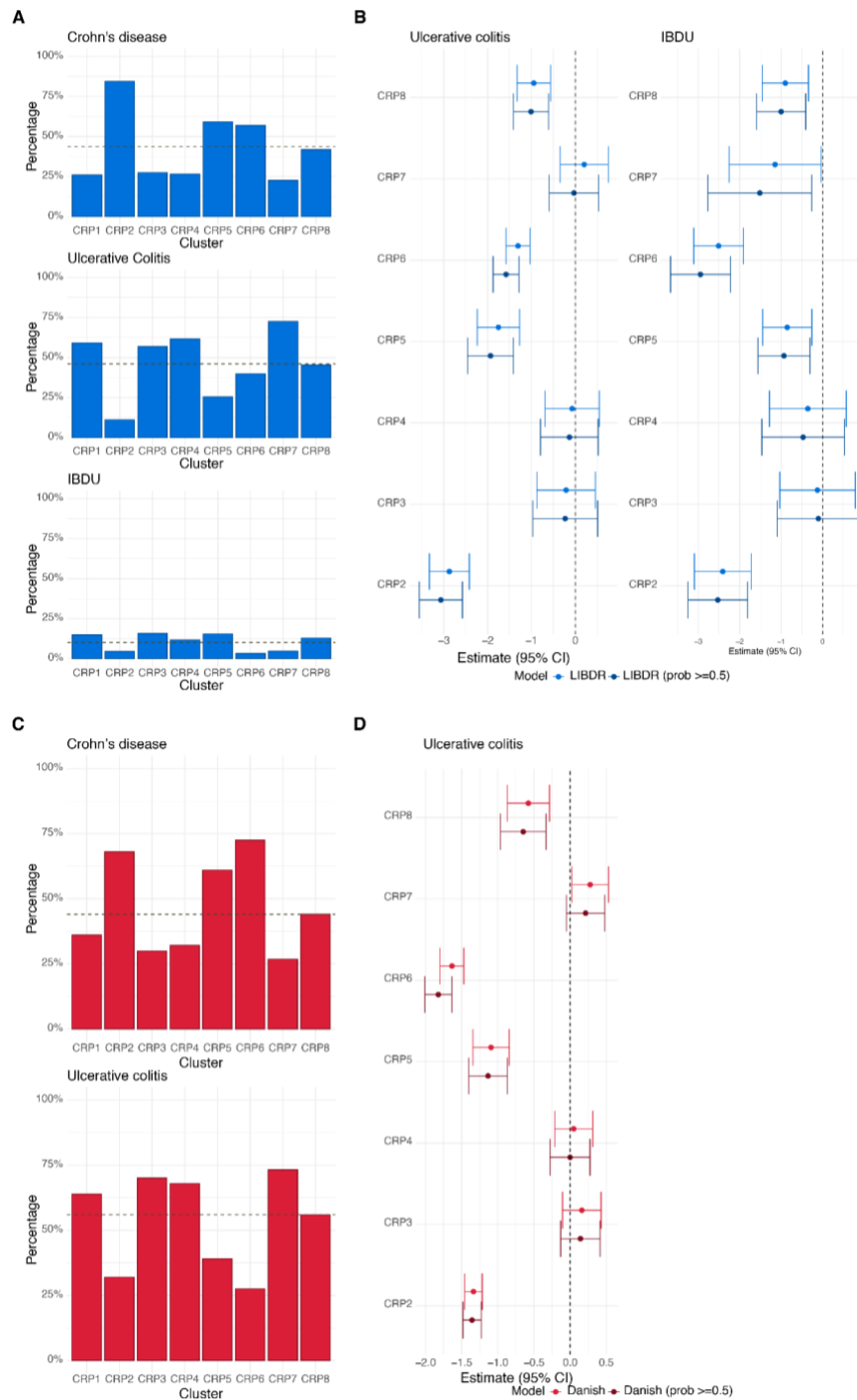
977

978

979

980

Figure S23. For each CRP cluster, barplots show the proportion of individuals with female and male sex. The dashed horizontal line represents overall proportions for (A) the Lothian IBD Registry and (B) Danish national registry data. (C) Forest plot showing the estimated effect sizes and associated 95% confidence intervals for male sex versus females (baseline category) in a multinomial logistic regression model that uses CRP cluster assignment as outcome. Subjects with a posterior probability of belonging to their assigned cluster greater than 0.5 were considered in addition to all subjects in the cohort. In (C), effect sizes are with respect to the reference cluster (in this case CRP1). The multivariate model includes age, sex and IBD type as covariates. The dashed vertical line is used as a reference to indicate no effect.



981

982 *Figure S24. (A) For each CRP cluster, panels show the proportion of individuals with Crohn's disease,*

983 *ulcerative colitis and IBDU respectively. The dashed horizontal line represents overall proportions*

984 *across the entire CRP cohort. (B) Forest plot showing the estimated effect sizes and associated 95%*

985 *confidence intervals for IBD type: ulcerative colitis and IBDU versus Crohn's disease (baseline*

986 *category) in a multinomial logistic regression model that uses CRP cluster assignment as outcome.*

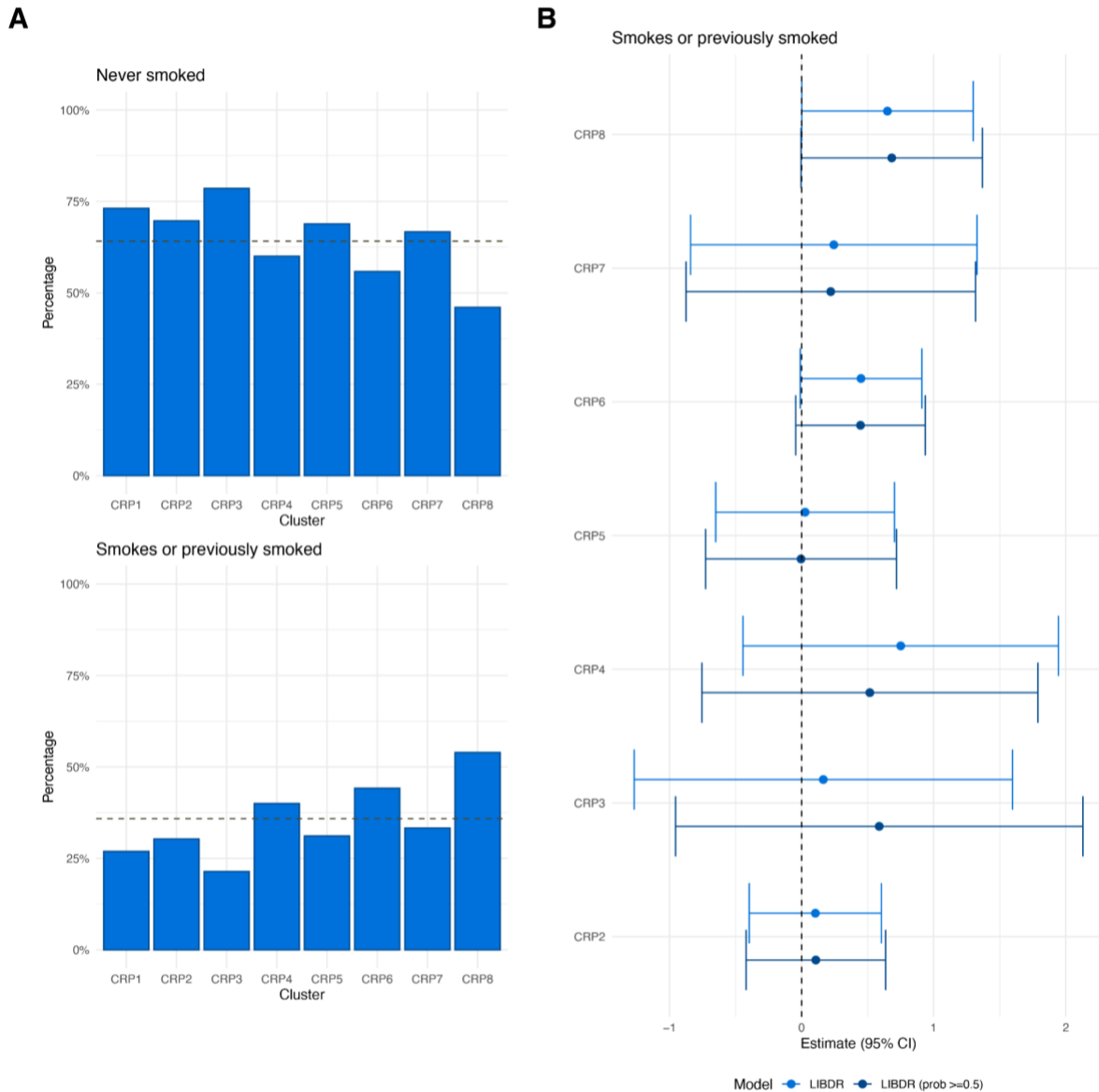
987 *(C) For each FC cluster, panels show the proportion of individuals with Crohn's disease and ulcerative*

988 *colitis respectively in the Danish cohort. (D) Forest plot showing the estimated effect sizes and*

989 *associated 95% confidence intervals for IBD type in the Danish cohort: ulcerative colitis versus*

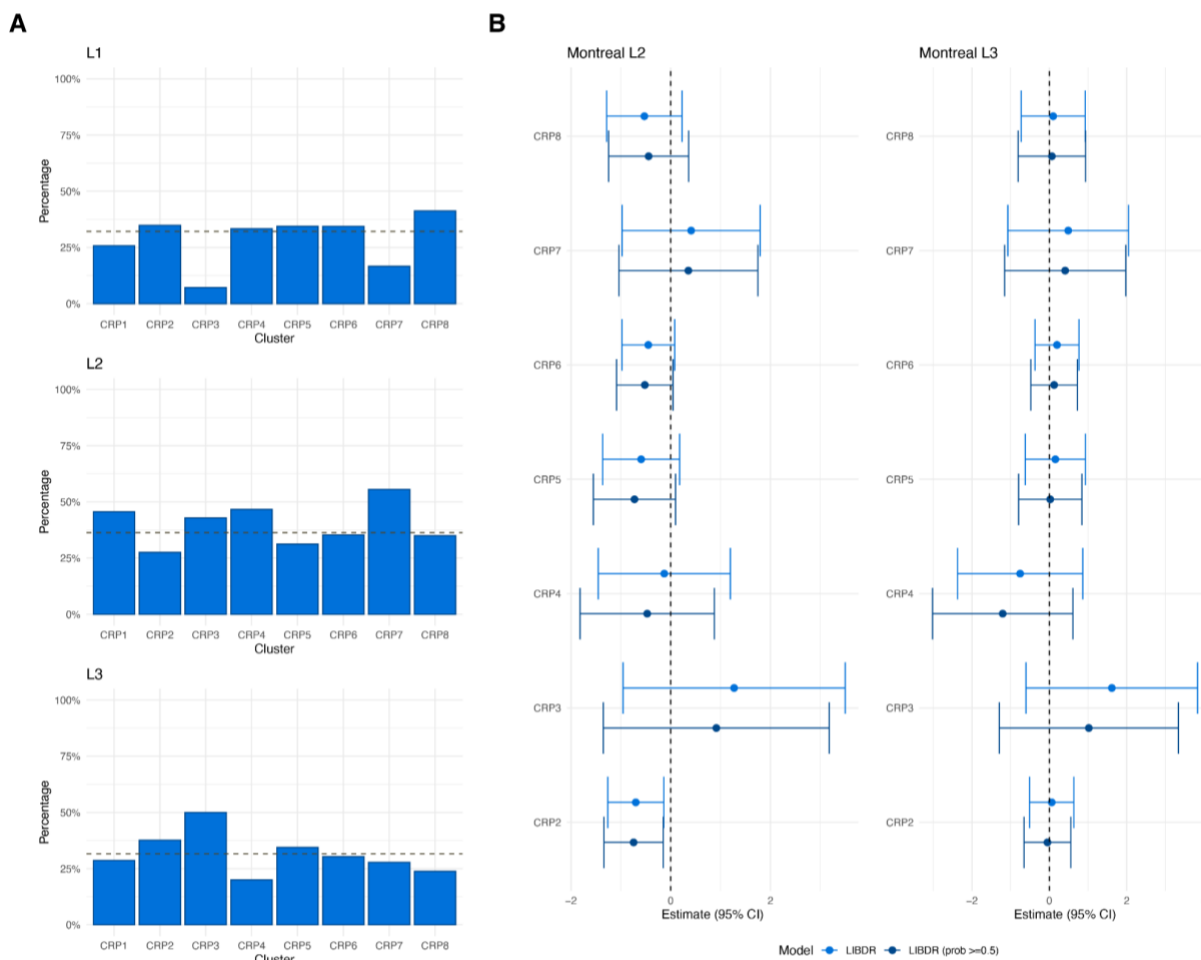
990 *Crohn's disease (baseline category) in a multinomial logistic regression model that uses FC cluster*

991 assignment as outcome. In the Danish cohort, subjects were not assigned a subtype of “IBDU”.
 992 Instead, they were assigned either Crohn’s disease or ulcerative colitis. Subjects with a posterior
 993 probability of belonging to their assigned cluster greater than 0.5 were considered in addition to all
 994 subjects in the cohort. Effect sizes are with respect to the reference cluster (in this case CRP1). In
 995 both cases, the multivariate model includes age, sex and IBD type as covariates. The dashed vertical
 996 lines are used as a reference to indicate no effect.

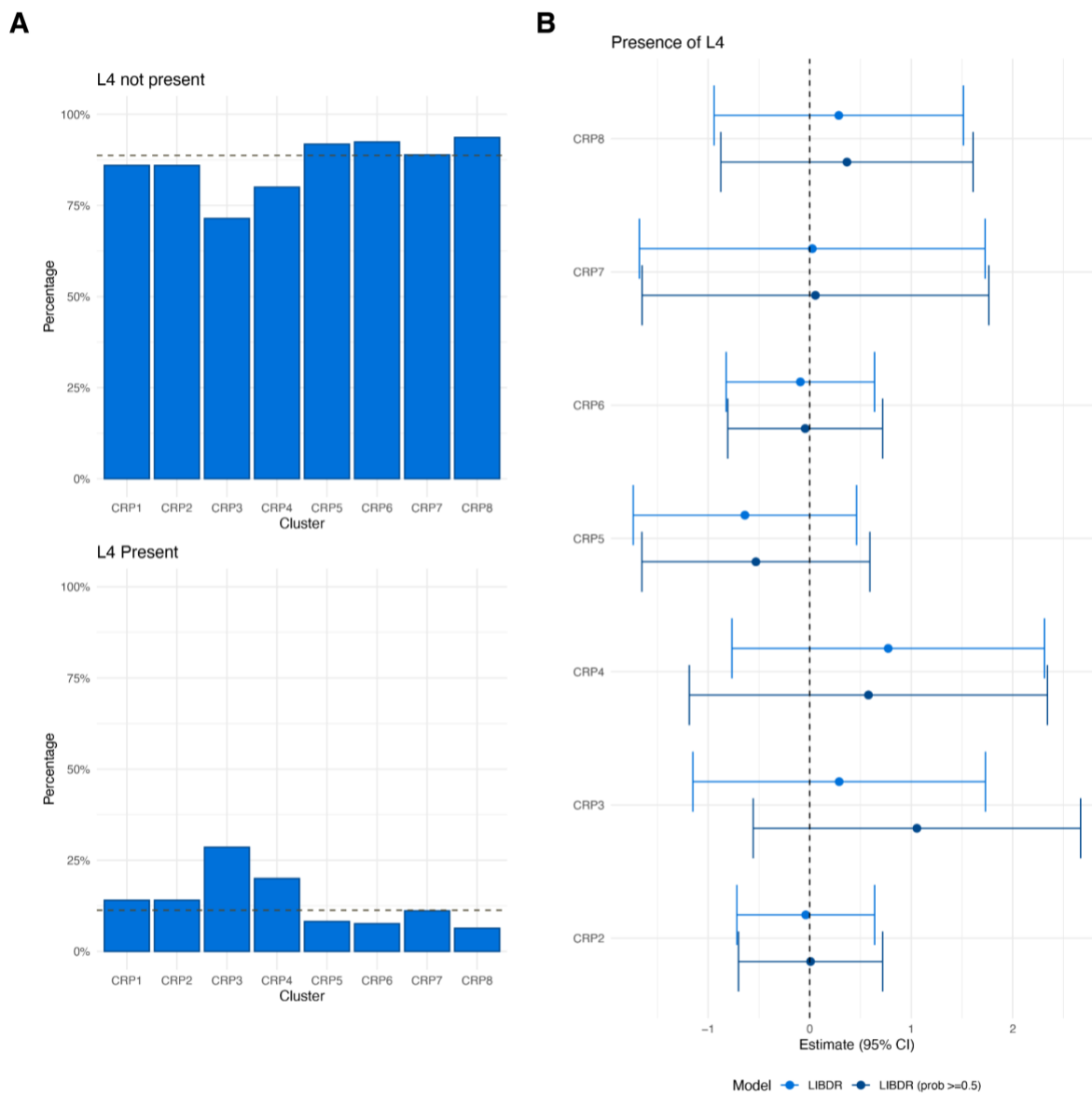


997
 998 Figure S25. Crohn’s disease patients in the Lothian IBD Registry only. (A) For each CRP cluster,
 999 panels show the proportion of individuals with smoking behaviour recorded as “no” (no and never) and
 1000 “yes” (current or previously smoked) at diagnosis respectively. The dashed horizontal line represents
 1001 overall proportions across the entire CRP cohort. (B) Forest plot showing the estimated effect sizes
 1002 and associated 95% confidence intervals for smoking: yes versus no (baseline category) in a
 1003 multinomial logistic regression model that uses CRP cluster assignment as outcome. Subjects with a
 1004 posterior probability of belonging to their assigned cluster greater than 0.5 were considered in addition
 1005 to all subjects in the cohort. Effect sizes are with respect to the reference cluster (in this case CRP1).

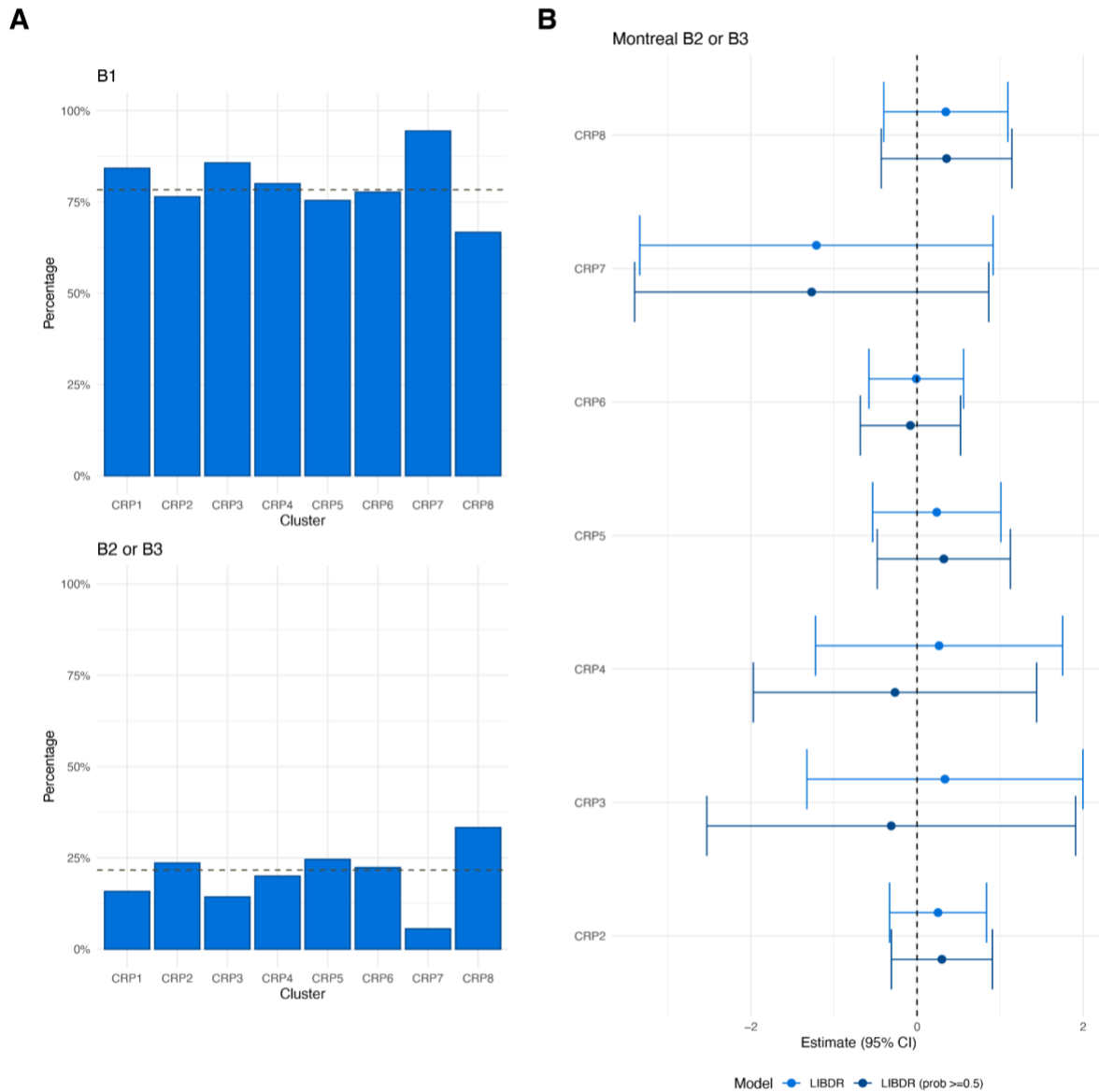
1006 *The multivariate model includes age, sex, smoking, Montreal location (L1, L2, L3), upper*
 1007 *gastrointestinal inflammation (L4), and Montreal behaviour (B1, B2/B3) as covariates. The dashed*
 1008 *vertical lines are used as a reference to indicate no effect.*



1009 *Figure S26. Crohn's disease patients in the Lothian IBD Registry only. (A) For each CRP cluster,*
 1010 *panels show the proportion of individuals with Montreal Location recorded as L1, L2 and L3*
 1011 *respectively. The dashed horizontal line represents overall proportions across the entire CRP cohort.*
 1012 *(B) Forest plot showing the estimated effect sizes and associated 95% confidence intervals for*
 1013 *Montreal Location: L2 and L3 versus L1 (baseline category) in a multinomial logistic regression model*
 1014 *that uses CRP cluster assignment as outcome. Subjects with a posterior probability of belonging to*
 1015 *their assigned cluster greater than 0.5 were considered in addition to all subjects in the cohort. Effect*
 1016 *sizes are with respect to the reference cluster (in this case CRP1). The multivariate model includes*
 1017 *age, sex, smoking, Montreal location (L1, L2, L3), upper gastrointestinal inflammation (L4), and*
 1018 *Montreal behaviour (B1, B2/B3) as covariates. The dashed vertical lines are used as a reference to*
 1019 *indicate no effect.*
 1020

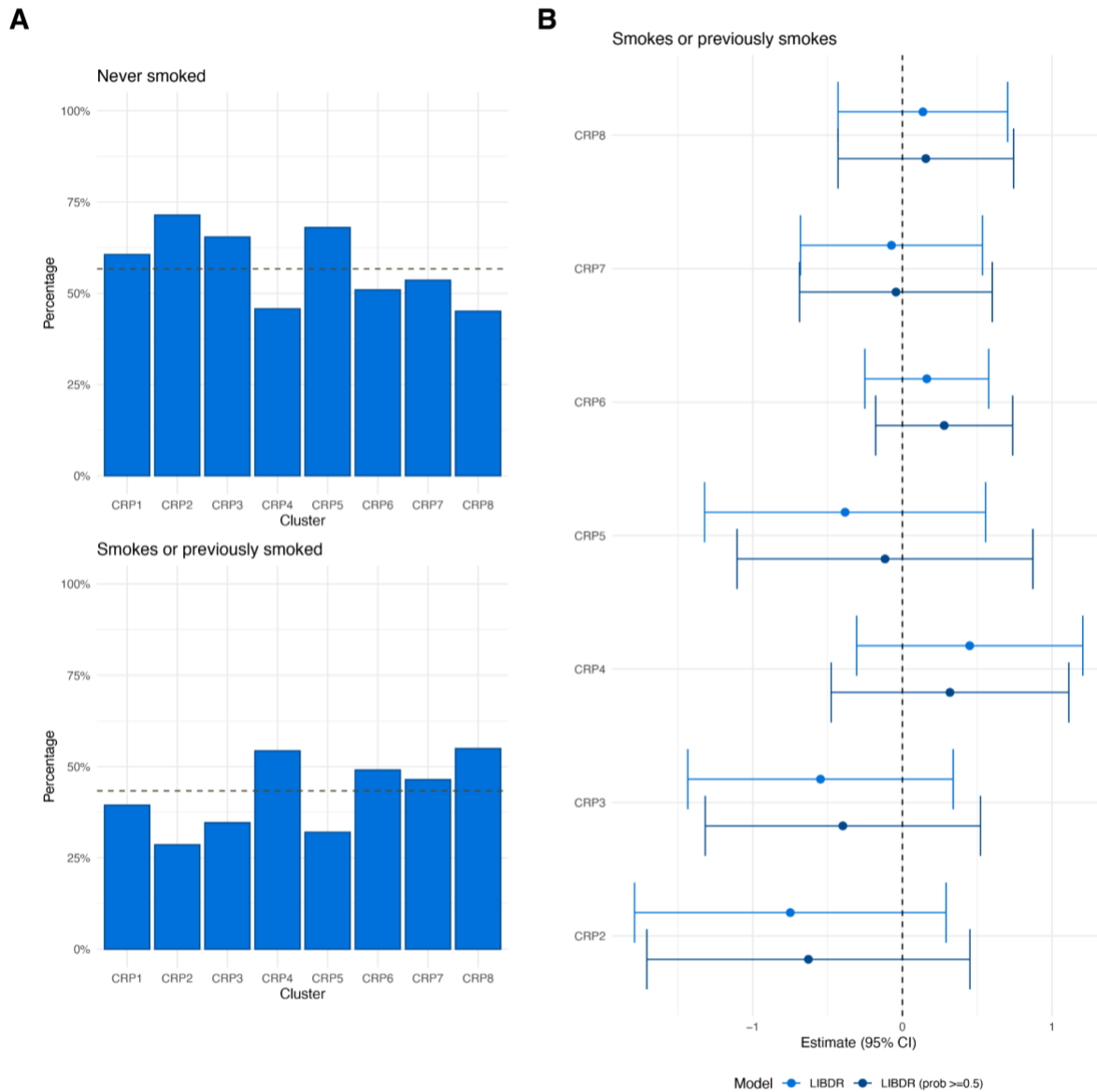


1021
 1022 *Figure S27. Crohn's disease patients in the Lothian IBD Registry only. (A) For each CRP cluster,*
 1023 *panels show the proportion of individuals with Montreal L4 (upper gastrointestinal inflammation),*
 1024 *recorded as present or non present. The dashed horizontal line represents overall proportions across*
 1025 *the entire CRP cohort. (B) Forest plot showing the estimated effect sizes and associated 95%*
 1026 *confidence intervals for L4: present versus not present (baseline category) in a multinomial logistic*
 1027 *regression model that uses CRP cluster assignment as outcome. Subjects with a posterior probability*
 1028 *of belonging to their assigned cluster greater than 0.5 were considered in addition to all subjects in the*
 1029 *cohort. Effect sizes are with respect to the reference cluster (in this case CRP1). The multivariate*
 1030 *model includes age, sex, smoking, Montreal location (L1, L2, L3), upper gastrointestinal inflammation*
 1031 *(L4), and Montreal behaviour (B1, B2/B3) as covariates. The dashed vertical lines are used as a*
 1032 *reference to indicate no effect.*



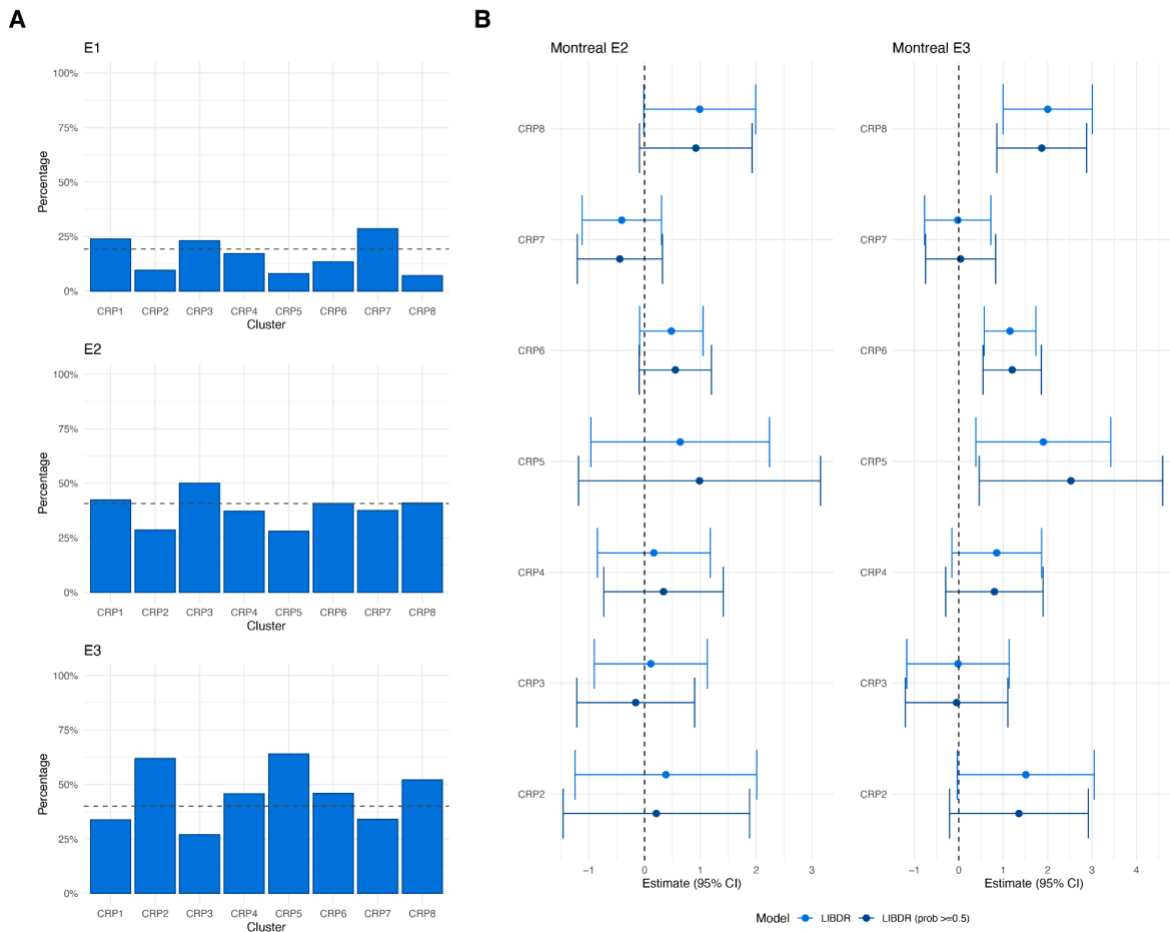
1033
1034
1035
1036
1037
1038
1039
1040
1041
1042
1043
1044
1045

Figure S28. Crohn's disease patients in the Lothian IBD Registry only. (A) For each CRP cluster, panels show the proportion of individuals with Montreal behaviour recorded as B1 or B2/B3 respectively. The dashed horizontal line represents overall proportions across the entire CRP cohort. (B) Forest plot showing the estimated effect sizes and associated 95% confidence intervals for Montreal behaviour: B2/B3 versus B1 (baseline category) in a multinomial logistic regression model that uses CRP cluster assignment as outcome. Subjects with a posterior probability of belonging to their assigned cluster greater than 0.5 were considered in addition to all subjects in the cohort. Effect sizes are with respect to the reference cluster (in this case CRP1). The multivariate model includes age, sex, smoking, Montreal location (L1, L2, L3), upper gastrointestinal inflammation (L4), and Montreal behaviour (B1, B2/B3) as covariates. The dashed vertical lines are used as a reference to indicate no effect.



1046
1047
1048
1049
1050
1051
1052
1053
1054
1055
1056

Figure S29. Ulcerative colitis patients in the Lothian IBD Registry only. (A) For each CRP cluster, panels show the proportion of individuals with smoking behaviour recorded as “no” (no and never) and “yes” (current or previously smoked) at diagnosis respectively. The dashed horizontal line represents overall proportions across the entire FC cohort. (B) Forest plot showing the estimated effect sizes and associated 95% confidence intervals for smoking: yes versus no (baseline category) in a multinomial logistic regression model that uses FC cluster assignment as outcome. Subjects with a posterior probability of belonging to their assigned cluster greater than 0.5 were considered in addition to all subjects in the cohort. Effect sizes are with respect to the reference cluster (in this case CRP1). The multivariate model includes age, sex, smoking and Montreal extent (E1, E2, E3). The dashed vertical lines are used as a reference to indicate no effect.



1057

1058

1059

1060

1061

1062

1063

1064

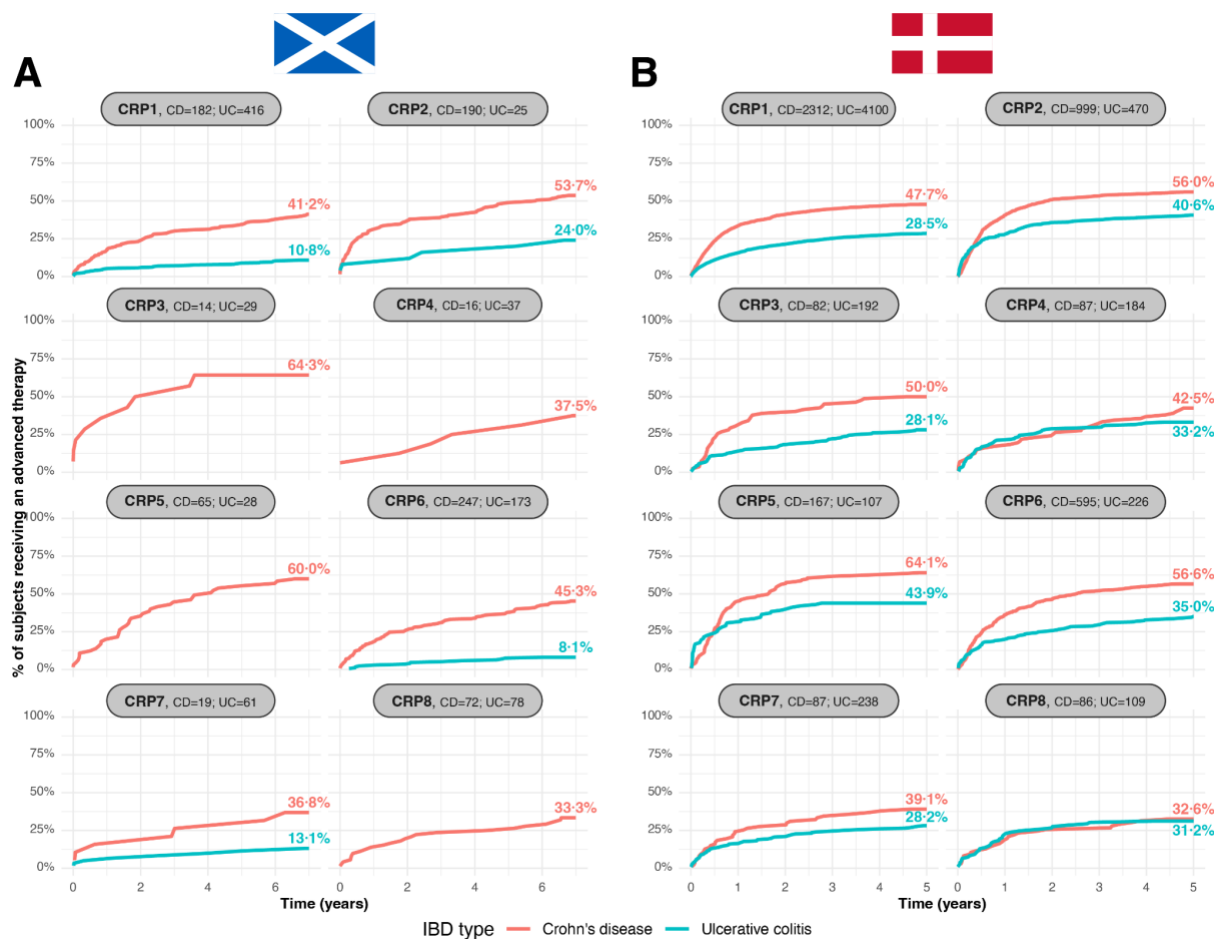
1065

1066

1067

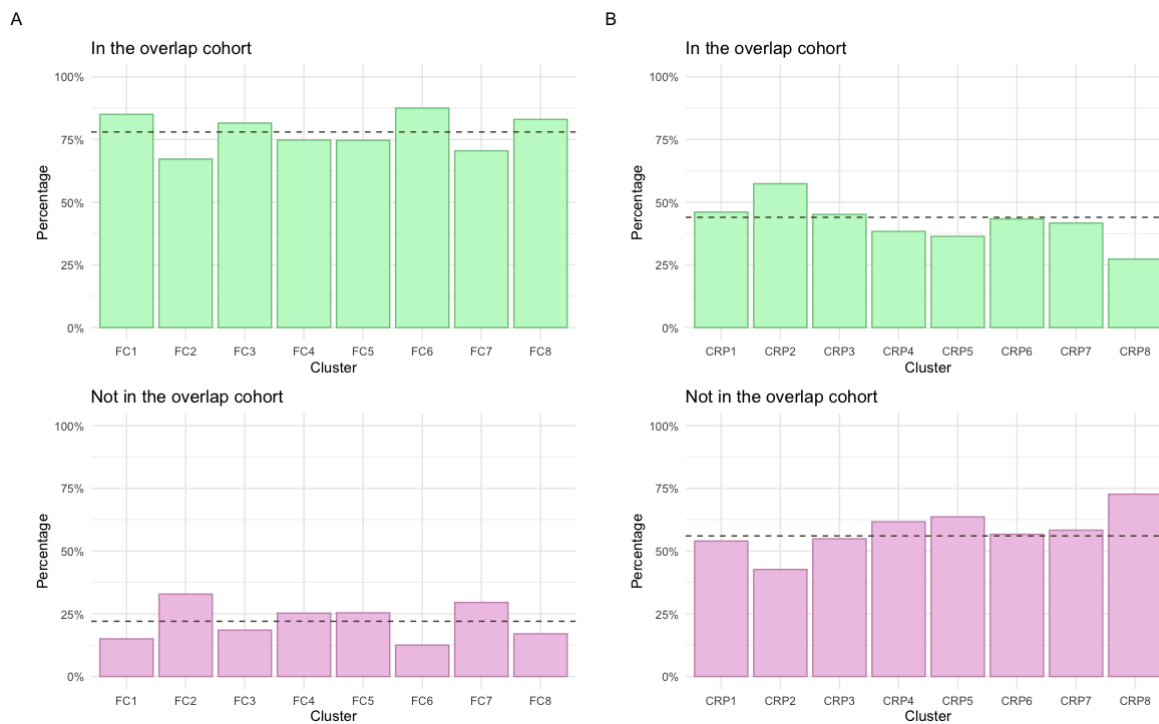
1068

Figure S30. Ulcerative colitis patients in the Lothian IBD Registry only only. (A) For each cluster, panels show the proportion of individuals with Montreal extent recorded as E1, E2 and E3 respectively. The dashed horizontal line represents overall proportions across the entire CRP cohort. (B) Forest plot showing the estimated effect sizes and associated 95% confidence intervals for Montreal extent: E2 and E3 versus E1 (baseline category) in a multinomial logistic regression model that uses FC cluster assignment as outcome. Subjects with a posterior probability of belonging to their assigned cluster greater than 0.5 were considered in addition to all subjects in the cohort. Effect sizes are with respect to the reference cluster (in this case CRP1). The multivariate model includes age, sex, smoking and Montreal extent (E1, E2, E3). The dashed vertical lines are used as a reference to indicate no effect.



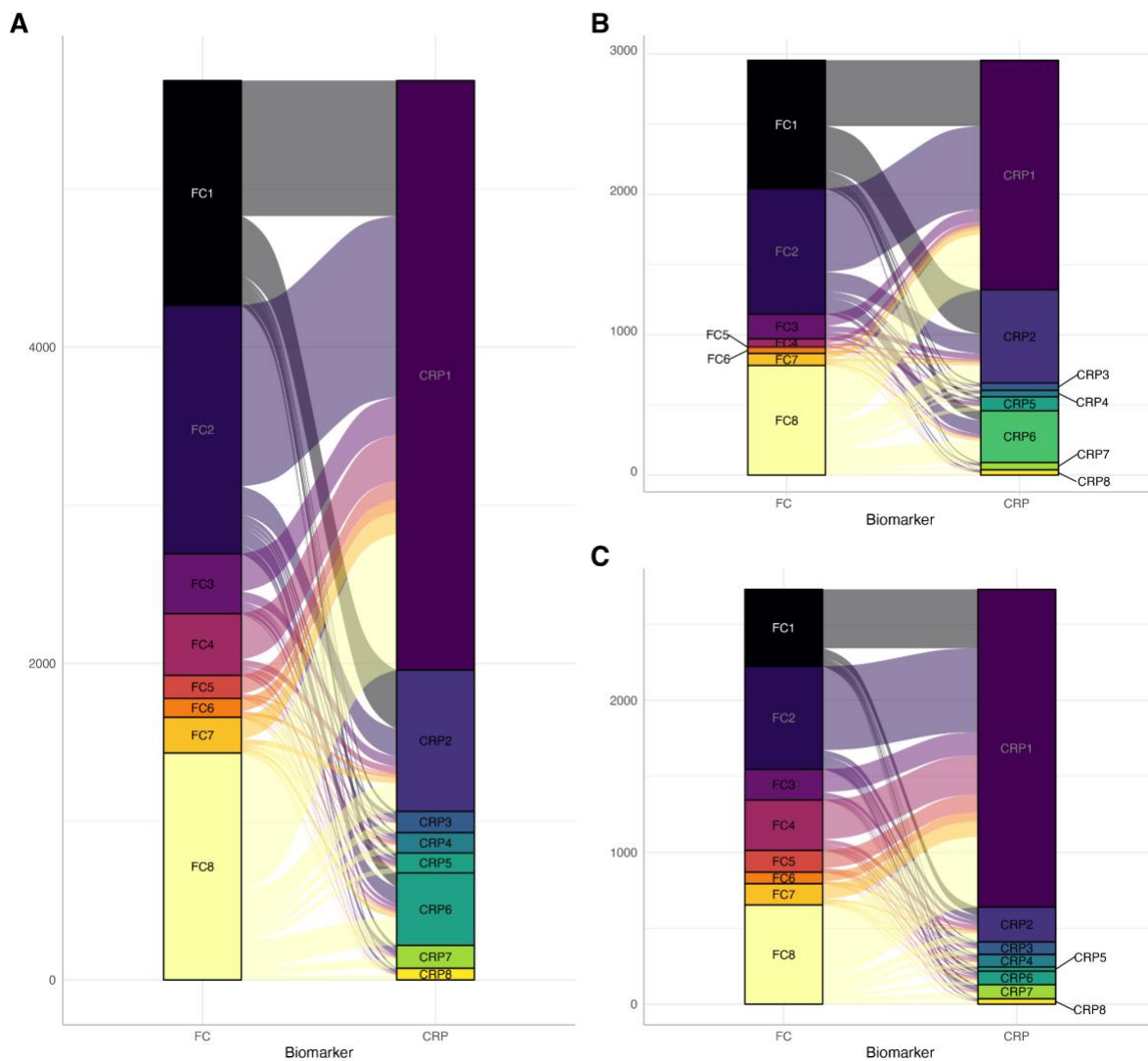
1069
1070
1071
1072
1073
1074

Figure S31. CRP cluster-specific cumulative distribution for first-line advanced therapy prescribing for Crohn's disease (red) and ulcerative colitis (teal) subjects in (A) the Lothian IBD Registry and (B) national Danish registry data. Clusters are ordered from lowest (CRP1) to highest (CRP8) cumulative inflammatory burden. The number of CD and UC subjects present in each cluster is displayed as panel titles. Curves which would describe fewer than five subjects are not shown.



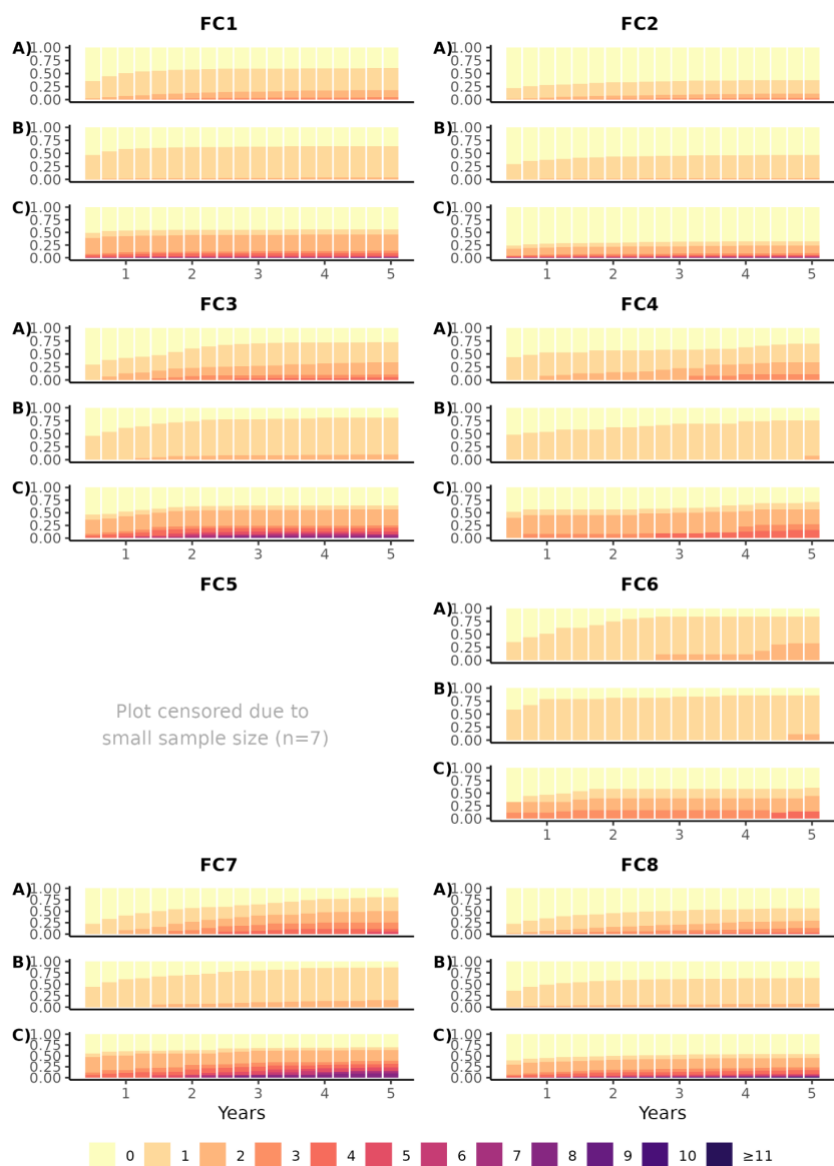
1075
1076
1077
1078
1079
1080
1081
1082

Figure S32. (A) For each FC cluster in the Lothian IBD Registry, panels show the proportion of individuals included in the overlap LIBDR cohort, which consists of LIBDR subjects included in both the FC and CRP analysis. The dashed horizontal line represents overall proportions across the entire FC cohort. (B) As in (A), but focusing on CRP clusters instead. The dashed horizontal line represents overall proportions across the entire CRP cohort.



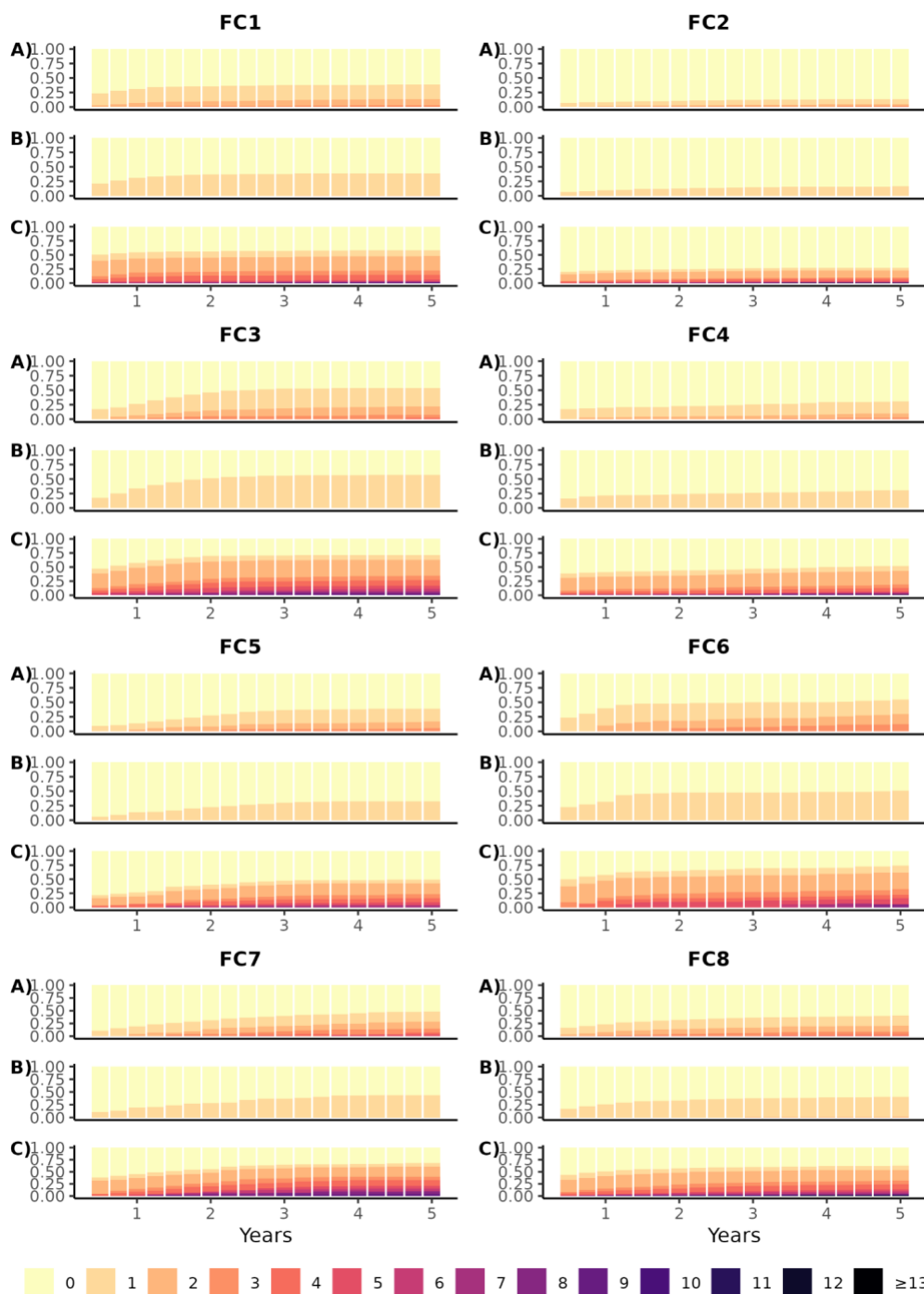
1083
 1084
 1085
 1086
 1087
 1088
 1089
 1090
 1091

Figure S33. Comparison between faecal calprotectin (FC) and processed CRP cluster assignment for the Danish cohort. Results are reported based on the overlap cohort, consisting of 5685 subjects included in both the FC and CRP analysis. (A) all subjects; (B) Crohn's disease; and (C) ulcerative colitis. Each segment denotes the size of the cluster whilst the alluvial segments connecting the nodes visualises the number of subjects shared between clusters.



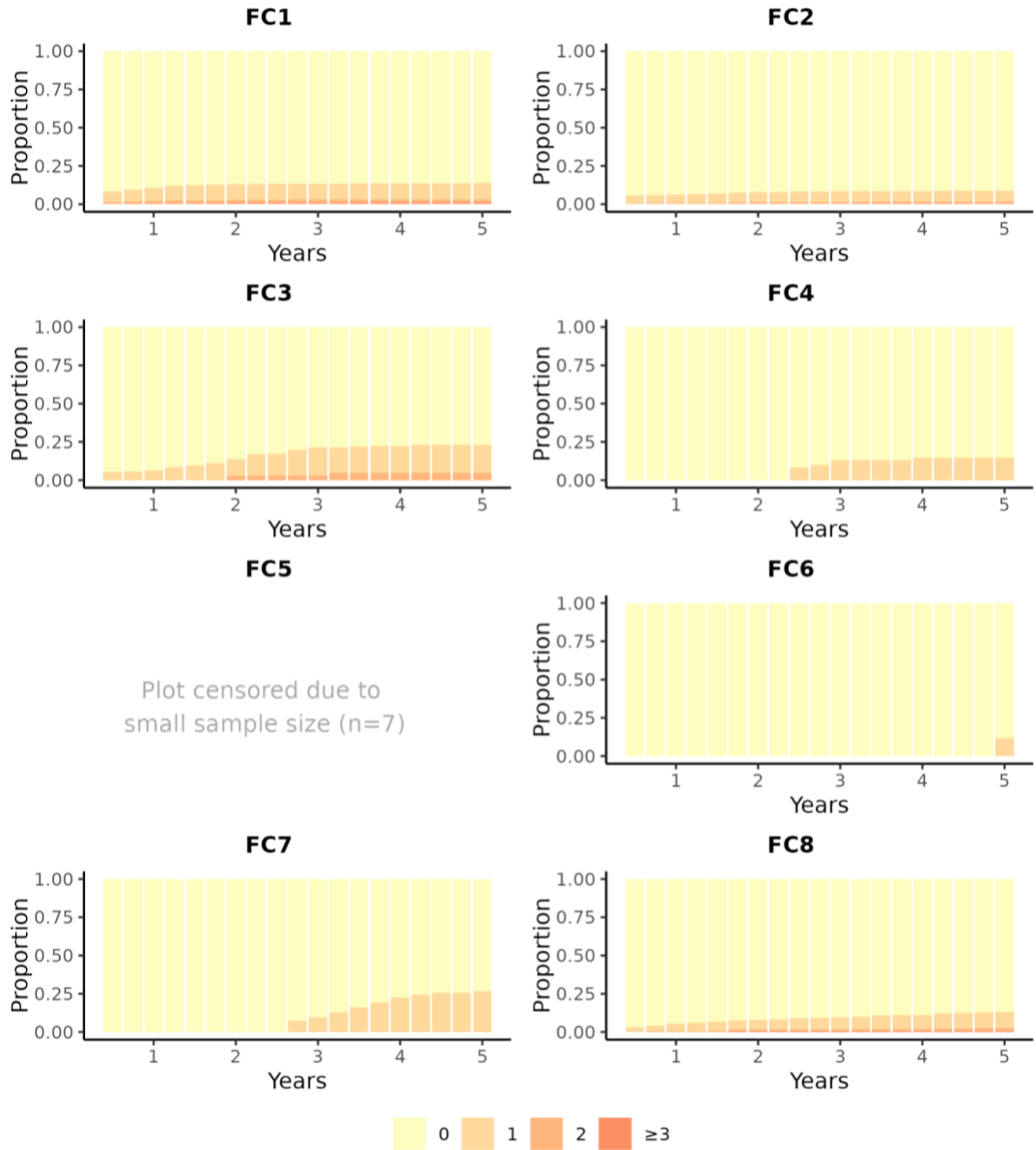
1092
1093
1094
1095
1096
1097
1098

Figure S34. Prescribing trends over time for Crohn's disease subjects in the Danish faecal calprotectin cohort for (A) commencement of an advanced therapy, (B) commencement of an immunomodulator, and (C) a course of corticosteroids (defined as 1500mg total). Subjects are stratified by FC cluster assignment. For confidentiality reasons, categories with <5 individuals at each time interval were merged with the category with one fewer treatment.



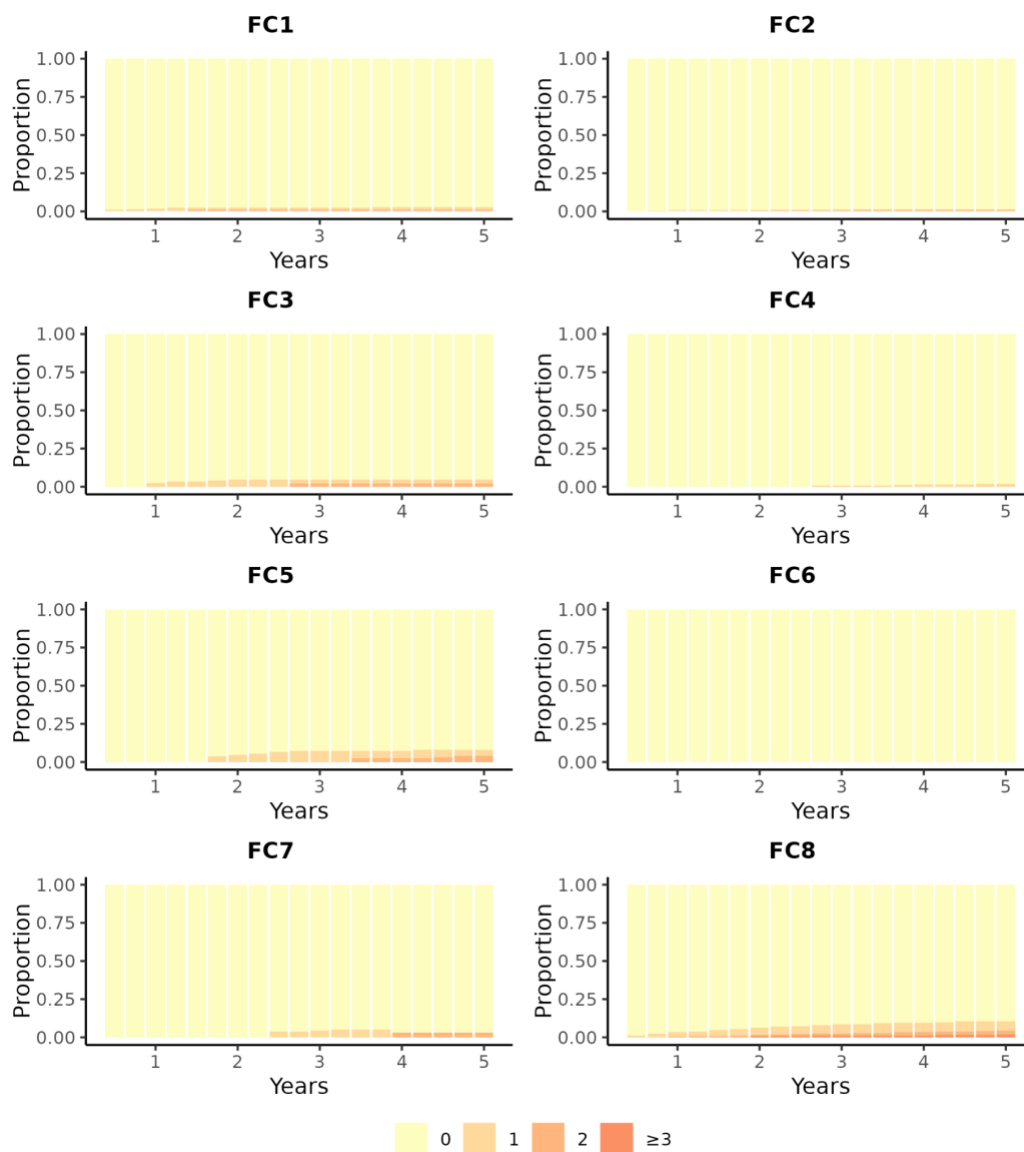
1099
1100
1101
1102
1103
1104

Figure S35. Prescribing trends over time for ulcerative colitis subjects in the Danish faecal calprotectin cohort for (A) commencement of an advanced therapy, (B) commencement of an immunomodulator, and (C) a course of corticosteroids (defined as 1500mg total). Subjects are stratified by FC cluster assignment. For confidentiality reasons, categories with <5 individuals at each time interval were merged with the category with one fewer treatment.



1105
1106
1107

Figure S36. Number of surgical bowel resections over time for Crohn's disease subjects in the Danish cohort. Stratified by faecal calprotectin cluster assignment.



1108
1109
1110

Figure S37. Number of surgical bowel resections over time for ulcerative colitis subjects in the Danish cohort. Stratified by faecal calprotectin cluster assignment.

1111 Supplemental tables

| Clusters | Maximum log-likelihood | AIC | BIC |
|----------|------------------------|-----------------|-----------------|
| 2 | -16532.10 | 33094.20 | 33168.35 |
| 3 | -16354.39 | 32754.78 | 32868.47 |
| 4 | -16260.21 | 32582.42 | 32735.66 |
| 5 | -16201.86 | 32481.71 | 32674.49 |
| 6 | -16141.82 | 32377.63 | 32609.96 |
| 7 | -16109.77 | 32329.54 | 32601.42 |
| 8 | -16076.89 | 32279.77 | 32591.19 |
| 9 | -16039.66 | 32221.33 | 32572.29 |
| 10 | -16015.29 | 32188.59 | 32579.09 |

1112 *Table S1. Likelihood-based model statistics for LCMMs fitted to faecal calprotectin data across 2–10*
1113 *clusters using the chosen model specification. Boldface font indicates optimal values.*

| Clusters | Maximum log-likelihood | AIC | BIC |
|----------|------------------------|-----------------|-----------------|
| 2 | -15451.41 | 30932.82 | 31015.57 |
| 3 | -15314.76 | 30675.52 | 30802.40 |
| 4 | -15240.15 | 30542.29 | 30713.30 |
| 5 | -15173.04 | 30424.09 | 30639.23 |
| 6 | -15106.25 | 30306.50 | 30565.78 |
| 7 | -15051.43 | 30212.86 | 30516.27 |
| 8 | -15016.96 | 30159.91 | 30507.45 |
| 9 | -15014.76 | 30171.53 | 30563.20 |
| 10 | -15014.40 | 30186.81 | 30622.61 |

1114 *Table S2. Likelihood-based model statistics for LCMMs fitted to processed CRP data across 2–10*
1115 *clusters using the chosen model specification. Boldface font indicates optimal values.*

Supplementary material for Constantine-Cooke and Vestergaard et al.

Nathan Constantine-Cooke^{1, 2}, Marie Vibeke Vestergaard³, Karla
Monterrubio-Gómez^{1, 2}, and Catalina A. Vallejos²

¹Centre for Genomic and Experimental Medicine, Institute of Genetics and Cancer, University
of Edinburgh, Edinburgh, UK

²MRC Human Genetics Unit, Institute of Genetics and Cancer, University of Edinburgh,
Edinburgh, UK

³Center for Molecular Prediction of Inflammatory Bowel Disease, PREDICT, Department of
Clinical Medicine, Aalborg University, Copenhagen, Denmark

Supplemental Note 1: Data definitions

1.1 Lothian IBD Registry

Additional phenotyping (at diagnosis)

When available, additional phenotyping information (at diagnosis) was manually extracted by the clinical team from electronic healthcare records (TrakCare; InterSystems, Cambridge, MA). For CD subjects, the following information was extracted:

- **Smoking:** recorded as a binary (yes/no) variable.
- **Montreal location:**
 - L1 (Ileal): limited to the ileum, the final segment of the small intestine.
 - L2 (Colonic): limited to the colon/large intestine.
 - L3 (Ileocolonic): inflammation is present in both the ileum and colon.
- **Montreal behaviour:**
 - B1 (Inflammatory): non-stricturing and non-penetrating
 - B2 (Stricturing): where the formation of fibrosis leads to the narrowing of the intestine.
 - B3 (Penetrating): where the inflammation causes the formation of fistulas or abscesses.

Due to small numbers, B2 and B3 are merged into a single group (complicated CD) when analysing Montreal behaviour.

- **Upper GI inflammation (L4):** whether any gastrointestinal inflammation is detected further up than the ileum. Usually, upper inflammation is considered a *modifier* for Montreal location. Recorded as a binary (yes/no) variable. L4 was missing for a high proportion of subjects. This is because the required investigations are only carried out where upper GI inflammation is suspected. As such, we have manually mapped missing L4 values as “No” (i.e. no upper GI inflammation for the associated patients).
- **Perianal disease:** considered a modifier for Montreal behaviour and is a severe complication of Crohn’s disease involving inflammation around the anus. Recorded as a binary (yes/no) variable.

For UC subjects, the following additional phenotyping information was considered:

- **Smoking:** recorded as a binary (yes/no) variable.
- **Montreal extent:**
 - E1 (Ulcerative proctitis): limited to the rectum.
 - E2 (left sided colitis): inflammation is present in the rectum, the sigmoid colon, and possibly the descending colon.
 - E3 (extensive colitis): inflammation extends beyond the splenic flexure.

List of advanced therapies relevant for IBD management

The following biologics and small molecules were considered to be advanced therapies relevant for the treatment of IBD. All other advanced therapies were ignored. If one of these advanced therapies were prescribed for a condition other than IBD, for example for rheumatoid arthritis, then these treatments were still considered given they are known to modify IBD outcomes. Only prescriptions given within the observation period (seven years since diagnosis) were considered.

- Adalimumab
- Certolizumab
- Golimumab
- Infliximab
- Risankizumab
- Tofacitinib
- Upadacitinib
- Ustekinumab
- Vedolizumab

1.2 National Danish registry data

Diagnosis adjudication

Subjects with IBD were defined as either

1. Having two different secondary care interactions linked to an ICD-10 IBD code (see Table 1.2) within a two year period, and/or
2. Two inpatient interactions assigned an IBD code (no period requirement).

If a subject meets only the first criterion, the first IBD secondary care interaction is used as the date of diagnosis. If a subject only meets the second criterion, then the date of the first inpatient record is used. If a patient meets both criteria, the earliest date is used.

Patients were assigned an IBD subtype (either CD or UC) based on the majority of the ICD-10 codes. If there were an equal number of IBD subtype diagnoses, the latest diagnosis was used.

Table 1.2 details the registry and codes used to obtain the data for each of the variables used in the Danish component of the study.

Prescribing and surgery data

As additional prescribing data were available for the Danish cohort, plots exploring these data were produced. Advanced therapy and immunomodulator plots were generated as the cumulative number of unique treatments over time for each patient. For systemic corticosteroids, one treatment course was defined as 1500 mg with the cumulative number of treatment courses plotted. For major surgeries related to IBD, the cumulative number of surgeries were plotted. For confidentiality reasons, categories with < 5 individuals in at each time interval were merged with the category with one fewer treatment.

| Variable | Definition and codes | Source |
|--|---|---|
| IBD-related hospital interactions | ICD-10: K50, K51 | Danish National Patient Registry |
| Biochemistry tests | | The Danish nationwide Register of Laboratory Results for Research |
| CRP | NPU: NPU19748 | |
| Fecal calprotectin | NPU: NPU19717, NPU26814 | |
| Biologic therapies and small molecules | | Danish National Prescription Registry |
| Infliximab | C_OPR: BOHJ18A1/ BOHJ18A | |
| Adalimumab | C_OPR: BOHJ18A3 | |
| Ustekinumab | C_OPR: BOHJ18B3 | |
| Vedolizumab | C_OPR: BOHJ19H4 | |
| Natalizumab | C_OPR: BOHJ26 | |
| Certolizumab | C_OPR: BOHJ18A5 | |
| Golimumab | C_OPR: BOHJ18A4 | |
| Risankizumab | C_OPR: BOHJ19N1 | |
| Tofacitinib | C_OPR: BOHJ28D | |
| Upadacitinib | C_OPR: BWHP107 | |
| Immunomodulators | | Danish National Prescription Registry |
| Azathioprine | ATC: L04AX01; C_OPR: BWHB83 | |
| Mercaptopurine | ATC: L01BB02 | |
| Methotrexate | ATC: L04AX03/L01BA01; C_OPR: BWHA115 | |
| Systemic corticosteroids | ATC: H02AB01, H02AB02, H02AB04, H02AB06, H02AB07, H02AB08, H02AB09 | Danish National Prescription Registry |
| IBD-related major surgery | | Danish National Patient Registry |
| Intestinal resections | NCSP: KJGB, KJFB (excl. KJFB10+13) | |
| Enterointerostomy | NCSP: KJFC | |
| Enterostomy | NCSP: KJFF | |
| Colectomy | NCSP: KJFH | |
| Intestinal stricture-plasty | NCSP: KJFA60, KJFA61, KJFA63 | |
| Other local intestinal surgery | NCSP: KJFA96, KJFA97 | |
| Other intestinal surgery | NCSP: KJFW | |
| Stenosis surgery without resection or adhesiolysis | NCSP: KJFL | |

Table 1.1: For each variable used in the Danish analyses, the corresponding registry and codes used to obtain the data.

Supplemental Note 2: Processing of CRP measurements

Further processing was applied to CRP data to smooth out short-term fluctuations. In the LIBDR, measurements were grouped into intervals of t : $[0, 0.5)$, $[0.5, 1.5)$, $[1.5, 2.5)$, $[2.5, 3.5)$, $[3.5, 4.5)$, $[4.5, 5.5)$, $[5.5, 7]$, where $t = 0$ (years) is the time of diagnosis. The median CRP for each interval was calculated for each subject and used as input for subsequent analyses. The centre of each interval was used as the corresponding observation time. The same approach was used for the Danish data, however intervals of t : $[0, 0.5)$, $[0.5, 1.5)$, $[1.5, 2.5)$, $[2.5, 3.5)$, $[3.5, 5]$ were used instead to take into account the differences in follow-up between the cohorts.

Supplemental Note 3: Latent class mixed model

Introduction

This note provides a formal definition of latent class mixed models (LCMMs)¹ and describes how the most appropriate model specifications were found.

All models were fit using the `lcmm` R package. In all cases, models were fit using a maximum of 24,000 Marquardt iterations and all other options left at the default settings. An automatic grid search approach with 50 repetitions was used to attempt to avoid local maxima. All models converged as per default convergence criteria.

Formal definitions

The LCMM consists of two sub-models. A longitudinal sub-model and a class assignment sub-model. The former will be introduced before the latter.

Longitudinal sub-model

We assume a population of N individuals is heterogeneous and composed of G latent classes (or clusters): each characterised by a distinct mean profile of a marker of disease activity (in logarithmic scale) across time. We assume each subject i has a vector of repeated measurements of length n_i , allowing the number of measurements to differ across subjects. A random effects specification is used to capture intra-individual correlation in measurements. We allow each subject i to belong to only one latent class and introduce a discrete random variable c_i which is equal to g if subject i belongs to the latent class g , where $g = 1, \dots, G$.

The logarithm of the biomarker measurement (FC or CRP) for the i th subject taken at time t_{ij} is denoted by Y_{ij} . Given that the subject i belongs to class g , the latter is modelled using a latent class mixed model LCMM:

$$Y_{ij}|_{c_i=g} = \mathbf{X}(t_{ij})' \beta_g + u_{ig} + \epsilon_{ij} \quad (3.1)$$

where the vector of regression coefficients β_g capture class-specific fixed effects, u_{ig} denote random effects distributed such that $u_{ig} \sim \mathcal{N}(0, \sigma_u^2)$ (we assume the variance σ_u^2 is shared across classes, but a more general form of the model allows for class-specific variance). In our analysis, we assume a single random effect (intercept) u_{ig} to account for correlation between longitudinal observations collected for the same individual. Finally, ϵ_{ij} indicates an independently distributed Gaussian error term with zero mean and variance σ_ϵ^2 .

Class membership sub-model

The probability of $c_i = g$ is given as a class-specific probability and is described by a multinomial logistic model:

$$P(c_i = g) = \frac{e^{\mathbf{X}_{c_i}^T \xi_g}}{\sum_{l=1}^G e^{\mathbf{X}_{c_i}^T \xi_l}}, \quad (3.2)$$

where \mathbf{X}_{c_i} is a vector of covariates and ξ_g is a vector of parameters whose first element corresponds to a class-specific intercept. For identifiability, the intercept associated to class G is assumed to be equal to zero. Note that the covariates in Equation (3.2) do not need to match those used in the longitudinal model. In our analysis, IBD type (CD, UC or IBDU for the LIBDR cohort; CD or UC for the Danish data) was included as a covariate in this model.

Posterior probabilities of class assignment

After inferring all model parameters, posterior class-membership probabilities for each subject are given by:

$$\hat{\pi}_{ig}^Y = P(c_i = g | \mathbf{Y}_i, \mathbf{X}(t_{i.}), \hat{\theta}_G) = \frac{\hat{\pi}_{ig} \phi_{ig}(\mathbf{Y}_i | c_i = g, \hat{\theta}_G)}{\sum_{l=1}^G \hat{\pi}_{il} \phi_{il}(\mathbf{Y}_i | c_i = l, \hat{\theta}_G)} \quad (3.3)$$

where \mathbf{Y}_i denotes a vector of length n_i containing all longitudinal measurements recorded for subject i , $\mathbf{X}(t_{i.})$ is a matrix ($n_i \times 4$) comprised of all the corresponding time-dependent covariates for subject i , $\hat{\theta}_G$ denotes the estimates obtained for all model parameters ($\beta_1, \dots, \beta_G, \sigma_u^2, \sigma_\epsilon^2, \xi_1, \dots, \xi_G$) and $\hat{\pi}_{ig}$ corresponds to Equation (3.2) evaluated on $\hat{\theta}_G$. Finally, $\phi_{ig}(\mathbf{Y}_i | c_i = g, \hat{\theta}_G)$ denotes a multivariate normal density function with mean $\mathbf{X}(t_{i.}) \hat{\beta}_g$ and variance covariance $\sigma_u^2 \mathbf{X}(t_{i.}) \mathbf{X}(t_{i.})' + \hat{\sigma}_\epsilon^2 I_{n_i}$, where I_{n_i} denotes an identity matrix with dimension n_i .

Fixed effects specified as natural cubic splines

The vector of time-dependent covariates $\mathbf{X}(t)$ (see Equation (3.1)) was defined using an intercept term and natural cubic splines (NCS)² to capture non-linear dependency between observations and time. The NCS were calculated as a pre-processing step prior to estimating the model in Equation (3.1) using the `ns()` function of the `splines` R library³. Knots were located at quantiles of measurement times across all measurements.

To determine the most appropriate number of interior knots for the LIBDR cohort, LCMMs with six clusters were fitted to the LIBDR FC data assuming two to four knots. Visual inspection, Akaike information criterion (AIC), and Bayesian information criterion (BIC) were used to determine the most appropriate NCS specification, which was then used to fit the models used in the main analysis.

The optimal AIC was reported for the NCS model with four interior knots whilst BIC favoured the three-knot specification (Table 3.1). However, visual inspection of the

four-knot specification appeared to result in overfitting of the data (Figure 3.1). As such, the three-knot approach was used to specify the fixed effects of the longitudinal sub-model for all further FC and CRP modelling in the LIBDR cohort. As such, the time-dependent covariate vector was defined as $\mathbf{X}(t) = (1, X_1(t), X_2(t), X_3(t), X_4(t))'$ (the first element ensures the model includes an intercept term).

A similar approach was used to define the number of knots when analysing the Danish data. Two knots were chosen for both FC and CRP analyses.

| Specification | Maximum log-likelihood | AIC | BIC |
|---------------|------------------------|-----------------|-----------------|
| 2 Knots | -19766.31 | 39614.61 | 39823.41 |
| 3 Knots | -19615.33 | 39324.67 | 39564.02 |
| 4 Knots | -19604.65 | 39315.30 | 39585.21 |

Table 3.1: Likelihood-based model statistics for LCMMs assuming six clusters with varying specifications for the fixed effects of the longitudinal sub-model. The models considered used natural cubic splines with varying knots. Boldface font indicates optimal values.

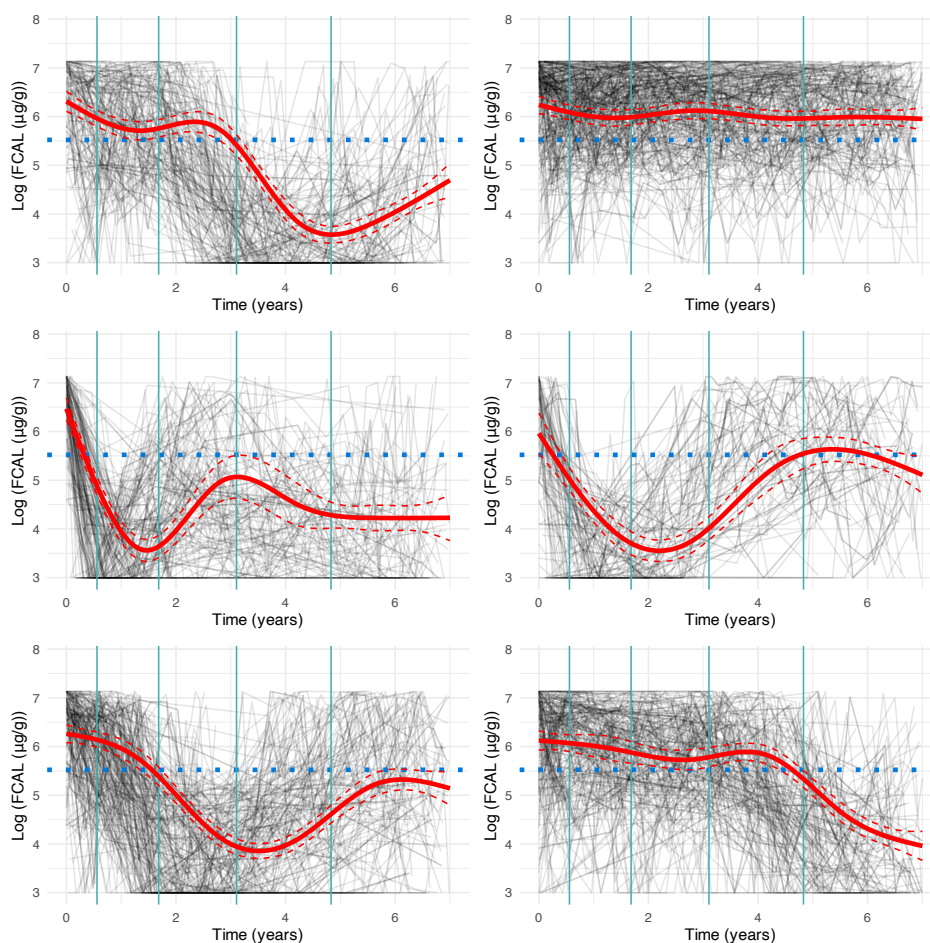


Figure 3.1: Cluster trajectories of FC for a LCMM using natural cubic splines with 4 knots. Vertical teal lines indicate knot locations. Dotted horizontal lines indicate $\log(250\mu\text{g}/\text{g})$ FC which is commonly used as a cutoff for disease activity.

Supplemental Note 4: Software versions

As LIBDR and Danish analyses were conducted on separate computational platforms, the software versions differed.

4.1 Lothian IBD Registry

R (v. 4.4.2),³ extended using the lamm (v. 2.1.0),¹ ggalluvial (v. 0.12.5),⁴ nnet (v. 7.3-19),⁵ and datefixR (v.1.7.0)⁶ packages, was used. Analytical reports have been generated using the Quarto scientific publishing system (v.1.4.551) and are hosted online (<https://vallejosgroup.github.io/IBD-Inflammatory-Patterns/>). An R package, libdr (v.1.1.0), has also been produced, supporting the reuse of our R code with other datasets.

4.2 National Danish registry data

R (v. 4.4.0) extended using the lamm (2.1.0), ggalluvial 0.12.5, and nnet 7.3.19 packages was used for the Danish analyses. The R code is shared in the VallejosGroup/IBD-Inflammatory-Patterns GitHub repository under the `source/dk` directory.

Bibliography

- [1] Proust-Lima C, Philipps V, Liquet B. Estimation of extended mixed models using latent classes and latent processes: The R package lmm. *J Stat Softw* 2017; 78(2): 1–56. doi: 10.18637/jss.v078.i02
- [2] Hastie T, Tibshirani R, Friedman J. *The Elements of Statistical Learning*. Springer Series in Statistics New York, NY: Springer . 2009
- [3] R Core Team . *R: A Language and Environment for Statistical Computing*. Vienna, Austria: R Foundation for Statistical Computing . 2022.
- [4] Brunson JC. ggalluvial: layered grammar for alluvial plots. *J Open Source Softw* 2020; 5(49): 2017. doi: 10.21105/joss.02017
- [5] Venables WN, Ripley BD. *Modern applied statistics with S*. New York: Springer. fourth ed. 2002.
- [6] Constantine-Cooke N. datefixR: fix really messy dates in R. <https://CRAN.R-project.org/package=datefixR>; 2024